HYBRID SOLAR PV–HYDRO CONTROLLER FOR AN AUTONOMOUS DC MICROGRID

By

PRIME NKUNDUKIZE

Submitted in partial fulfilment of the requirements for the degree

Master of Engineering in Energy

Faculty of Engineering and Built Environment

Cape Peninsula University of Technology

Supervisor: Dr. M. Adonis

Bellville Campus

November 2022

DECLARATION

I, **PRIME NKUNDUKIZE**, declare that the contents of this dissertation/thesis represent my own unaided work, and that the thesis has not previously been submitted for academic examination towards any qualification. Furthermore, it represents my own opinions and not necessarily those of the Cape Peninsula University of Technology.

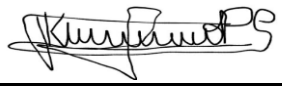

November 2022

Signed **Date**

ABSTRACT

The negative impact of global warming and general environmental pollution associated with the use of fossil fuel as a source of energy has become more visible in the past decade. Hence, the need to operate a more sustainable electrical grid network using renewable resources such as wind, solar PV, hydroelectric, biofuel and biomass. Solar PV is a reliable source of energy to solve the energy crisis and environmental pollution associated with it. This is mostly informed by the advancement in technology and reduced cost of solar PV panels. The power supply and consequent power output from a microgrid network with high solar-PV penetration is normally unstable due to the intermittent nature of solar PV supply. Hence, the need to incorporate a pumped hydro storage system as the energy storage system of choice.

In this study, a control method for an off-grid hybrid DC microgrid that consists of solar PV and pumped hydro storage system was developed to provide sustainable, reliable, flexible and accessible energy for a remote community. The developed off-grid DC microgrid system consists of a solar PV system of 100 kWp as a distributed energy resource and a pumped hydro storage system as energy storage system (ESS). an energy management system (EMS) was designed and developed using a fuzzy logic controller (FLC) in the MATLAB/Simulink environment. A pumped hydro storage system (PHSS) is used as an energy storage system to improve the DC microgrid system stability and also operates as a backup power system. A load shedding scheme is part of the system to bring support to the supply by automatically disconnecting or re-connecting the secondary load to ensure reliability and continuous supply of power to the primary load and secondary load depending on the available power and the water level in the reservoir. A DC-DC boost converter connects the solar PV to the rest of the DC microgrid system thereby improving the quality of power generated and allow the flow of power in the system. The performance analysis of the research design considered the intermittent power supply of the solar PV and the flexibility of the load demand under different circumstances and time of the day.

The study developed different scenarios using the energy management system algorithm to evaluate the performance of the system. The results showed that the adopted EMS ensured DC microgrid stability, improved reliability, increased system flexibility and effective power distribution. In addition, the developed algorithm provided adequate power distribution between the solar PV and the PHSS and maintained the charging and discharging of the reservoir within acceptable level. The results also showed that the PHSS was able to augment power shortage in the system based on the different scenarios that were implemented. The developed energy management system also provides an opportunity to

remodel and change any parameter within the DC microgrid system. The results obtained were compared with other similar DC microgrid system's and the results proved that the EMS was effective and the load demand was adequately met.

Key words: DC microgrid, energy storage system, MATLAB/Simulink, pumped hydro storage system, renewable energy, solar PV.

ACKNOWLEDGEMENTS

I would like to acknowledge and give my heartfelt thanks to my supervisor Dr Marco Adonis, without his contribution, this work was not going to be achieved. His undivided support and assistance carried me through all the stages while writing my project. I would also like to thank different member of staff at CPUT, who contributed from distance, during different assessment for their brilliant comments and suggestions, thanks to you.

I would also like to give special thanks to my wife Nadege Nduwayo and my sons, Brian, Ela and Simon, for their continuous support by allowing me to use most of the family time when undertaking my research and writing my project. Your prayers and good wishes for me were what kept me strong this far.

Last but not least, I would like to thank God for letting me through all the difficulties during the duration of this work and finish my degree, may you continuous to guide me in my responsibilities ahead. I will always trust you.

DEDICATION

This thesis is dedicated to my wife, Nadege Nduwayo, and my sons, Brian, Ela and Simon. Without their love and support I would never have been able to complete my graduate studies. I will forever adore you; you are the reason why I wake up in the morning and go to work, and I appreciate everything that you have done for me.

This thesis is also dedicated to my late grandmother, Colette Nintunze, for teaching me the importance of hard work. I will always miss you.

TABLE OF CONTENTS

TABLE OF FIGURES

LIST OF TABLES

LIST OF ACRONYMS AND ABREVIATIONS

AC: Alternative Current

DC: Direct current

DCMG: Direct current microgrid

DER: Distributed Energy Resource

DER: Distributed energy resources

DP: Dynamic programming

EMS: Energy management system

EPS: Electronic power system

HESS: Hybrid Energy Storage System

HPFD: High pass-filter Droop Controller

IMG: Intelligent Microgrid

LCOE: Levelized cost of energy

LPSP: Loss of power supply probability

MPPT: Maximum Power Point Tracking

PHSS: Pumped hydro storage system

Ppv: Power output of the solar PV panel

PSH: Pump storage hydroelectric system

PV: Photovoltaic

RES: Renewable Energy System

SC: Supercapacitor Converter

SDR: Supply to demand ratio

SOC: State of change

VCD: Virtual Capacitor Droop

YRE: Year-round efficiency

CHAPTER 1: INTRODUCTION

1.1 Background

The negative impact of global warming and environmental pollution associated with the use of fossil fuel as a source of energy has become more visible in the past decade. Hence, the focus on more sustainable sources of energy generation such as: wind, solar photovoltaic, hydroelectric, biofuel, and biomass (Philip et al., 2016). According to Singh (2016) , the solar PV system was identified as the most reliable source of energy in an attempt to solve this energy crisis and environmental pollution. This is due to available technology, ease of mounting solar PV panels and cost of power which has been reduced significantly in recent years (Aliyu et al., 2018). The power supply and consequent power output from a microgrid network with high solar-PV penetration is normally unstable due to the intermittent nature of solar PV supply (Rehman et al., 2015).

Solar PV systems are usually complemented by energy storage systems (ESS) to enhance the stability and efficiency of the energy supply (Xu et al., 2019). Therefore, to improve the system, a hybrid system comprised of a solar PV and pumped hydro storage energy system (PHS) was identified as a system that is capable of increasing the power production capacity (Mahmoudimehr & Shabani, 2018). The implementation of this system has the capacity to salvage the intermittent power supply from the solar PV. Among the various types of storage technologies available, the battery is generally utilised in stand-alone renewable energy systems regardless of the obvious limitations such as high initial investment cost, short lifespan, environmental damage, explosion and maintenance difficulties confronting its usage (Mahmoudimehr & Shabani, 2018).

As highlighted by Aliyu et al.(2018) in his study, photovoltaic backed up by pumped hydro energy storage has shown to be a major solution that will adequately eradicate the intermittent characteristic of solar PV power supply to achieve the continuous energy supply required by consumers. Pumped storage plant represents the most mature approach among the peaking power sources (PSS) and this is one of China's major investments for the future (Rehman et al., 2015). The pumped hydro energy storage (PHES) is in the form of potential energy where water is pumped from a lower reservoir to a higher-level reservoir to be used during high power energy demand period (Swe, 2018).

According to Dong et al. (2018) the design of any microgrid is determined by the need of the consumers because the power supply must be equal to the load in order to maintain stability. Although the power produced by solar photovoltaic and hydropower (PV/PHES) hybrid is

continuous and reliable, emergency conditions can arise due to active power deficiency in an islanded microgrid which decreases the system frequency and cause the microgrid to collapse (Khoa et al., 2016). In a traditional power system, when an unbalanced situation occurs between the energy supply and the load, the system automatically uses its rotating inertia to give rise to a change in frequency of the grid network, which is underlying the principle of P-f droop control method (Wang et al., 2015). In the DC microgrid system, the inertia does not exist due to the intermittent character of most of the renewable energy sources (Baboli et al., 2014). Most research has tried to understand which of the AC and DC-based microgrid is best when it comes to the control of the system. AC system present problems linked to the power quality and synchronization, while the DC microgrid has presented positive improvements when the system control is taken into consideration (Zhou & Ngai Man Ho., 2016).

According to Liu et al.(2018), pumped hydro energy storage is currently considered as the most promising technology to enhance reliable and clean energy production, especially in autonomous islanded microgrid (Liu et al., 2018). The microgrid is formed by the hybrid interconnection of various units such as AC and DC energy sources, storage device, AC and DC loads AC/DC, or DC/AC converters (Aliyu et al., 2018). Different researchers have shown that a lack of controllers in the microgrid system to regulate power flow from the solar PV to the load has a significant impact on different load components in the system. This is because of power supply and load imbalances in the system. When operating in islanded mode, a microgrid (MG) is expected to supply the needed active power, reactive power, and frequency to the load, and must operate within the specific range of voltage (Chong et al., 2016).

Different control methods have been used in microgrid system; master-slave, peer-to-peer, multi-agent control, fuzzy logic control, PID and sliding mode controller in order to ascertain the best control method capable of managing the power flow from the different energy supplies and the energy demand (Zhou & Ngai Man Ho., 2016). Philip et al.(2016) provides more details on how recently DC microgrid systems (MGs) have been receiving lots of attention with their flexibility and expandability. The key of promoting DC MGs lies in the advanced technology that enhances reliability during fault conditions, reduces overall costs and losses by the removal of AC-DC conversion, as well as achieves user-friendly operations (Muhsen et al., 2018).

1.2 Statement of the research problem

A stable power supply is essential for effective and efficient operation of a solar PV based microgrid system. This is because, the intermittent nature of renewable resources causes imbalance and unreliable power supply, especially with solar PV based microgrid system. In the past, most solar PV based microgrid system used batteries for energy storage and as a backup system. These batteries have limited capacity, are costly and can only last for few hours depending on the load demand. As a result, it affects the operation of the microgrid system.

Again, solar PV-diesel hybrid system have shown to be very expensive and environmentally harmful as explained by Philip et al.(2016). The regulation and balancing of the intermittent solar supply and the fluctuating load demand continue to be the bigger issues (Verma et al.,2013). The need for low cost and environmentally friendly power system with the capacity to solve the problem of both supply and demand imbalances is of great importance and addressed in this research.

1.3 Significance of the research

- Implementing the results obtained will help achieve the sustainability and reliability aim of the hybrid system by balancing the power flow between solar PV, energy storage and the load.
- It will enhance the ability of the system to automatically shed some of the load in case of a considerable decrease in the energy back up.
- The results will further position hydropower system as an energy storage in the renewable energy mix thereby enhancing the robustness of hybrid systems.
- Successfully achieving desired results will reposition solar PV as the prime choice in future energy mix policy, which is in line with most Governments' policy on the provision of autonomous clean electrical energy programs.
- The anticipated model is a smart and efficient system that will provide a complete result capable of assisting the independent power producers to better understand the behaviour of hydropower system in power stability.
- The research will strengthen the use of solar PV and hydropower systems in microgrid systems thereby discouraging over dependence on coal powered grid network.
- Lastly, the results of this research will assist both researchers and government in providing electricity to remote areas that are not connected to the national grid.

1.4 Aim and objectives of the research

The aim of this research is to implement power flow control in an autonomous solar PV-hydro DC microgrid system by means of fuzzy logic controller strategy. To achieve the abovementioned aim, the research needs to accomplish the following objectives:

- Carry out a literature review on autonomous hybrid Solar PV-hydro applications to DC microgrid.
- Conduct a feasibility study on fuzzy logic controller as a mechanism capable of DC microgrid power control.
- Model a solar PV-hydro system using MATLAB/Simulink.
- Model a control system capable of balancing the unstable solar power supply and the ever-changing load demand using fuzzy logic controller in the MATLAB/Simulink environment.
- Develop a system that will control the amount of power generated and consumed in the system using fuzzy logic controller in the MATLAB/Simulink environment. The results obtained will be measured against existing literature and its effectiveness to meet the power demands when required.
- Ensure that load is shared equally between the different distributed power supply system depending on the prevailing power demand and availability.
- Model a system that will implement a load-shedding strategy when the power generated is less than the power demand.
- Model varying solar irradiances that will mimic the unbalanced power supply from the solar PV using MATLAB/Simulink.

1.5 Research Methodology

To achieve the expected results, the research process is conducted in the following order:

- Different research papers relative to the subject were reviewed in order to gather in-depth knowledge on microgrid concepts, control, modelling, solar PV system, and energy storage systems.
- This research is implemented in the MATLAB/Simulink environment using various load and power supply scenarios. The system includes solar PV systems, System controller algorithms, DC-DC converters, MPPT, ESS and various components of the DC load.
- An investigation into different control strategies in DC microgrid is conducted, and a selection of a suitable control strategy for an autonomous solar PV-Hydro microgrid is proposed based on its reliability.

- The results after modelling and simulation were tested, evaluated, and compared to others obtained from different isolated DC microgrids controlled by another type of controllers.

1.6 Delineation of the research

Different control strategies in DC microgrid, load sharing and load shedding in solar PV-Hydro microgrid system.

- The research concentrated only on the control of power flow in solar PV-Hydro hybrid standalone microgrid.
- The research investigated the power flow in an islanded Hybrid solar PV-Hydro system using MATLAB/Simulink and not grid connected system.

1.7 The contribution of the Research

This research adds value in the control of power flow in solar PV-hydro microgrid, which can be used in rural areas where renewable resources such as solar power and hydropower are readily available in large amount. Most often, rural areas are the most disadvantaged due to lack of basic electricity infrastructures and are not connected to the existing grid. By implementing a hybrid solar PV–hydro microgrid system, communities within such an environment will be reliably supplied with electricity thereby improving the standard of life.

- With results obtained according to established parameters and values, a thesis will be compiled, and a paper will be published in a peer reviewed academic journal as an input to the body of knowledge in electrical engineering.
- The research will introduce a low-cost control of the system to balance the power between the power supply and the load demand.
- The study will improve the friendly environmental characteristic of solar PV-hydro as one of the solutions to environmental pollution.

1.8 Thesis outline

Chapter 1 introduces the thesis by presenting a brief background of hybrid solar PV–hydro autonomous DC microgrid controller. Thereafter, the statement of research problem, significance of the research, aims and objectives and methodology, delineation of the research and the contribution of the research are discussed.

Chapter 2 provides literature review on different renewable energy sources and corresponding energy storage systems with much emphasis on solar-PV pumped hydro storage system.

Chapter 3 presents a detailed literature on the concept of DC microgrid systems focusing on some advantages and disadvantages of different types. Thereafter, presents the different control systems highlighting distinct applications and technology advancements as it relates to DC microgrids.

Chapter 4 presents the system design and methodology. It covers research design, design model of the solar PV system, hydropower system, controllers, inverters, MPPT and adequate DC load.

Chapter 5 presents the simulation results of a hybrid solar PV–hydro autonomous DC microgrid with adequate controllers coupled with a detailed discussion of the results evaluating it against previous studies.

Chapter 6 concludes the research and identifies areas that will require further research.

CHAPTER 2: RENEWABLES AND ENERGY STORAGE SYSTEMS

2.1. Introduction

The past decade has experienced significant shortage in the supply of fossil fuel which happens to be the main source of power supply in most electrical grid networks around the world (Yang et al., 2014). Studies have also shown that global demand for power and electricity will continue to increase as the population increases (Ellabban et al., 2014). This is because more people are migrating to the major cities in search of a better life which must also be provided with electricity daily. The grid network is no longer sustainable nor environmentally friendly due to obsolete equipment, poor technology, and the need to operate more efficient and cost-effective grid network. Hence, an efficient renewable energy powered grid network has started attracting more attention because of the obvious advantages it has over the conventional grid network system (Vijayaragavan, 2017). Again, technological advancement in energy storage systems has offered a suitable platform for utility operators as well as power consumers to integrate more renewable energy resources to existing grid network (Adefarati & Bansal, 2016). Furthermore, integrating energy storage systems have the capacity to provide primary and sensitive loads enough power that will ensure stability without overloading the grid (U.S. Department of Energy Microgrid Exchange Group, 2011). Therefore, this chapter discusses hydropower system and solar PV as renewable energy sources, battery energy storage system (BESS), flywheel energy storage system, supercapacitor and pumped hydro storage system as energy storage systems utilised in microgrid systems.

2.2. Renewable energy sources

Renewable energy sources are naturally renewed but intermittent depending on the weather and environmental conditions of that particular location. Examples of renewable energy sources are wind, biomass, hydropower, geothermal, and solar as shown in figure 2.1. Some of the fundamental and general characteristics of these type of energy sources are, environmental friendly, less pollution, and renewable (Adefarati & Bansal, 2016). Compared to fossil fuels, renewable energy resources are generally spread in equal amount in specific geographical location at no cost. The amount of renewable energy resources added to the grid network, standalone power systems and as microgrid network has grown significantly in the past seven years as shown in figure 2.2 (REN21, 2020).

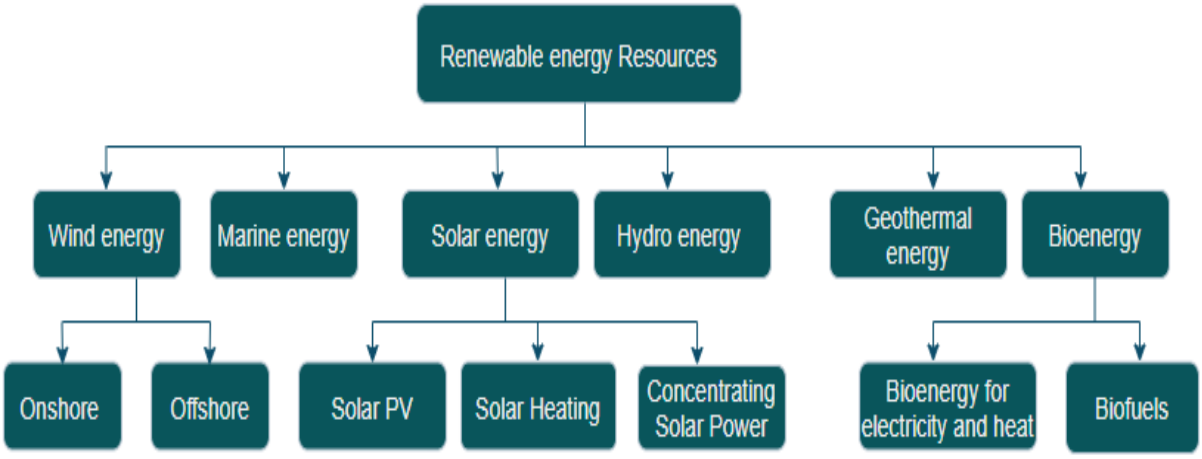

Figure 2.1 : Overview of renewable energy sources (Ellabban et al., 2014)

Again, figure 2.2 shows a significant addition of renewable power capacity to the power mix with Solar power appearing to be the highest in 2020 followed by wind, hydropower, then a combination of biomass, geothermal, ocean power and concentrated solar power (CPS) (Hossain et al., 2020).

Presently, the world is burdened with its over reliance on fossil fuel for power generation both for commercial, residential, industrial, and transportation purposes. Electricity has become a basic requirement for human existence and must be met at all material times but the commitment to meet this need in a sustainable manner has occupied the centre stage of global discussion. In addition, the need for electricity has grown significantly in the past decade due to the obvious increase in the population combined with huge urban migration (Showers, 2019). In addition, fossil fuel alone accounts for 60% of electric energy production globally by burning coal, gas, and oil. However, this pattern of power generation using fossil fuel as the primary source is no longer sustainable because of the environmental pollution and cost of extraction associated with its operation. Furthermore, fossil fuel is unequally distributed amongst different countries making it difficult for the most industrialised countries to meet their energy need while the countries with abundance of it does not have the technological skils to extract it from the ground (Abolhosseini et al., 2014; Somano & Shunki, 2016).

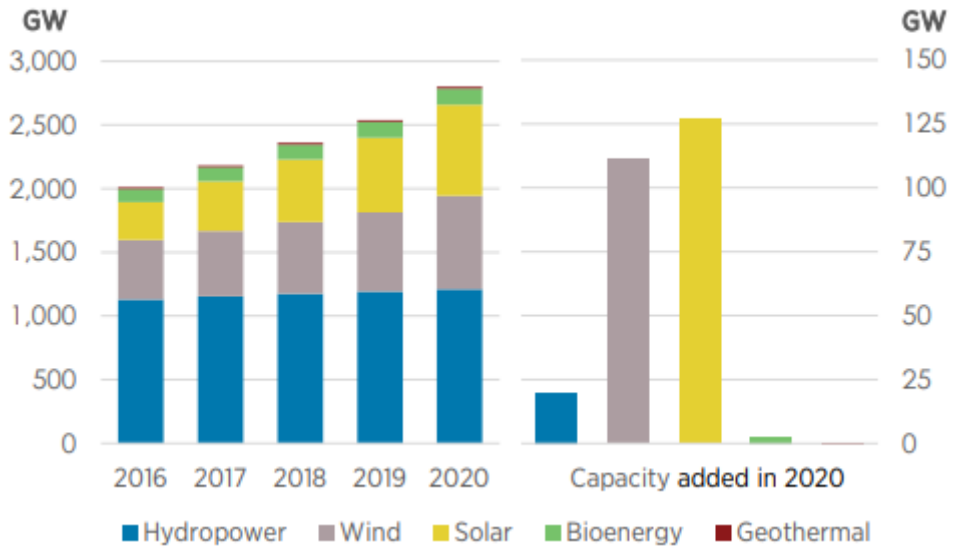

Figure 2.2 : Annual additions of Renewable power capacity, by technology and total, 2013-2019 (Somano & Shunki, 2016)

Again, renewable energy resources have demonstrated huge potential in meeting the global energy need if adequately managed for the common good of humanity. There is an ongoing debate amongst scholars and government officials on the viability of renewable energy as the primary source of power generation with the capacity to meet total demand. This debate is tilting towards renewable energy resources due to the obvious benefits and advantages it has over fossil fuel combined with the improvement in technology in recent years. Furthermore, research have shown that the total solar energy striking the earth hourly is equal to the total global power production from all fundamental sources for a year (Yang et al., 2014).

Recent research results have shown that an average of 1.1 billion people in the world are living without access to electricity while significant number are experiencing unstable power supply (REN21, 2020). All these together with concerns of environmental pollution, which is growing daily, has informed research in alternative forms of power generation and microgrid systems. Adequate implementation of renewable energy resources will open up a sustainable route for environmentally friendly and cost-effective power generation (Bajpai & Dash, 2012). Hence, effective design, implementation, operation and maintenance of DC microgrid system will definitely provide the much-needed alternative. Therefore, there is the urgent need to provide a brief literature on hydropower and solar PV as renewable energy resources. This will offer a detailed knowledge on the nature of these resources and suitability in DC microgrid system not failing to understand individual complexities during operation.

2.2.1 Hydropower

Hydropower is a form of renewable energy that is generated using the potential energy resident in water which travel from a region of higher potential to that of lower potential caused by gravitational force (Dhivya & Prabu, 2018). This form of energy has been in existence for the past century with significant development in technology and personnel. Electricity is generated by moving the stored water across turbines that activates rotation of the shafts that further energises electric generator. This type of technology is at an advanced stage with available skills needed to execute the conversion of water to electricity (Šćekić et al., 2020). Presently, hydropower is an exceptionally flexible power technology that has shown one of the best conversion efficiencies compared to other forms of renewables because hydraulic energy is converted directly to electricity. It has an operational efficiency or conversion of water to electricity of 90%. Because of the high efficiency it enjoys, hydropower has applications in different sectors such as mechanical power production, power generation industries, domestic applications, and used for textile processing. Regardless of its high efficiency, there is ongoing research in an attempt to improve its impact on the environment, reduce cost of operation, and adopt new environmental requirements (Swe, 2018; Somano & Shunki, 2016).

In rural areas or areas not connected to the electricity grid, hydropower plants are seen as the prime choice of power generation because it is cost effective, and water is readily available most time of the year without much drought. Hydropower technology is reliable, robust, and flexible with low operational and maintenance cost but huge initial investment including a favourable operational lifecycle (Somano & Shunki, 2016). Presently, hydropower generation is unstable as it changes from year to year determined by the installation capacity and changes in the weather patterns and other localised operating conditions. At the end of 2019, global electricity generation from hydropower was around 4,306 TWh, which represents an increase of 2.3% from 2018 or approximately 15.9% of the global electricity generation and represents 25% of total electricity from renewable energy resources as shown in figure 2.3 and figure 2.4, respectively (Swe, 2018; Somano & Shunki, 2016).

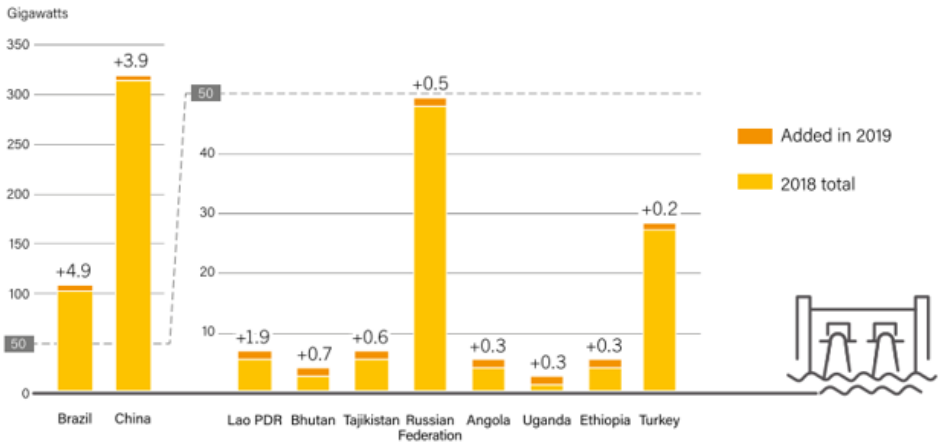

Figure 2.3 : Additions and capacity of Hydropower, 2019 top 10 countries for added capacity (REN21, 2020)

Hydropower is strategically positioned in the power generation and management sector providing energy managers the desired flexibility that would enhance proper regulatory services my evaluating maximum load demands hence, adding variable renewable energy resources in the anticipated energy mix of the future. There are three basic types of hydropower technologies available based on operation and type of water flow, reservoir hydroelectric plants, pumped storage hydroelectric plants, and run-of-river hydroelectric plants (Dhivya & Prabu, 2018).

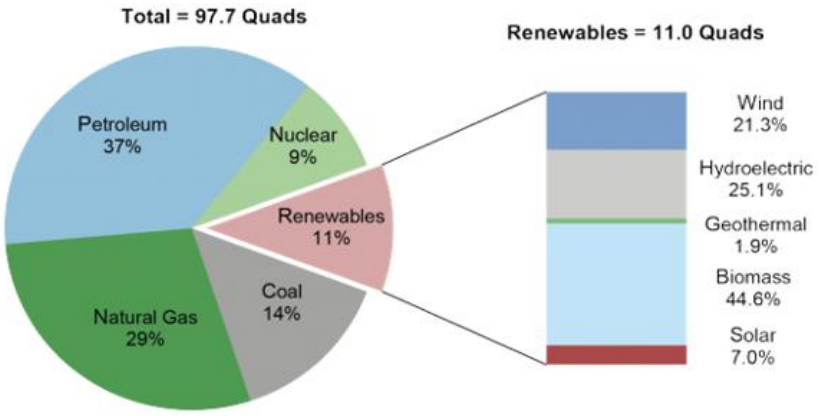

Figure 2.4 : Percentage of Renewable energy in global electricity production (REN21, 2020)

From figure 2.4, 1 quad is equivalent to 1 quadrillion BTU (British thermal unit) which is the unit used to measure energy consumption. Again, 1 BTU is the amount of heat energy required to increase the temperature of 454 grams of still water by 1℉ (REN21, 2020).

2.2.2 Solar Energy

This type of energy converts the sun's energy directly into electricity, provide heat, or hot water for general consumption. It can be utilised for water purification purpose, cooking, store food and medicines, and pump water. Solar energy is broadly classified into three categories: solar photovoltaic (PV), concentrating solar power (CSP), and solar thermal. All three technologies are well developed with significant number of installed capacities globally in the past two decades (Picco & lotero, 2019; Bhattacharjee & Nayak, 2019). Global solar PV capacity added in 2020 regardless of the Covid-19 pandemic was approximately 107 GW in the main case as shown in figure 2.5. In concentrating solar PV module, the sunlight is concentrated on smaller surface area and utilizes mirrors to produce electricity through direct-beam solar concentration of solar radiation trapped as heat. The accumulated and trapped heat triggers chemical reaction that produces electricity. The concentration or accumulation of heat is either implemented along a line (linear focus) through a linear Fresnel device or as a dish system (Ma et al., 2014; Yang et al., 2014), while solar thermal heating and cooling technologies uses the thermal energy of the sun to provide space heating, cooling, pool heating, and hot water for commercial, industrial, and domestic purposes (REN21, 2020; Ellabban et al., 2014).

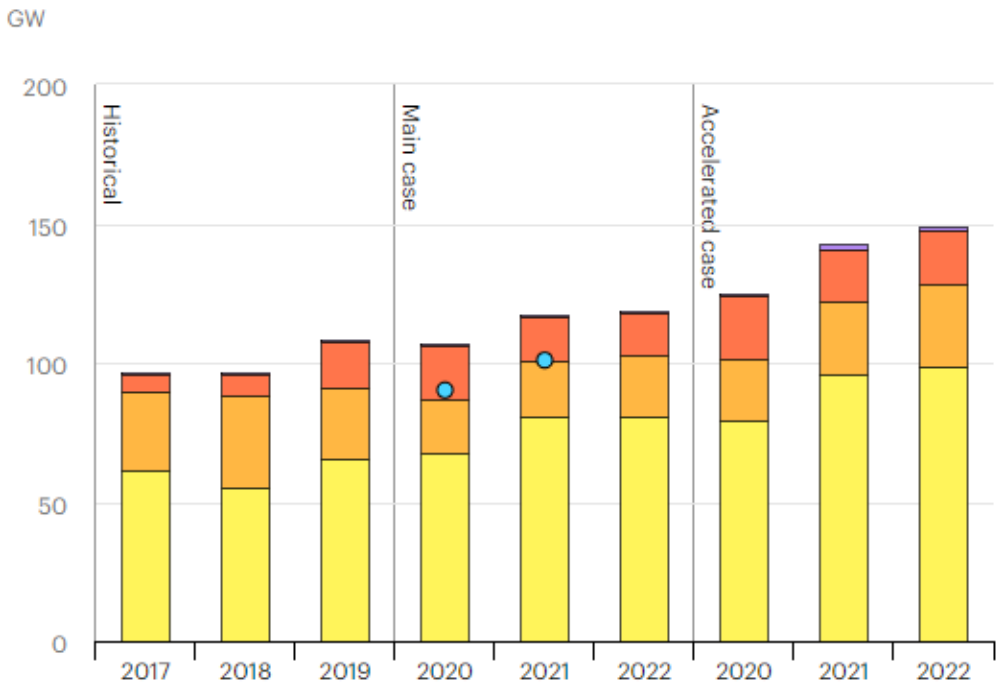

Figure 2.5 : Solar PV net capacity additions by application segment (REN21, 2020)

2.2.2.1 Solar photovoltaic (PV)

The basic structure of the PV system is the PV cell, a semiconductor device that converts the solar energy directly into electricity (DC). PV cells are connected in series, parallel, or series-parallel to form a module which might be between 50 to 250 W (Showers, 2019). These modules are further fused with other application dependent system components such as electrical devices, batteries, mounting parts, and inverters to create a complete PV system. Presently, silicon-based PV system is the most advanced and utilised PV system due to its high-power output and the chemical structure of the silicon device (Ma et al., 2015; Mahmoudimehr & Shabani, 2018).

Solar PV like other renewable energy sources is broadly classified into two major types: grid-connected and off-grid (standalone) power systems. In the past decade standalone (off-grid) systems have gained significant acceptance and utilisation in power generation especially in areas were connecting to the grid is not economically viable. Off-grid localised PV microgrid power system has become a workable alternative for most rural electricity needs because of the economic opportunities this type of application presents. Integrated and localised power systems possess somewhat technical advantages with regards to reduced storage needs, energy availability, electrical performance and changing characteristics of the system which has shown significant potential in becoming the most cost-effective power system for specific amount of service requirement (Singh, 2016; Swe, 2018; Ellabban et al., 2014; Eid et al., 2016; Bhandari et al., 2015; Philip et al., 2016; Aminu & Solomon, 2016). This type of system has the advantage of component and system optimisation of installation and operating costs by acquiring significant and cost effectiveness of the solar PV components and stability of the larger system. Furthermore, the robustness of centralised solar PV system is greater than distributed solar PV system due to the fact that they combine maintenance systems with monitoring devices which in most instances less than the cost of the entire system (Reddy et al., 2017; Mahmoudimehr & Shabani, 2018).

Solar PV modules have shown to have significant advantages over concentrated solar PV (CSP) and solar thermal PV. Some of such advantages are, solar PV can be produced in huge plants that provides avenue for scalability, reduced cost of production and flexibility. In addition, solar PV produces electricity through the direct conversion of sunlight and produces electricity during night because it uses the diffuse component of sunlight deposited on the silicon particles even when the weather is cloudy. This unique characteristics of producing electricity even without sunlight has created the platform for mass deployment of solar PV in most parts of the world where CSP deployment is not technically and economically feasible (Singh et al., 2012). Hence, in this study the solar PV system is used as the primary

renewable energy source to supply power to the load and recharge the pumped hydro system.

2.3 Energy storage systems

Researchers in the past two decades have been working diligently to provide stability in the current grid network, as it gets smarter. The effort has increased in the past decade due to the intermittent nature of power supply in the grid and the type of loads connected to the network (Connolly et al., 2012; Chen et al., 2009). This situation has informed the intentional drive for energy storage system. However, in microgrid, effective energy storage system can provide the needed stability such as improved power quality, smoothening the production of different power sources, offering energy boosting in the network and voltage control. Furthermore, having an effective energy storage system in a microgrid system will provide better level of flexibility especially, network with high level of renewable energy sources (Torres, 2015; Prakash et al., 2016). Integrating renewable energy sources such as solar PV and wind to existing grid network will create significant variations. Hence, to compensate for this fluctuation in power supply and to operate a reliable power network, it is necessary to strengthen the grid and at the same time establish a power backup system. The energy stored can be supplied to the grid in the event of power shortage using different technologies, depending on the form of energy at hand and cost effectiveness. The different technologies are broadly categorised into electrochemical, mechanical, electrical and thermal (Bhattacharjee & Nayak, 2019; Diaz et al., 2014).

2.3.1 Battery Energy Storage System (BESS)

Battery energy storage system over the century have been the standard of electrochemical energy storage technology (Šćekić et al., 2020). A standard electrochemical battery consists of one or more electrochemical cells with each cell having a liquid, paste, or solid electrolyte in combination with both negative and positive electrodes as shown in figure 2.6 (Hesse, 2017). Electrochemical reactions take place in both electrodes during discharging by generating a flow of electrons triggered by an external circuit. However, these batteries are rechargeable through the application of external circuit over the electrodes hence, making these reactions reversible. This unique characteristic makes electrochemical batteries suitable for large electrical energy storage in grid-connected and off-grid applications. However, one of the major drawbacks of electrochemical batteries is the energy density and power density ratio which several studies have been carried out in the past century with several still ongoing with the focus of increasing the ratio between the energy and power densities (Showers, 2019). The search to improve the energy and power density ratio has

resulted in the introduction of various battery technology topologies in the past two decades based on the type of electrolytes. However, lithium-ion based battery is the most technologically advanced at the moment but still not economically viable in large-scale power system applications and storage. Batteries also have fast response time and high reliability making it highly suitable for smart grid application even as the more renewable energy resources are integrated into the grid network. In addition, batteries are harmful to the environmental because of the toxic contents in it and also have high degradable charge and discharge rate (Siad, 2019; Chen et al., 2009; Torres, 2015; Ma et al., 2015).

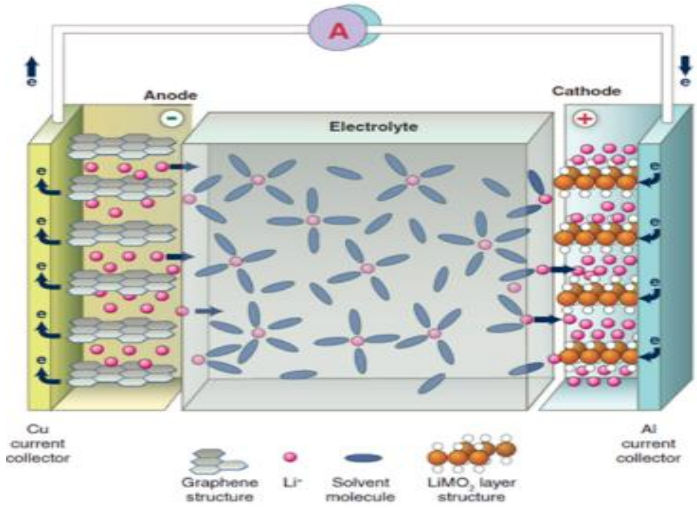

Figure 2.6 : Lithium-ion battery (Hesse, 2017)

2.3.2 Flywheel Energy Storage System (FESS)

The energy in a flywheel energy storage system (FESS) is stored by accelerating a rotor to a high speed and stored in a kinetic form. Flywheels store kinetic energy and does not generate potential energy (Subkhan & Komori, 2011). This process is reversed by utilising the motor as a generator when the flywheel releases the stored energy. However, this reversal process continues until the stored energy is completely released. Weight is seen as a major problem in implementing this technology hence, improved organic materials are seldom used for the rotor during exceptionally high-speed operations. Flywheels have high charging and discharging abilities and not susceptible to temperature changes thereby making it suitable for frequency regulation and power quality control. Flywheels occupy very little space as shown in figure 2.7, have increased lifespan, not affected by deep discharge, and requires less maintenance compared to other types of energy storage technologies. FESS was initially intended for applications in the aerospace and automobile industries but later finds its applications in the power sector because it is cost effective, respond rapidly,

has high reliability, and enhances power quality (Prakash et al., 2016; Torres, 2015; Baboli et al., 2014).

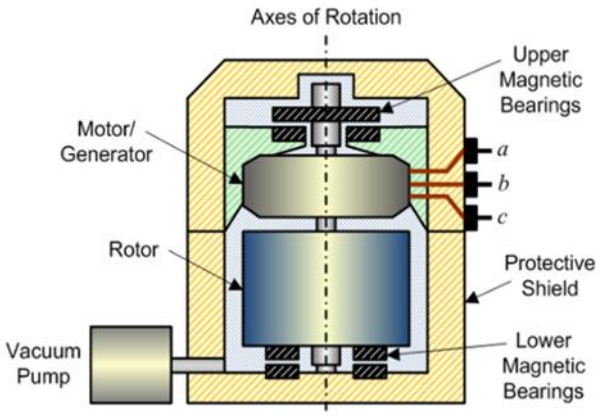

Figure 2.7: Flywheel (Torres, 2015)

2.3.3 Supercapacitor (SC)

Supercapacitors (SCs) are known to be amongst the most effective and direct technology for electrical energy storage. SCs are made up of modules of single cells connected in series and arranged in parallel with other modules in combination with two metal plates separated by a dielectric material (non-conducting material) as shown in figure 2.8 (Aneke & Wang, 2016). The energy generated is either absorbed or supplied to the grid in a grid connected system using a DC/DC bidirectional converter. However, the supercapacitor capacitance which is the capacity of the SC is basically determined by the load demand including other factors (Benavente et al., 2019). Again, one of the plates usually induces a negative charge when the other is charged with electricity thereby ensuring that the plates are either positively or negatively charged at all times making it suitable for short-term storage applications. SCs are developed for energy storage during peak hours, charges faster than standard electrochemical batteries, and can be cycled several thousands and still maintain high efficiency. The main advantages of SCs are less weight, high cycle efficiency, fast rates of charge and discharge while the disadvantages are low energy density and high cost of production (Siad, 2019).

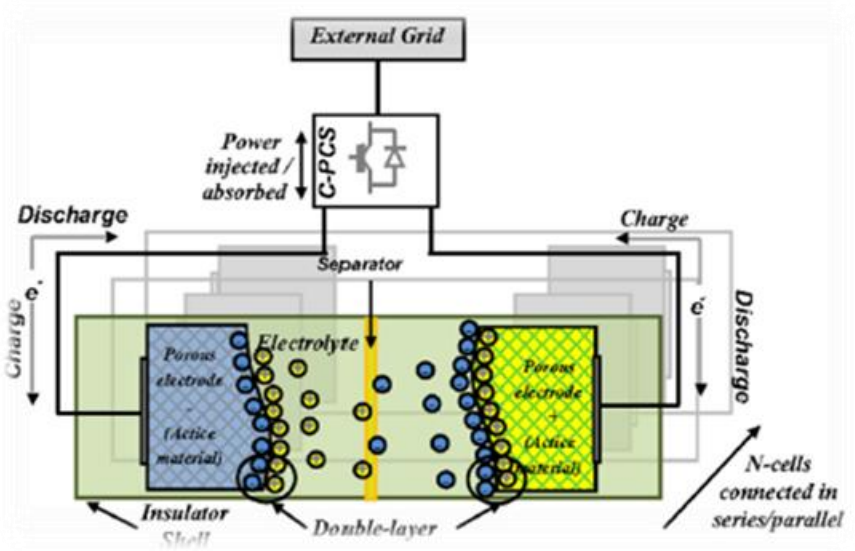

Figure 2.8: Supercapacitor Energy Storage technology (Aneke & Wang, 2016)

2.3.4 Pumped Hydro Storage (PHS)

According to Bhattacharjee & Nayak, (2019) PHS is the largest and oldest form of energy storage technologies available. It was mostly used in the older grid network and it has two big water reservoirs stationed at different elevations as shown in figure 2.9. Water is normally pumped from the lower reservoir to the higher reservoir during off-peak periods to ensure that the surplus energy from the grid is stored in the reservoir. During peak hours, the water stored in the higher reservoir is sent to the lower reservoir through a hydraulic turbine thereby generating electricity. PHS is suitable for long term energy storage because it has low self-discharge rate, extended lifecycle, low cost, and high efficiency conversion rate. However, the main disadvantage of this technology is that it requires the destruction of trees and related ecosystems because of its low energy and power densities. For stand-alone microgrids, there are presently small hydro schemes of few kilowatts and megawatts depending on the size of the network and the load demand (Bhattacharjee & Nayak, 2019; Alam et al., 2017; Rehman et al., 2015).

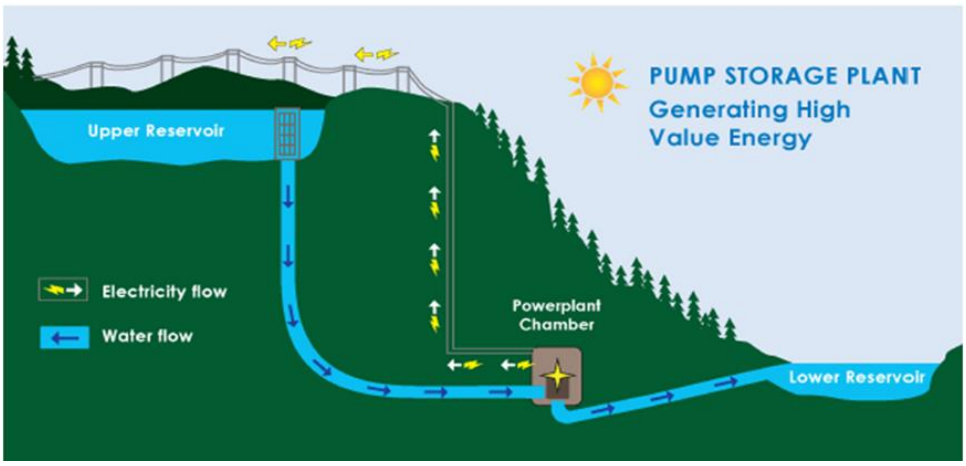

Figure 2.9: Pumped hydro storage system (Bhattacharjee & Nayak, 2019).

2.3.4.1 Solar-PV pumped hydro storage system

As highlighted previously, modelling of a solar-PV pumped hydro storage system is very complex but vital because it ensures optimisation and increases efficiency (Baboli et al., 2014). The system usually consists of a solar-PV (power generator), pumped hydro storage reservoirs (energy storage subsystem), loads (end-users), and a dedicated control system as shown in figure 2.10. The control station is the heart of the system, making it the most vital component of the whole system because it is saddled with the responsibility of energy distribution and management. Having an effective energy management system will ensure that the whole system is operated optimally. However, when the power generated by the solar-PV is greater than the load demand, the excess power is used to pump water from the reservoir at the lower elevation to the reservoir at the higher elevation hence storing gravitational potential energy as shown in the figure 2.10a. However, during peak hours, the water from the higher reservoir is released to flow downwards through the turbine as shown in figure 2.10b. This process ensures the availability of water both day and night thereby eliminating environmental problems associated with electrochemical batteries but with little conversion losses in the system (Ma et al., 2015).

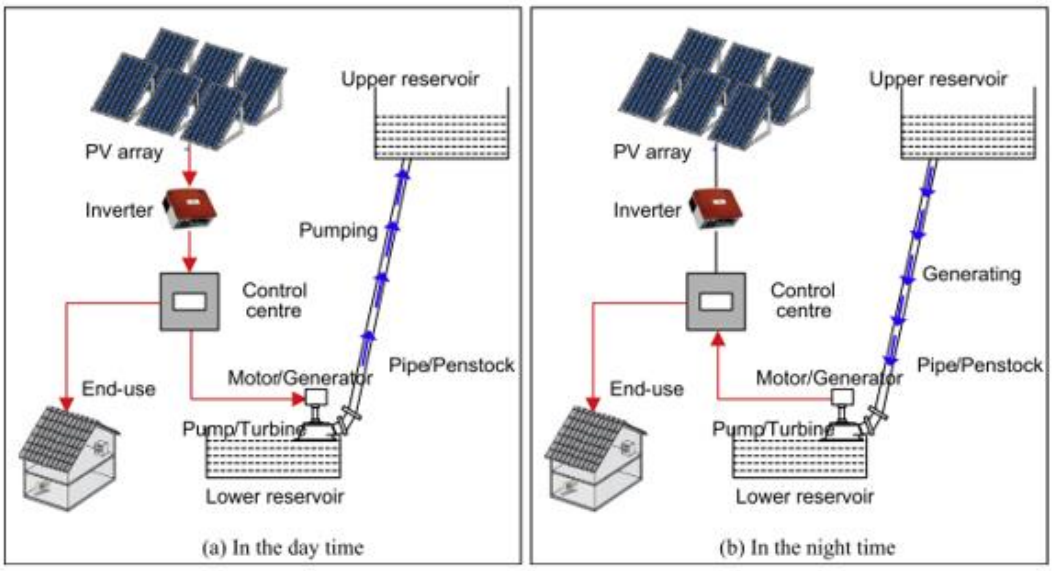

Figure 2.10: Solar-PV based standalone PHSS (Ma et al., 2015)

In this study, a pumped hydro storage (PHS) system is used as the energy storage system because it has the potential to reduce harmonic distortions as well as regulate the challenges of voltage drops associated with other energy storage systems. PHS has a very long lifecycle that produces regular electricity created by the continuous water circulation that can be used to supplement power supply during high load demand hours and frequency regulation in a microgrid system. It has a relatively high efficiency and quick response time that is coupled with its ability to supply power to the grid in grid connected network. This makes it an ideal energy storage option capable of providing power during peak hours. PHS has low operational and maintenance cost and the least in lowest levelized cost of electricity (LCOE) compared to other energy storage technologies.

CHAPTER 3: DC MICROGRID SYSTEMS

3.1 Introduction

A microgrid (MG) is composed of different components and generally, MGs are classified according to the type of sources, storage, loads, and interconnection to either grid or off-grid. In this study, the primary power source is a photovoltaic (PV) system, and the secondary power source is a pumped hydro storage system while the load is a DC load. Conventional power systems are generally centralised to include large power generation plants that transfers electricity to consumers over long transmission lines (Ellabban et al., 2014). Hence, DC microgrids (DCMGs) are designed to replace or complement these existing power systems that consist of large nuclear and fossil fuel plants to provide a more energy sustainable and environmentally friendly power system. These are usually small power systems that comprises distributed energy sources, storage systems and loads that can function whilst connected to the grid or as standalone power systems. They provide power stability by ensuring that the power generated is equal to the amount consumed at all times by using energy storage systems and other power electronic devices within normal operating conditions (Zhang et al., 2018; Hinov et al., 2016; Singh, 2016). DCMGs are grouped into various categories according to type such as residential, campus, commercial, industrial and military, according to size such as small, medium and large systems, according to application such as reduced losses, stability focused and power quality according to connectivity such as grid-connected and off-grid. Furthermore, a DCMG can be classified using the type of currents and voltage and distribution network as either monopolar, bipolar or homopolar (Lotfi & Khodaei, 2017a). The concept of a typical DCMG system is shown in figure 3.1.

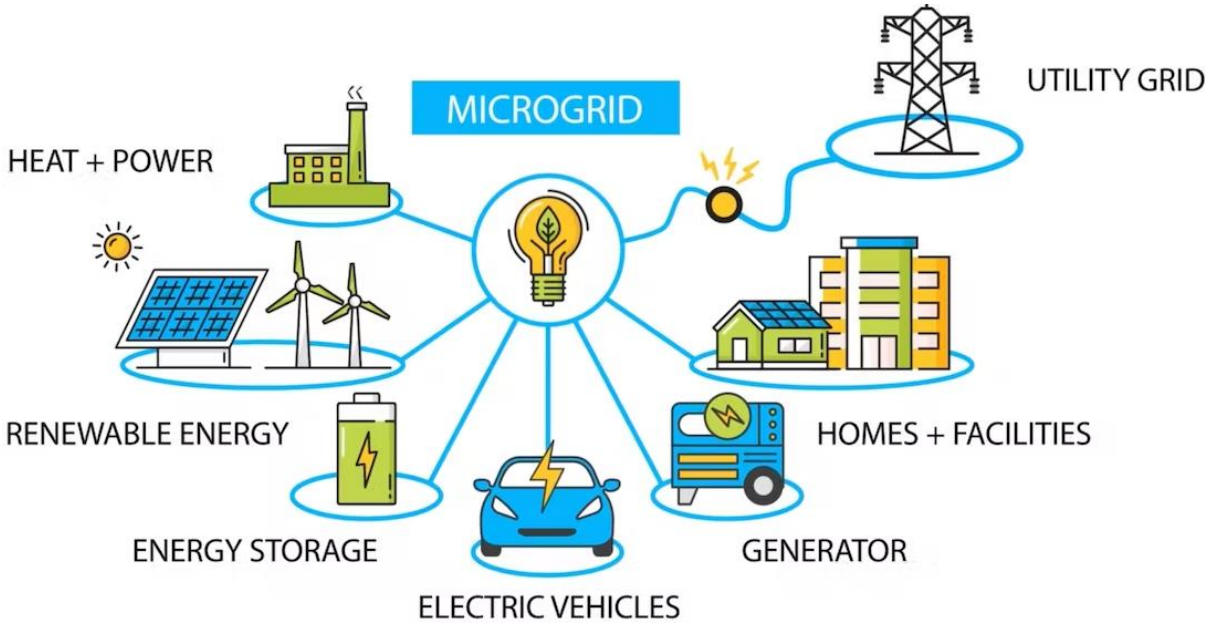

Figure 3.1: A typical microgrid structure (Siad, 2019)

"A microgrid is a group of interconnected loads and distributed energy resources within clearly defined electrical boundaries that acts as a single controllable entity with respect to the grid. A microgrid can connect and disconnect from the grid to enable it to operate in both grid-connected and island-mode." (U.S. Department of Energy Microgrid Exchange Group, 2011, p. 1)

Distributed power generation systems are gaining popularity due to increasing energy demand (Kakigano et al., 2013). According to Aneke & Wang, (2016), high reliability, remote electrification, low distribution losses, reduced chances of blackout and easy scalability are some of the key advantages of distributed systems. Zhou & Ngai Man Ho (2016), review microgrid architectures and control methods, individual structures of DC, AC and hybrid microgrid were studied and analysed. The results showed that AC MGs were dominant due to their long historical technology and power component availability, while DC microgrids were classified first due to improved and better power quality, efficiency, and control flexibility (Zhou & Ngai Man Ho, 2016). The above mentioned findings were supported by Wang et al (2015) in his study on a similar topic where a number of control methods in AC and DC microgrids were analysed and compared. As a result, each control method exhibited a unique advantage in different MGs depending on the topology, scale, system architecture and application. Therefore, this chapter provides a general overview of DCMG system including DCMG architecture and different control strategies and techniques used in DCMG systems.

3.2 DC Microgrid system

In DC microgrid system, all the distributed energy resources (DERs) are connected to a common DC bus then supplied to DC loads (Siad, 2019). AC-to-DC rectifiers are used to connect the AC generating systems and all energy storage systems to the common DC bus then supplied to the DC load as shown in figure 3.2 (Gao et al., 2019).

A typical DCMG configuration is a combination of microsources and corresponding loads that functions as a single system offering both electricity and heat with most of the microsources in the system as power electronic based devices that offers the necessary flexibility that will ensure the regulated system functions as a single combined system (Shehadeh et al., 2019). A DCMG usually consists of one or multiple microsources and several customers in a specific or confined geographical location (Lu et al., 2014). The integration of different sources of power to the DCMG provides energy autonomy for regional power generation and consumption while the MG is operated in low or high voltage.

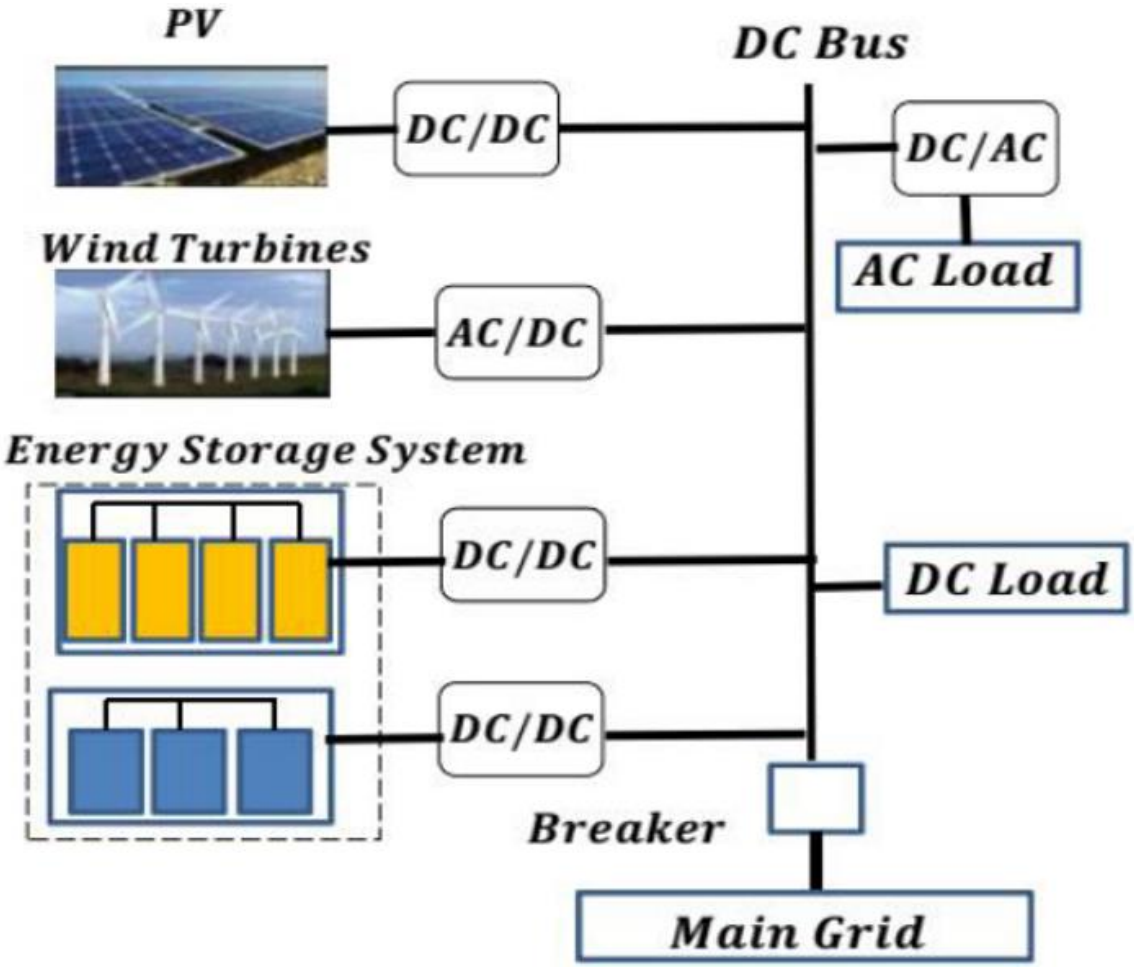

Figure 3.2: DCMG system (Gao et al., 2019)

However, the primary purpose of this regulated flexibility is to ensure that the DCMG system is presented to the large power system as a regulated unit in a manner that meets the electricity needs of consumers within established constraints. These needs will ensure developed localised sustainability and necessary power stability because DCMGs have control mechanism for each microsource that manages the power flow and operational voltage (Lotfi & Khodaei, 2017a; Lotfi & Khodaei, 2017b; Siad, 2019; John, 2017; Kumar, 2016).

DCMG is normally operated within a small geographical area and the distribution length is shorter than conventional AC distribution lines. Hence, DCMG systems are considered and treated as resistive networks (Augustine et al., 2018). The operation of DCMG system is different from conventional power system generators as it uses power converters such as DC-DC, AC-DC, DC-AC to integrate the microsources like fuel cell, small turbines, solar PV, biomass etc., energy storage devices and DC loads. The different microsources and corresponding converters used in a DCMG system provides less physical inertia thereby affecting the system stability (Blasi, 2013).

3.2.1 DC MG topologies

Assessing the DCMG connection using the different DERs and loads, DCMGs can be broadly categorised into three topologies (Augustine et al., 2018):

3.2.1.1 Single-bus DCMG

The single bus DCMG topology, which is also referred to as radial, or feeder structure is the fundamental topology and the most implemented topology in DCMG system due to its design simplicity and configuration. The topology has a single DC bus where all the microsources, energy storage systems and loads are connected directly or via a power converter. This topology is scalable and other types of configurations can be built on a single bus topology with the ease that it presents. A simple bus topology having different energy sources and an energy storage system is shown in figure 3.3. This topology is very effective for Low voltage (LV) DCMG systems and its reliability can be improved by adding more energy storage systems (Kumar et al., 2019).

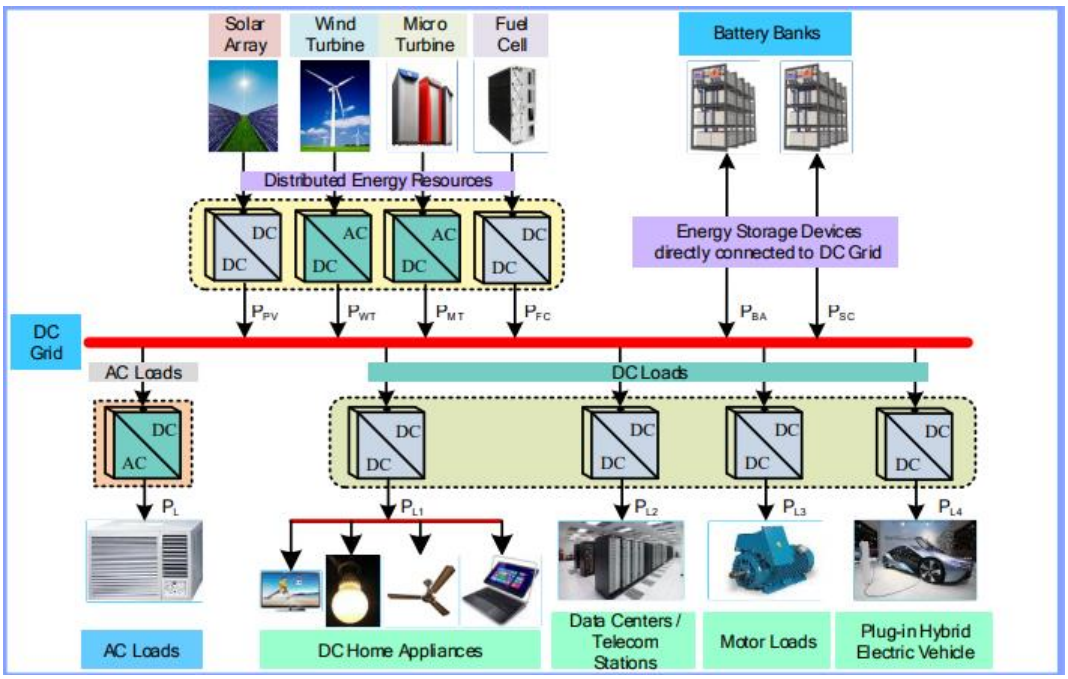

Figure 3.3: A single bus DCMG topology (Augustine et al., 2018)

This type of configuration has been commonly deployed to power telecommunication devices in the past decade due to voltage stability including shorter transmission lines. Again, this topology can be used to regulate the DCMG voltage and make it more flexible to adopt multiple microsources. The energy storage system can be connected directly to the DCMG while the voltage is regulated using the battery state-of-charge (SOC). This configuration requires systematic design and evaluation of the different power converters and other control components to ensure stability where additional energy storage system can be integrated to the DCMG through the DC-DC power converters (Augustine et al., 2018; Jia & Tong, 2016). In this topology, a failure in any of the source interface would not trigger total power failure due to the presence of other sources within the DCMG network.

3.2.1.2 Multi-bus DCMG

In a multi-bus DCMG system, the configuration can be either series or parallel and the power is shared amongst the various MG systems within the network as shown in figure 3.4. This type of configuration supports the disconnection/isolation of a faulty MG within the network where the communication part between the DERs are employed to exchange control parameters that will enhance performance and stability of the DCMG system (Shafiee et al., 2014). Again, DCMG system with multiple buses is more reliable because it provides the option of reconfiguration during faulty situation and prioritise sensitive loads within the system. This configuration is flexible and provides different voltage levels to different consumers based on their power demand thereby making it suitable for both low and high voltage consumers. While this is an extended version of the single-bus DCMG topology, it is more accessible with enhanced reliability (Blasi, 2013; Ma et al., 2016).

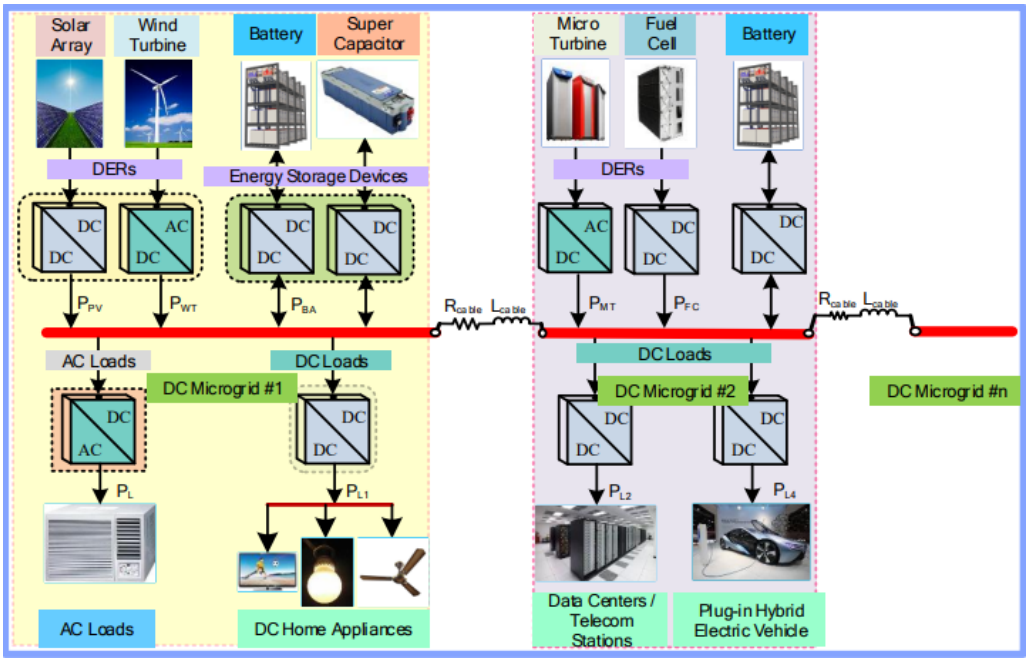

Figure 3.4: Multi-bus DCMG configuration (Augustine et al., 2018).

3.2.1.3 Reconfigurable DCMG

Reconfigurable DCMG topology is broadly classified into mesh and ring configurations (Lotfi & Khodaei, 2017b). Mesh type configuration offers the best flexibility and improves redundancy by providing several other connections to all the nodes within the network. These are intended to provide support for the basic purpose of redirecting power during failures to a major line. However, it makes it difficult to provide adequate protection for the microgrid because it is usually connected at high or medium voltage levels (Ma et al., 2015).

Although, distribution systems provide compensation for the three phases and the period of peak power output is evenly distributed between all phases providing a more stable peak power output. In addition, mesh configuration is the most complex configuration because of the multiple power sources, several connections between nodes, and the task to maintain effective power distribution. This is the fundamental reason why mesh uses existing configuration for its operation without installing new network (Prakash et al., 2016; Zhang et al., 2018). Mesh configuration is effective in short distance transmissions, it is cost effective, has high reliability and control over fluctuating power generation and provides a balanced voltage profile.

Another type of reconfigurable DCMG topology is the ring-based configuration. In this configuration, the DCMG system is divided into zones and made up of lines that produce a geometrical loop or ring shape which ensures the flow of power from two different directions to any path of the network as shown in figure 3.5. This configuration when properly implemented provides improved voltage stability and reduces power losses, but at the same time needs improved protection system (Siad, 2019; Bevrani et al., 2014).

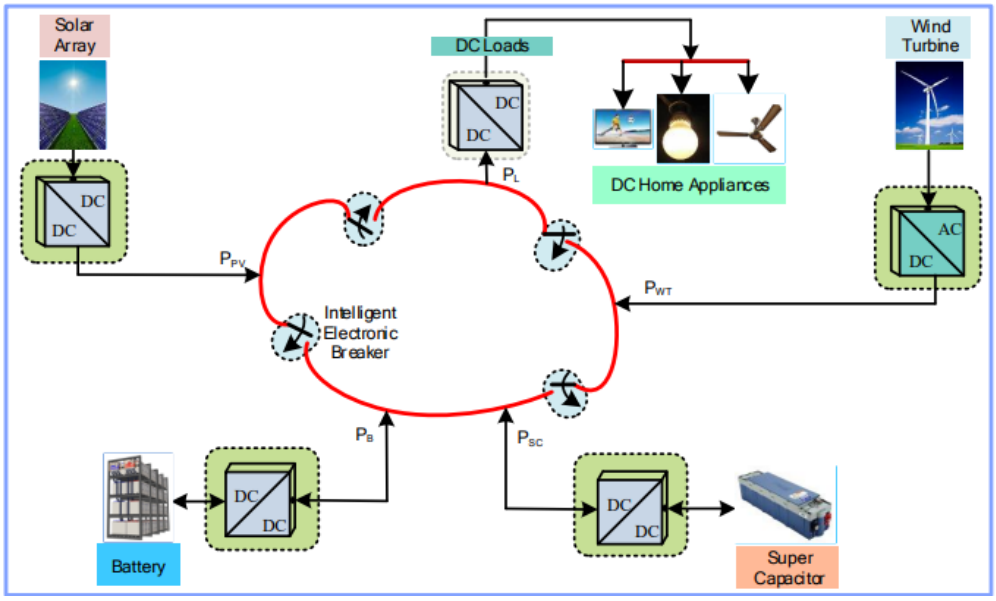

Figure 3.5: Ring DCMG configuration (Siad, 2019)

Energy storage system provides much needed stability in grid-connected renewable energy resources when the power supply is less than the load with combined support for Distributed Generation (DG) power capacity. MGs enhances the power capability of the grid, reduces the amount of CO_2 produced, decreases power losses in the power distribution network, improves grid stability, it can be used for ancillary services such as voltage and frequency regulation and it reduces the huge investment cost required for transmission and distribution

networks (Ma et al., 2015). Again, MGs have shown to be the perfect and suitable method of integrating distributed generation into the grid network. This is informed by the high flexibility and power stability capacity exhibited by MGs (Alanazi et al., 2017). Furthermore, there are several opportunities and notable benefits of integrating distributed generation resources into the MG network for utility operators and electricity consumers at residential, commercial, and industrial levels. Implementing MGs will benefit utility operators by ensuring maintenance without disrupting supply to consumers, reduce electrical stress on the transmission and distribution lines and permit dispatchable load during peak hour. Operating MGs in island mode have the capacity to reduce the negative impact of defects on the upstream network. Although, this approach will require a control mechanism, an effective communication structure, and a reliable protection system that will disconnect faulty sections and offer reliable independent system (Lotfi & Khodaei, 2017a). Achieving the above will ensure stable power supply to users, secure the distribution network, and provide required performance using generation redundancy.

DCMGs in the past ten years have experienced significant technology growth and improvement. Again, a substantial increase in the number of DC appliances and loads such as LED lights, telecommunication devices, consumer electronics and shortage of other devices operated within the 50 Hz and 60 Hz AC systems coupled with enhanced technology in the past decade have the capacity to position DCMGs as the prime solution to the energy needs of the future (Ma et al., 2016). DCMG system as against ACMG system provides improved efficiency and reduced power losses because DC loads does not require inverters, bus ties in DCMG systems are operated without using synchronizing buses and DCMGs reduces over reliance on fossil fuel-based energy sources thereby reducing greenhouse gas emissions. In addition, DCMGs have improved power quality due to reduced number of power converters, DERs such as solar PV, fuel cells, and energy storage systems are easily connected to the common bus using enhanced interfaces, DC loads such as electric vehicles and general DC powered consumer electronics are effectively supplied and synchronising generators which allow rotary generating parts operate optimally are eliminated (Lotfi & Khodaei, 2017a; Augustine et al., 2018). A DCMG is either off-grid or grid-connected as indicated in section 3.1 but, this study focuses only on off-grid DCMG because of the advantages that it has over an AC grid-connected microgrid system.

3.3 DCMG control

Present DCMG system has different levels of control (primary, secondary and tertiary) according to the International Society of Automation-95 (ISA 95) standard (Shafiee et al., 2014). Unlike the ACMG system that considers frequency and voltage, the control in a

DCMG system considers a single parameter. This provides an obvious difference between both systems where the DCMG control algorithm is easier to implement. DCMG control configuration is a key component that ensures improved stability and efficient operation of DCMG system and broadly classified as shown in figure 3.6 (Siad, 2019) Again, power electronic converters functions as the interface between the different sources and the load in a DCMG system. It also ensures effective control of the grid parameters such as voltage and current distribution. Hence, having an effective control mechanism reduces the non-linearity effect that is associated with power converters because of the constant power characteristics that it possesses. However, control system has become more complex in recent years due to intermittent power sources and loads in a DCMG system (Smith, 2014).

In addition, having an effective power management system in a DCMG system is an integral component that will ensure balance between power generation and consumption in order to operate optimally. This phenomenon is becoming common as power from renewable energy resources increases and applies to utility grids, grid-connected and off-grid networks. To maintain power stability and ensure adequate frequency regulation in a utility grid or MG, generators and storage system are utilised (Gao et al., 2019). In the past decade, DCMG has gained popularity because of its high efficiency and the capacity to provide better power quality. This is partially because of the absence of frequency regulation and reactive power quality issues which are seen to be major problems in ACMG (Ma et al., 2015).

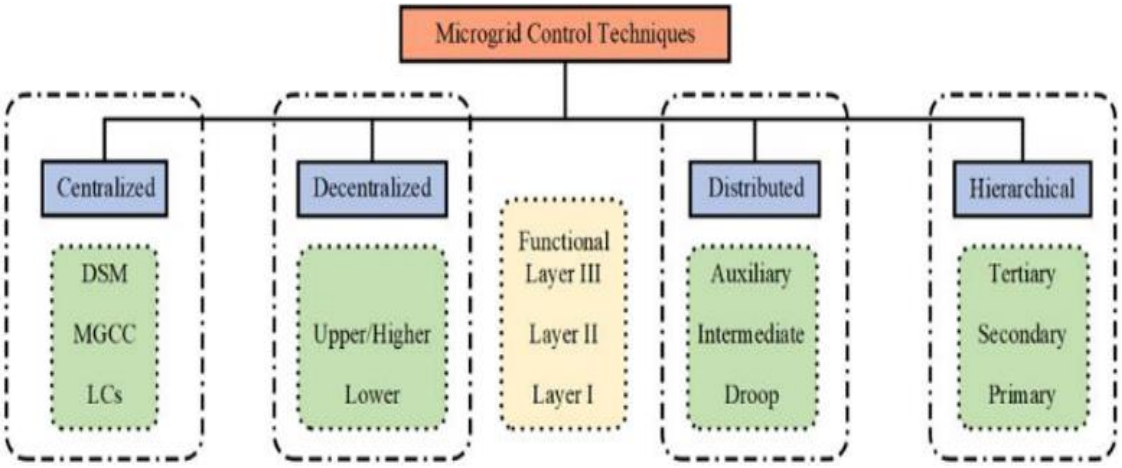

Figure 3.6: Classification of MG control techniques (Siad, 2019)

3.3.1 Model Predictive Control (MPC)

Using previous and present information of a MG system, MPC make predictions of the future and anticipated outcome within an established set of rules with the aid of a quadratic cost function and component categorization based on tested MG system (Bagyaveereswaran et

al., 2016). It reduces the error associated with predicting an outcome while concentrating on trailing a perfect current parameter (Torres, 2015). Aiming at achieving a stable power system, the model predicts anticipated values required for the envisioned MG system using present values of the different components within the system. This technique is based on a diminishing horizon control set of rules with an embedded predictive system that is implemented by initially establishing the optimal input parameters over a predictive zone that is aimed at reducing the primary function of established operational restrictions. After achieving and implementing the initial parameters of the obtained optimal parameters in real-time, the entire prediction horizon is set ahead and the process repeated until the desired result in achieved. However, this method is complex and vulnerable to natural interference because of the complex mathematical equations associated with its implementation (Hu et al., 2021). Figure 3.7 presents the block diagram of a typical MPC with different input constraints and aims as the primary input to the controller which is determined by the control signal modelled for the actual system.

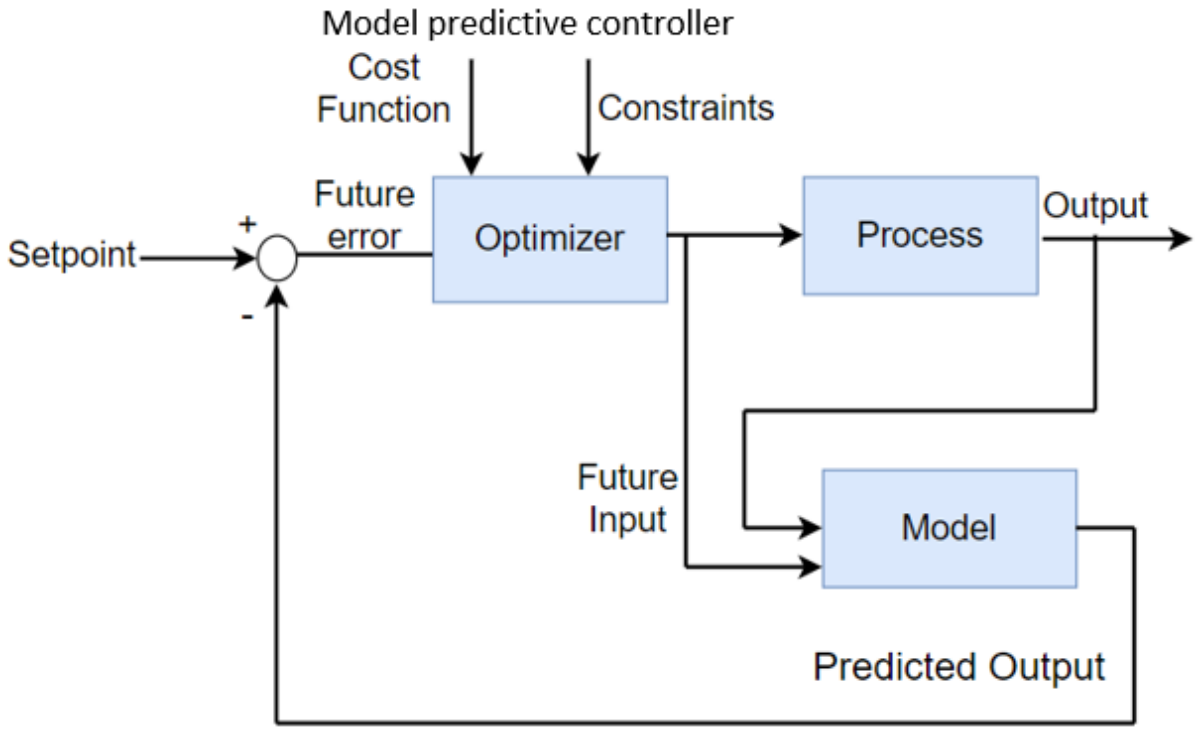

Figure 3.7: Basic structure of a MPC (Bagyaveereswaran et al., 2016)

3.3.2 Maximum power point tracking (MPPT) control

MPPT control techniques are mostly implemented in huge power generation stations including photovoltaic plants and wind turbine generators because of their intermittent nature (Showers, 2019). The amount of power generated by a solar photovoltaic is determined by the environmental conditions, solar irradiation, and temperature while that of a wind turbine

is determined by the wind speed and other atmospheric conditions (Torres, 2015). However, in microgrid network, MPPTs are utilised at the local converter level for effective optimisation and best impact. MMPT controller is used to indicate the maximum operating point of renewable energy sources such as solar PV by extracting the maximum power from the resource as shown in figure 3.8. Some of the techniques used in the MATLAB environment to indicate the maximum point of a solar PV are Incremental Conductance (IC) method, Fuzzy Logic method, Perturb and Observe (P&O) method, and Artificial Neural Network method. This is the point in the V/I characteristic of a PV string where the value of P and V equals zero (Dragi & Guerrero, 2016; Zhou & Ngai Man Ho, 2016).

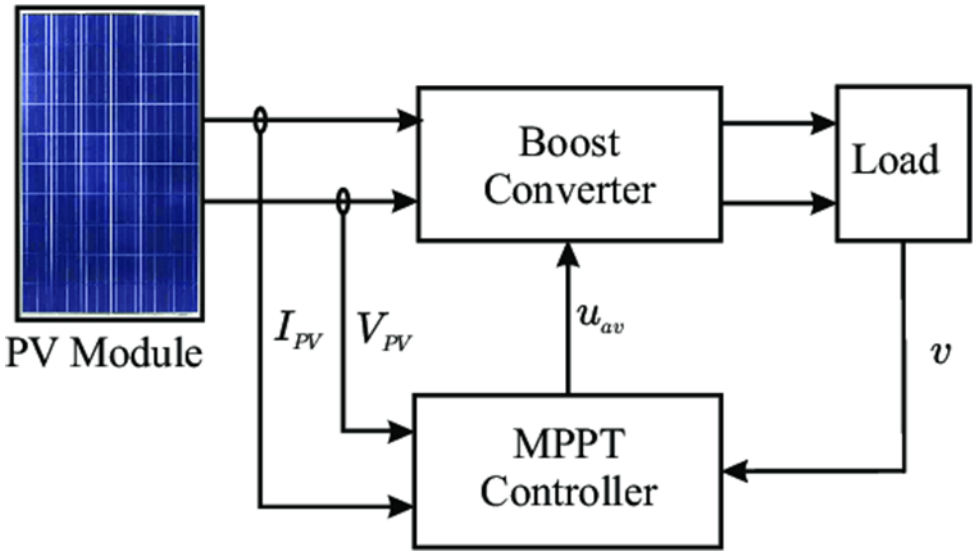

Figure 3.8: PV system under MPPT controller (Gil-Antonio et al., 2019)

3.3.3 Hysteresis control (HC)

Hysteresis control technique is mostly utilised in grid-connected networks or for power factor correction (PFC) applications because of its fast dynamic response abilities, which ensures increased power quality of the grid and load (Han, 2014). In addition, as current oscillate between the lower and upper regions of a band and combining the disadvantages of variable frequency, hysteresis control is used to set operational boundaries that will maintain power stability and appropriate load distribution. Again, HC technique can be used for frequency control and other ancillary services in grid connected VSI applications due to its fast dynamic response (Aminu & Solomon, 2016).

3.3.4 Fuzzy Logic Controller (FLC)

Fuzzy logic controller is a logical controller that communicate and deals with different linguistic values with one another while removing the logic complexities associated with

values common in decision making. It translates the human experiences and reasoning into a set of conditional statements (Cordón, 2011). FLC provides quantitative expression between zero and one for a specific parameter. The process starts with input parameters referred to as “fuzzification”, then fuzzy inference which is where the input parameters are processed and end with an output referred to as “defuzzification” as shown in figure 3.9. The fuzzified input parameters are fed into the fuzzy inference stage to evaluate the fuzzy rules that are stored in the fuzzy rule base and the Deffuzzifier transforms the inferior engine’s fuzzy package into a crisp value. Hence, the Deffuzzifier produces an out signal based on the received output signal. However, the level of complexity or crisp feedback is determined on individual fuzzy collection introduced in the first step (Velázquez-Abunader, 2013; Zhang et al., 2014; Kakigano et al., 2013).

For any transformation process, different membership functions are utilised depending on its suitability for that specific application. Its performance is defined using membership duty and fuzzy set of rules and conditions at the level of fuzzy thinking (Reddy et al., 2017). Fuzzy logic (FL) does not depend on complex mathematical model of any control system but possesses the capacity to handle multi-domain and non-linear configurations that are common in DC MG systems (Chauhan et al., 2015). Fuzzy logic controller is widely used in microgrid control and stability because it is extensively robust and user friendly. Furthermore, fuzzy logic controller has been widely utilized for the minimization of overshoots and enhanced tracking performance due to its simple decision-making characteristics (Bharath et al., 2019).

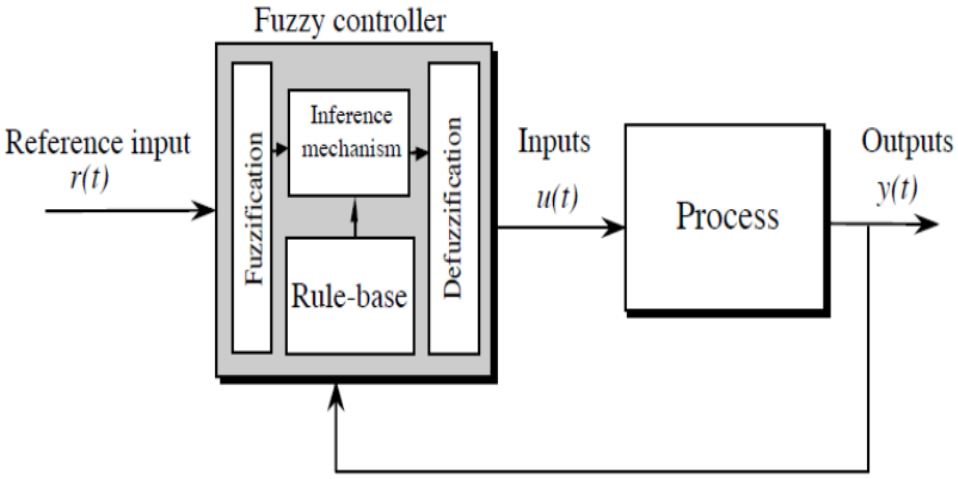

Figure 3.9: FLC architecture (Vijayaragavan, 2017)

In this study, the fuzzy logic controller must always consider the water level in the reservoir and the discharge rate. The load demand is not the only critical factor to be considered by

the FLC but the water level in the reservoir as well. It is obvious that the reservoir cannot accept water when it is full up to 80% of its capacity and cannot discharge water when it is less than 20% of the capacity. Hence, fuzzy logic controllers are most appropriate controllers for this type of condition due to its robustness. Fuzzy logic controller uses human expertise, fuzzy characteristics, and experiences to control the system against other controllers where the behaviour of the system must be precise for it to function properly. Although, when designing a fuzzy logic controller for any system such as the DC MG system, the designer must ensure that the system is controllable and noticeable. This is because fuzzy logic controller offers high flexibility and efficiency. It also provides a proper process of expressing, controlling and executing a result close to human heuristic precision (Zhang et al., 2014; Kakigano et al., 2013).

The choice of fuzzy logic in this study was informed by the fact that it is cheaper to develop compared to other conventional controllers, it has no effect through parameter changes, it can easily be reconfigured, it can be implemented on both small and large non-linear power systems and implemented on a wider operating situation. In addition, FLC provides effective solution to complex problems, the logic is robust and simple, it can handle multiple input variables and make a precise decision with the aid of the precise function. Generally, FLC is seen as an artificial decision maker that functions in a closed-loop system in real-time that is flexible and robust with four primary components as follows (Bharath et al., 2019):

- Rule base: This component houses the knowledge that is programmed as a set of rules trained on how to control the system.
- Interference: This is the component that accesses the relevance of all the controls at any specific time and then decides the type of input to the plant. It uses membership functions, logical operations and “If then” conditions in arriving at a particular decision. These can be expressed in shapes such as Gaussian, Trapezoidal and Triangular.
- Fuzzification interface: This stage processes the input variables into a form that can be decoded and compared to the set of rules established within the rule base. It basically produces an output fuzzy set based on the established set of rules.
- Defuzzification interface: It converts the changes arrived at this level by the inference interface to an acceptable input to the plant. In this study the centroid method was used due to its simplicity as compared to others.

CHAPTER 4: SYSTEM DESIGN AND METHODOLOGY

4.1 Introduction

This chapter presents the modelling of a hybrid solar PV–hydro controller for an autonomous DC microgrid and the proposed fuzzy logic controller algorithm in the MATLAB/Simulink environment. The modelling and selection of appropriate values for the different components of the DC-MG is important to ensure effective control and operation of the system. Hence, this chapter provides the methodology of modelling the photovoltaic system, the DC-DC boost converter, DC-DC bi-directional converter, energy storage system (pumped hydro storage system), the primary and secondary loads and the fuzzy logic controller. The research design that covers the fundamentals of the study together with all variables and set conditions are presented in section 4.2. The modelling of the photovoltaic system together with its particular control mode including calculations and power rating is presented in section 4.3. In section 4.4 is the design process of the DC-DC boost converter showing formulae and calculations used. The energy storage system (pumped hydro storage system) similar to a battery is presented in section 4.5 and the load profile in section 4.6. Lastly, section 4.7 presents the fuzzy logic controller algorithm, where the fuzzy logic controller is used to ensure effective power distribution, control, and supply of adequate power to meet the load demand. The fuzzy logic controller is operated based on the load demand and availability of power in switching “ON” or “OFF” the different switches within the system to maintain energy balance between the power produced by the Solar PV, pumped hydro storage system and the total load demand. This is because, in an autonomous DC microgrid system, effective power distribution and availability of power are crucial.

4.2 Research Design

This research is based on a DC control mechanism for an autonomous hybrid microgrid system. The system consists of various components such as: solar PV as the main energy source, hydropower as storage system acting as energy back up, and the load, which comprises of essential and non-essential load based on level of importance in the household. The above-mentioned components are connected with a boost converter and a control element for the bidirectional flow of active and reactive power in the system. A fuzzy logic controller strategy will be utilized to control the power flow in the system. However, the fundamental design of the solar PV and the amount of power it can deliver depends on the solar irradiation and environmental condition of the site.

Primarily, the solar PV system will generate enough power to supply the load demand and use the extra amount of power to charge the hydropower system to be used later. The number of reservoirs filled with water will depend on the extra charging energy available from the solar PV. All the energy generated by the solar PV will be stored by increasing the number of reservoirs accordingly. The DC controller is designed to automatically disconnect or connect non-essential loads in events that the power supply is less than the load demand. This makes the system an intelligent system capable of sensing the available power and load demand in the system including the storage capacity of the reservoir. The different variables used in modelling the system is shown in table 4.1 and the load curve of a typical solar PV-hydro system with its corresponding characteristics is shown in figure 4.1.

Table 4.1: System variables

Symbol	Designation and SI unit
P	Power (W)
PV	Photovoltaic
P_(PV)	Power produced by the solar PV system (W)
P_Load	Load demand (W)

Furthermore, to accomplish the desired objective of effective power supply and equal power distribution between the solar PV and the pumped hydro storage system using the load demand, the following scenarios are implemented:

- If P_ (PV) $\geq$ 77.2 kW, the supply source will supply both essential and the non-essential load.
- If P_ (PV) > P_Load, the supply power source will supply the load and the excess energy will be used to pump water from the lower reservoir to the upper reservoir to constitute potential energy when needed.

- If P_ (PV) < P_Load, the potential energy from the hydropower will be used to compensate the power needed, and the non-essential load will automatically be disconnected if necessary.

The system is implemented in the MATLAB/Simulink environment to demonstrate the feasibility of the system using different data sets and parameters sourced under different conditions. This will ensure the robustness and reliability of the system at different time and environmental conditions.

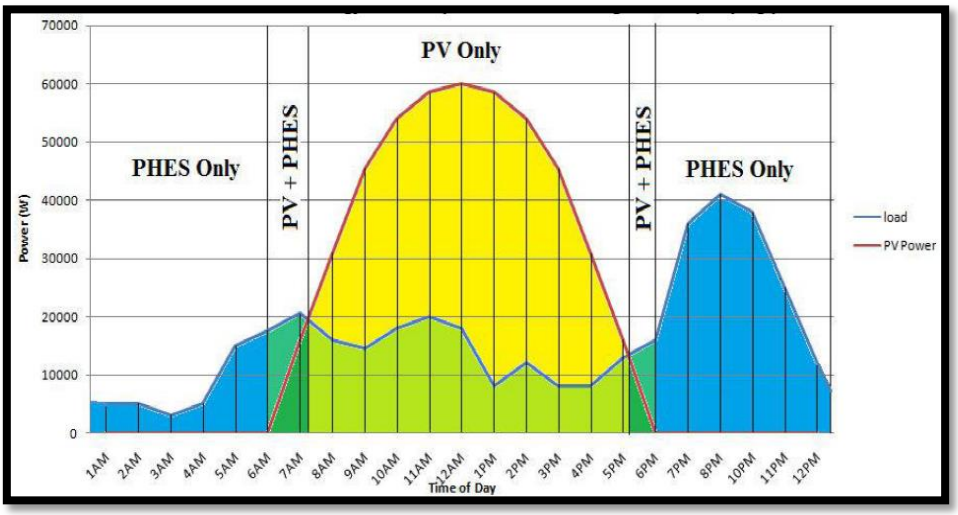

Figure 4.1: Solar PV-Hydro power supply scheme (Swe, 2018)

4.3 Photovoltaic (PV) system modelling

Proper modelling of the photovoltaic system in the MATLAB/Simulink environment provides an in-depth understanding of the inner performance of the system which is determined by the cell temperature in degrees Celsius (℃) and the solar irradiance in W/m^2. These two parameters must be properly selected because it determines the power output of the photovoltaic system. In addition, PVs are modelled to operate at its maximum power point with the assistance of the maximum power point tracker.

4.3.1 Ideal PV module

The cell temperature, available solar irradiance, and the output voltage of the solar array determines the output characteristics of an ideal photovoltaic array. Therefore, careful selection of these parameters is critical to ensure maximum power output from the PV. Again, this is informed by the fact that the short circuit current of the PV is linearly controlled

by the ambient radiation and an increase in the solar irradiance automatically increases the open circuit voltage of the PV.

The PV array block as provided in the MATLAB/Simulink environment is a combination of several well organised photovoltaic (PV) modules. These PV array modules are arranged in series but connected in parallel with each module connected in series. Each PV array block comprises of a diode, current source Iph (light-generated current), series resistor (Rs), and shunt resistor (Rsh) used to characterise the temperature reliant characteristics and solar irradiance I-V characteristics of the modules as shown in figure 4.2.

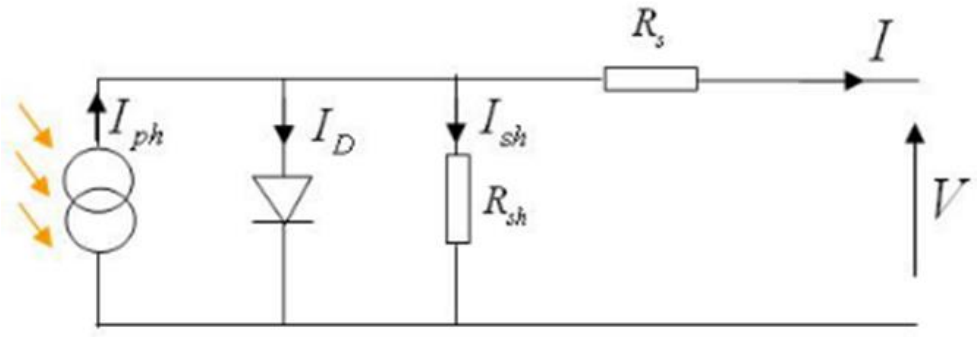

Figure 4.2: Equivalent circuit model of a PV Cell

The short circuit current is significantly affected by the ambient cell temperature because an increase in the cell temperature leads to an increase in the short circuit current but a decrease in the open circuit voltage. Therefore, an increase in the cell temperature reduces the cell efficiency and the power output. This is further expressed as the electrical circuit of the solar cell as represented using a photocurrent but defined by a constant current source connected in parallel to a diode and a shunt resistor. This is indicative of the leakage current that is connected in series with the series resistance showing the internal resistance to current flow.

The solar cell voltage-current characteristics from figure 4.1 is represented in equation 4.1:

$$I = I_{ph} - I_s\left(exp\frac{e(V + IR_s)}{mkT_c} - \frac{(V + IR_s)}{R_{sh}}\right) \tag{4.1}$$

Where:

- $I_{ph} = Photocurrent\ generated\ by\ the\ solar\ irradiance\ (A)$
- $I_D = Current\ passing\ through\ the\ diode\ (A)$
- $I_{sh} = Current\ passing\ through\ the\ parallel\ resistance\ (A)$

- $I = Output\ current\ of\ the\ solar\ cell\ (A)$
- $V = Output\ voltage\ of\ the\ solar\ cell\ (V)$
- $R_s = Junction\ resistance(\Omega)$
- $R_{sh} = Loss\ of\ dissipative\ effect\ of\ the\ solar\ cell\ (\Omega)$
- $k = Boltzman's\ constant, 1.3810^{-23}\frac{J}{K}$
- $T = cell's\ working\ temperature\ (℃)$

The photocurrent I_{ph} significantly depends on the operating temperature of the solar cell and radiation as shown in equation 4.2:

$$I_{ph} = \frac{\left(I_{SC} + ki\left(T_c - T_{ref}\right)\right)\lambda}{1000} \tag{4.2}$$

The cell saturation current was shown earlier to be significantly dependent on the temperature and can be expressed using equation 4.3 as:

$$I_s = I_{RS}\left(\frac{T_C}{T_{Ref}}\right) exp\left(\frac{qE\left(\frac{1}{T_{Ref}} - \frac{1}{T_C}\right)}{KA}\right) \tag{4.3}$$

Where; $q = electron\ charge;\ 1.610^{-19}\ C$

$$I = I_{ph} - I_D \tag{4.4}$$

Again, figure 4.2 represents an ideal equivalent photovoltaic system with different components such as series resistor, shunt resistor connected in parallel with the diode but inversely proportional to the shunt leakage current. However, a change in the value of the shunt resistor does not affect the PV array hence its corresponding leakage resistance will increase significantly without the leakage current connected to ground. But a little change in the value of the series resistor will have a significant impact on the power output of the PV array.

The ideal model of a photovoltaic cell with its intricacies is represented using equation 4.5 as:

$$I = I_{ph} - I_0\left(exp\frac{q(V + IR_S)}{mkT_C} - 1\right) \tag{4.5}$$

The solar cell is characterised using the following parameters as:

- Short circuit current: the maximum current generated by the solar cell when the voltage is equal to zero (V = 0)
- Open circuit voltage, V_{oc}: the maximum voltage of the solar cell when, $I_D = I_{ph}$ while the generalised current is normally taken as zero.
- Mathematically, the cell voltage without light is expressed as:

$$V_{OC} = \frac{mkT_C}{e} ln\left(\frac{I_{ph}}{I_O}\right) = V_t ln\left(\frac{I_{ph}}{I_O}\right) \quad (4.6)$$

Where: $T_C = absolute\ cell\ temperature$

$V_t = \frac{mkT_C}{e} = thermal\ voltage$

- Efficiency: ratio of the maximum power to the incident light power expressed as:

$$Efficiency\ (\eta) = \frac{P_{max}}{P_{in}} = \frac{I_{max}V_{max}}{AG_a} \quad (4.7)$$

Where: $G_a = local\ irradiance\ on\ the\ solar\ cell\ surface$

$A = cell\ area$

- Maximum power point (MPP): the point on the I-V characteristic curve where the product of the voltage and the current is highest, i.e., the point that shows the highest value of the power in the curve.

4.3.2 Photovoltaic system design in MATLAB/Simulink

In the MATLAB/Simulink environment, there are different types of solar panels available with each having distinct specifications of maximum current, maximum voltage, and power rating. The solar radiation and temperature were carefully selected to depict the actual weather condition of the chosen geographical location. In this study, the incremental conductance method was used to track the maximum power point under the South African weather condition. Hence, the details of the solar PV which includes the current, voltage, power, solar irradiance, and temperature used in this study is shown in figure 4.3.

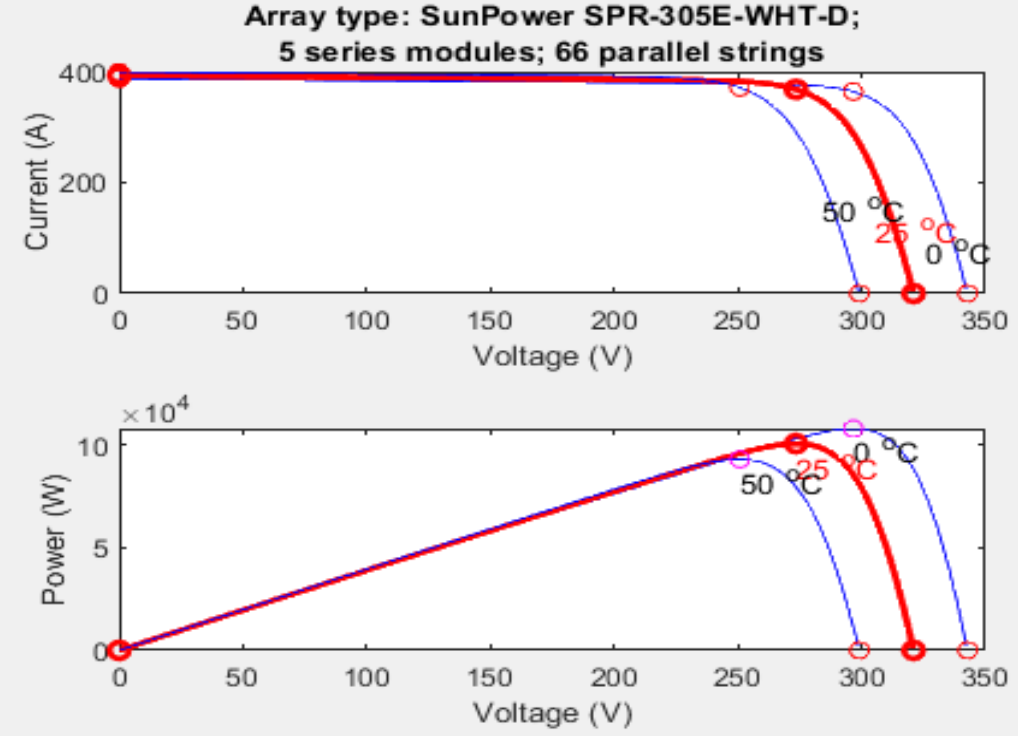

Figure 4.3: 100 kW PV array at an irradiance of 1000 W/m^2, temperature at 25 ℃ and 50 ℃ respectively

Calculations on how the total number of modules needed in both series and parallel to achieve a total power output of 100 kW.

Number of panels required in series = $\frac{V_{dcmax}}{V_{mp}} = \frac{273.5}{54.5} = 5$

$$\therefore \textit{the total number of panels needed in series} = 5$$

Therefore, the actual output voltage from the PV system: 5 × 54.7 = $273.5\ V_{dc}$

The output current generated by the PV system $(I_{out}) = \frac{P_{out}}{V_{out}} = \frac{100\ kW}{273.5} = 365.5\ A$

The number of panels connected in parallel $(N_p) = \frac{I_{PV}}{I_{mp}} = \frac{365.631}{5.58} = 65.53$

Because it is not practical to have 0.53 panels, the number of panels needed in parallel is rounded up to 66.

The actual power is then calculated as:

Actual power = (No. of panels in parallel × I_{mp}) × (No. of panels in series × V_{mp})

Therefore, the actual power = (66 × 5.58 Amperes) × (5 × 54.7 Volts)

= 10072458 W

= 100.7 kW

The actual values of the power output, output voltage, and output current is shown in figure 4.4 with the solar irradiance showing significant impact on the power output of the solar PV system.

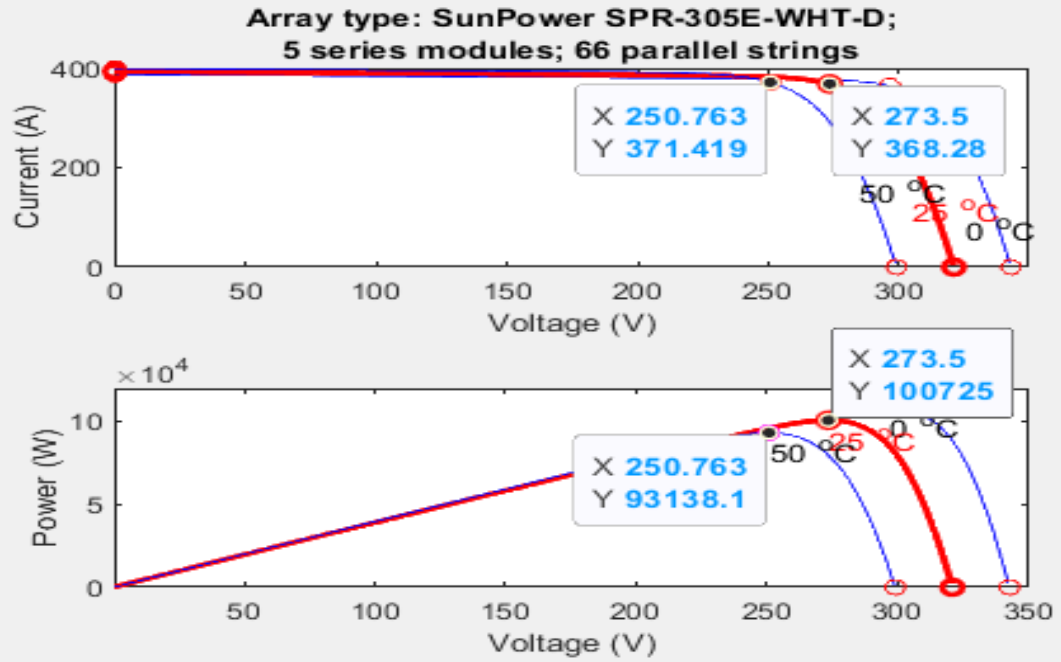

Figure 4.4: 100 kWp PV showing the actual values at 25℃ and 50℃ respectively

4.4 DC–DC Boost Converter modelling

A DC-DC boost converter is required to step-up the input voltage from the PV to a value greater than the PV system output voltage that is suitable for the DC-link voltage. The DC-DC boost converter comprises of an inductor, a capacitor, a diode, a pulse width modulator, and a semi-conductor switch as shown in figure 4.5.

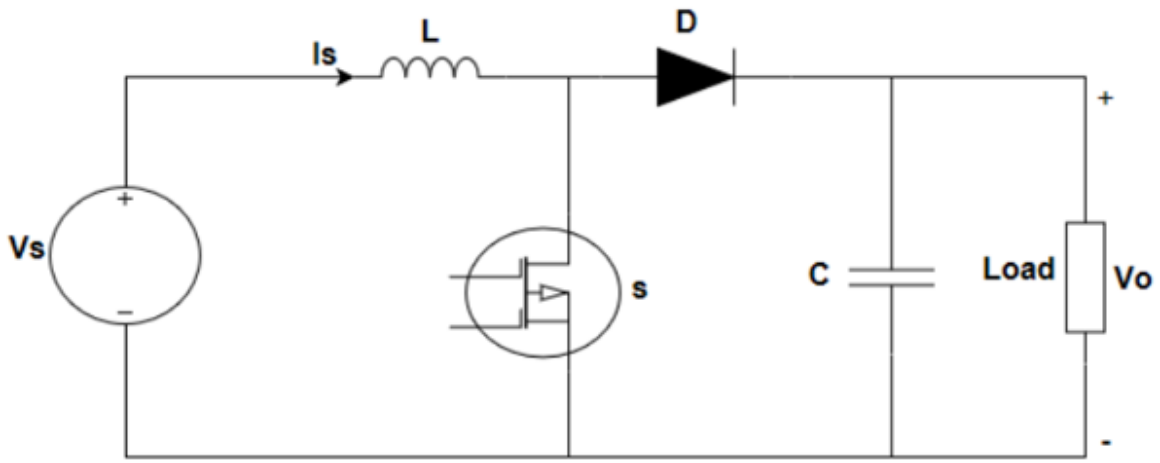

Figure 4.5: A boost converter circuit with diode and MOSFET

The study used the volt-second balance technique and capacitor charge balance technique to design the boost converter for the PV system. The small ripple approximation method was also used to obtain the approximate values of the voltage and current appropriate for the boost converter. The above methods were adopted to establish appropriate values of all the components in the boost converter with necessary assumptions made regarding modelling and components selection.

The voltage drop across the inductor is expresses using equation 4.8 as:

$$V_L = \frac{Ldi}{dt} \tag{4.8}$$

$$V_L = V_{in} \tag{4.9}$$

$$i_C = -\frac{V}{R} \tag{4.10}$$

Equation 4.10 can further be expressed including the small ripple approximation as:

$$i_C = -\frac{V_{out}}{R} \tag{4.11}$$

Where:

$$V_{in} = input\ voltage, V_L = inductor\ voltage, i_C = capacitor\ current, V_{out} = output\ voltage,$$
$$R = resistor$$

The duty cycle of the boost converter can be obtained using the boost conversion ratio as:

$$M(D) = \frac{V_{out}}{V_{in}} = \frac{1}{D'} = \frac{1}{1-D} \tag{4.12}$$

Hence, the duty cycle of the DC-DC boost converter is obtained using equation 4.13 as:

$$D = 1 - \frac{V_{in}}{V_{out}} = \frac{V_{pv}}{V_{DClink}} \tag{4.13}$$

$$\therefore D = 1 - \frac{273.5}{584} = 0.53$$

Again, when operating at steady state, the value of the critical inductance L is defined by the limit between the continuous conduction mode (CCM) and the discontinuous conduction mode (DCM) using equation 4.14 as:

$$L = \frac{V_{in} * D}{\Delta i_L * f_S} \tag{4.14}$$

Where: $i_L = \frac{P_{in}}{V_{in}} = \frac{100\ kW}{273.5} = 365.631\ A$

$\Delta i_L = 30\%\ of\ i_L$

$\therefore \Delta i_L = \frac{30}{100} * 365.631 = 109.69\ A$

The period $T_S = \frac{1}{f} = \frac{1}{5\ kHz}\ (seconds)$

Therefore, substituting these values into equation 4.14 gives:

$L = \frac{273.5*0.53}{109.69*\ 5\ kHz} = 264\ \mu H$

However, to ensure continous conduction for various voltages and loads, the value of the inductance is mostly chosen to be 10 times hgreater than the calculated value.

Hence, the value of the capacitor can be calculated using equation 4.15 as:

$$C = \frac{I_0 * D}{f_S * \Delta V_C} \tag{4.15}$$

Where: $I_O = \frac{P_{out}}{V_{out}} = \frac{100\ kW}{584} = 171\ A$

The capacitor voltage is equal to the output voltage i.e.., $V_C = V_O$ and the ΔV_C is assumed to be 1% of the output voltage

$$\therefore \Delta V_C = \frac{1}{100} * 584$$

$$= 5.84\, V$$

Therefore, substituting the values obtained into equation 5.24 gives:

$$C = \frac{171 * 0.53}{5\ kHz * 5.84}$$

$$= 3\ mH$$

Again, the load resistor is obtained as:

$$R_{load} = \frac{V^2}{P} = \frac{584^2}{100\ kW} = 3.41\ \Omega$$

In addition, a solar cell is basically a current source, therefore, to ensure voltage stability, a capacitor must be connected in parallel across the PV output to enable it to appear as a voltage source to the DC-DC boost converter. Hence, the boost converter, its controller and components as modelled in the MATLAB/Simulink environment is shown in figure 4.6.

Hence, the PV capacitor (C_{PV}) is expressed as:

$$C_{PV} = \frac{DV_{PV}}{4\Delta V_{PV} f_s^2 L_{boost}} \tag{4.16}$$

Where:

$D = duty\ cycle$

$V_{PV} = PV\ voltage$

$\Delta V_{PV} = PV\ ripple\ voltage$

$f_S = switching\ frequency$

$L_{boost} = boost\ converter\ inductor$

Therefore, substituting the values obtained into equation 4.16 gives:

$C_{PV} = 128\ \mu F$

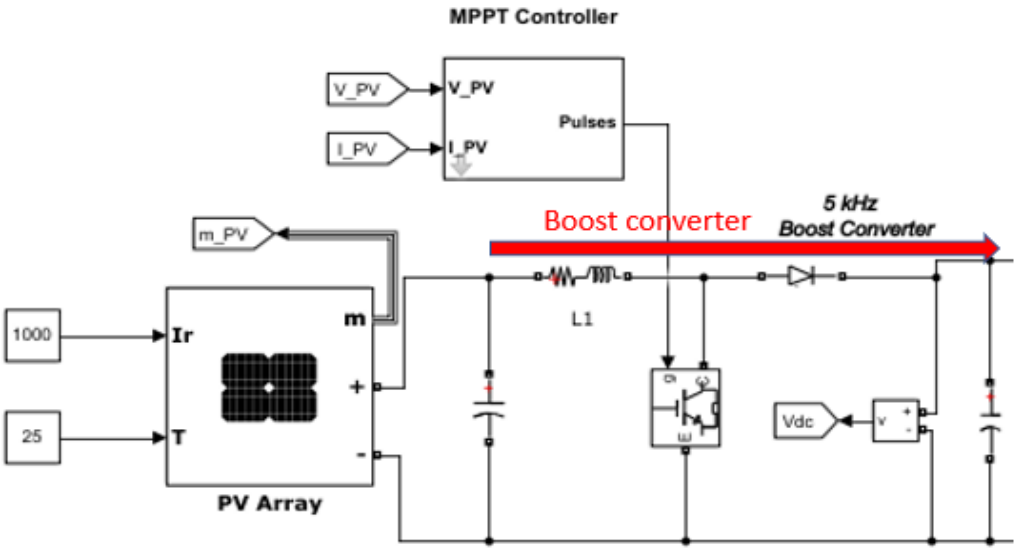

Figure 4.6: DC-DC boost converter with controller

4.5 Pumped hydro storage system (PHSS)

The pumped hydro storage system (PHSS) is the basic and only energy storage system used in this study. The PHSS is made up of the pump/motor subsystem, hydro turbine/generator subsystem and the reservoir unit. However, the most important parameters of the pumped hydro storage system are the hydro pumping coefficient expressed in m^3/kWh and the turbine generating coefficient expressed in kWh/m^3. This section provides a detailed information of the pumped hydro storage subsystem with corresponding application in DC microgrids. Again, it is aimed at offering realistic model that has all the necessary practical parameters. Hence, the turbine power capacity is calculated using the water level in both reservoirs without considering the fittings, turbine losses and pipes. The model is evaluated using suitable blocks in the MATLAB/Simulink environment. The pumped hydro storage system contains the upper reservoir, a hydro turbine, and a pump that stores electrical energy as gravitational potential energy. The volume of water and the height difference between the upper and lower reservoirs determines the capacity of the PHSS. However, the losses in individual components are considered and adequately compensated in the design within allowable design range.

4.5.1 Pump-motor unit

The water flow rate from the lower reservoir to the upper reservoir using the pump is obtained using equation 4.17 as:

$$P_t(t) = \eta_t \rho g h \times q_t(t) = c_t \times q_t(t) \qquad (4.17)$$

In this study, the solar PV is the primary power source designed to meet the load demand when generating at the maximum point and the flow rate can be likened to the rate of charge of a battery in the MATLAB/Simulink environment and expressed as:

$$q_p(t) = \frac{\eta_p \times P_{h\to p}(t)}{\rho g h} = c_p \times P_{h\to p}(t) \quad (4.18)$$

Where:

$\eta_t =$ overall efficiency of the turbine/generator unit

$q_t(t) =$ water volumetric flow rate input into the turbine (m^3/s)

$c_t(t) =$ turbine generating coefficient (kWh/m^3)

g = acceleration due to gravity ($9.8\ m/s^2$)

ρ = water density ($1000\ kg/m^3$)

$\eta_p =$ total pumping efficiency

c_p = water pumping coefficient of the pump (m^3/kWh)

h = elevation head (m)

$P_{h\to p}(t)$ = charging power from the solar PV to the pump (W)

The pumped hydro storage model calculates the water flow rate using the pump (Q_p) as the input power (P_m). Where the pump unit is made up of electric motor and the pump. The electric motor converts the electrical energy into mechanical energy that drives the pump to send water from the lower reservoir to the upper reservoir. The efficiency and effectiveness of the motor (η_m) indicates the losses in the system due to energy conversion from electrical to mechanical. The power efficiency of motors is presented in the data sheet because η_m is a function of P_m. Therefore, the input mechanical power of the pump (P_p) can be represented and calculated as:

$$P_m = P_m \eta_m \quad (4.19)$$

$$\eta_m = \phi(P_m) \quad (4.20)$$

But because the Q_p is a function of P_p, the entire head of the pump (H_p) together with the pump efficiency(η_p) can be expressed as:

$$Q_p = \frac{P_p \eta_p}{\rho g H_p} \tag{4.21}$$

$$\eta_p = \phi(Q_p) \tag{4.22}$$

Again, the efficiency-power flow rate curve shows that η_p is a function of Q_p and H_p is the sum of the static head (H_S). Therefore, the head loss of the pump mode (H_{pl}) can be expressed as:

$$H_p = H_s + H_{pl} \tag{4.23}$$

Where; H_s represents the vertical distance between the water level in the upper reservoir and the water level in the lower reservoir. This distance is controlled by the charging and discharging rate which is a function of the power dynamics in the system.

Again, the water level and the internal surface of the fittings and pipes which is beyond the scope of this study can be calculated using Darcy equation as follows:

$$H_{pl} = K \frac{V^2}{2g} \tag{4.24}$$

Where:

$g = gravity\ (9.81\ m/s^2)$

$K = \ resistance\ coefficient$

$$K = K_{pipe} + K_{fittings} \tag{4.25}$$

$$K_{pipe} = \frac{f L_p}{D_p} \tag{4.26}$$

$K_{fitting} = resistance\ coefficient\ of\ the\ fitting$

$$V = velocity = \frac{Q_p}{0.25 \pi D_p^2} \tag{4.27}$$

4.5.2 Turbine-generator unit

The hydro turbine evaluates the output power as a function of the flow rate and the turbine head where the kinetic energy of the water is converted to electrical energy. This occurs when the power from the primary power source (solar PV) is less than the primary load (load

1) in this case. Water is drawn from the upper reservoir to the lower reservoir to operate the hydro turbine using equation 4.17. Mathematically, the hydro turbine can be expressed as:

$$P_t = Q_t H_t \rho g \eta_t \tag{4.28}$$

The turbine valve is installed at the outlet of the upper reservoir to enable absolute and effective control of the flow rate (charge) into the turbine. The flow rate is also affected by the pipe diameter during the charge and discharge modes.

4.5.3 The reservoir model

The reservoir estimates the volume of water stored in it by using the difference between the incoming flow and the outgoing flow including losses due to evaporation but assuming zero leakage. Evaporation depends on the relative humidity, net radiation, wind velocity and temperature. In this study, the quantity of water is always adequate to generate enough power to meet the primary load (load 1) when the solar PV is not generating. Hence, the water level in the upper reservoir is considered as the state of charge (SOC) of the storage of the reservoir which is similar to the state of charge of a battery. The gravitational potential energy in the upper reservoir is achieved using equation 4.29.

$$E_c = n_{day} \times E_{load} = \frac{\eta_t \times \rho \times V \times g \times h}{3.6 \times 10^6} \tag{4.29}$$

Where:

$E_c = energy\ storage\ capacity\ of\ the\ reservoir\ (Joules)$

$n_{day} = number\ of\ days\ of\ independent\ supply$

$E_{load} = daily\ load\ demand\ (kWh)$

$V = storage\ capacity\ of\ the\ reservoir\ (m^3)$

Therefore, the total quantity of water stored (charge in the case of battery) in the reservoir at any particular time can be achieved by:

$$Q_{UR}(t) = Q_{UR}(t-1)(1-\alpha) + q_p(t) - q_t(t) \tag{4.30}$$

Where: α is the leakage and evaporation losses. Although, these losses are not considered in this study, but the minimum water quantity was set at 20% in order to ensure efficiency and avoid failure in case of emergency load demand.

Precipitation is another parameter that has the capacity to influence the water level in the reservoir, but this was not considered in this study because the reservoir is assumed to be properly covered on top. However, in tropical rainforest regions, the average annual rainfall is estimated between 150 and 400 centimetres (Mousavi, 2020). Therefore, not including this parameter in the design of the reservoir with open top will increase the error in calculating the stored water level in the reservoir. This is most critical in energy management systems because the management of the entire system and the power output depends on the volume of water stored in the reservoir.

4.6 Load demand profile

The study modelled an autonomous DC microgrid system that has both residential and commercial loads. However, the solar PV output power is modelled to meet both loads when generating at the maximum power point. The DC microgrid system is connected to the DC load directly at 584 V_{dc} and classified as primary load or secondary load. The pumped hydro storage system is used as a backup system during peak demands and when the power produced by the solar PV is less than the DC load demand. The load profile was carefully selected using a publication from the UK department of energy to reflect a typical average DC load demand for a residential and commercial neighbourhood. The total load demand for both residential and commercial buildings is 77.2 kW. Where, each residential building has a load demand of 13600 W (13.6 kW) daily during peak hour and each office building has a load demand of 7600 W (7.6 kW) daily during office hours making it a total load demand of 21.2 kW daily. In this study, 4 residential buildings and 3 office buildings were considered. Hence, the total load demand for the community is 77.2 kW.

The controller is implemented using the flowchart shown in figure 4.7. Implementing this process requires information such as the available solar PV power output, water level in the reservoir, and load demand. These values are used to determine the charging and discharging mode of the system at any particular moment. If the solar PV power output is greater than the load demand and the water level in the reservoir is less than 20%, then the excess power will be used to charge the reservoir. But if the solar PV power output is less than the load demand and the water level in the reservoir is between 20% and 80%, then, the pumped hydro storage system will be used to meet the load (discharge mode).

The load 1 (L_{D1}) is 54.4 kW, load 2 (L_{D2}) is 22.8 kW, solar PV power output is 100 kW and the PHS is 30 kW respectively. However, the following assumptions were made regarding the scenarios and the system operation start:

- Solar PV is always “ON”

- Cloudy days were not considered in this study
- The upper reservoir is full at the start of the simulation.

The flowchart operates as follows:

- Measure the solar PV power output, pumped hydro storage water level, primary load and secondary load to ascertain their respective values.
- A condition is set to check if the solar PV power output is greater than the total load (primary and secondary loads).
- If “YES”, supply primary and secondary loads (L_{D1} & L_{D2}) and return back to measure the solar PV power output, pumped hydro storage water level, primary and secondary loads.
- If “NO”, disconnect the secondary load (L_{D2}) and check if solar PV power output is greater than the primary load.
- If “YES”, supply the primary load and charge the pumped hydro storage system if the solar PV power output is greater than 54.4 kW and thereafter, return to measure P_{PV} against the primary load.
- If “NO”, check if pumped hydro storage water level is greater than 20%.
- If “YES”, discharge pumped hydro storage, supply primary load and charge pumped hydro storage if solar PV power output is greater than 54.4 kW.
- If “NO”, charge pumped hydro storage and check if pumped hydro storage water level is greater than 97%.
- If “NO”, continue charging the pumped hydro storage
- If “YES”, stop charging and return to measure the solar PV power output, pumped hydro storage water level, primary load and secondary load

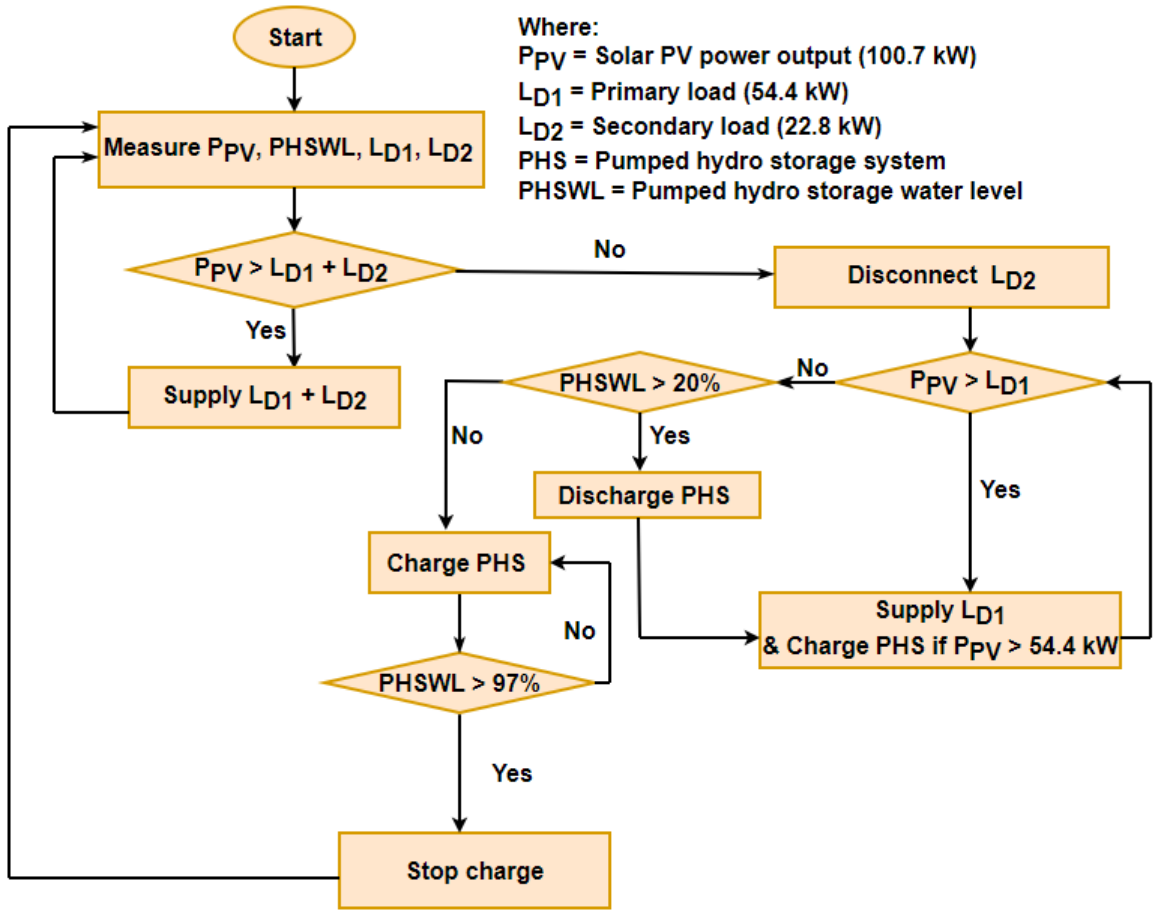

Figure 4.7: Flowchart of the microgrid optimization process

4.7 Fuzzy logic controller algorithm

Fuzzy logic controller is a smart tool used to control a combination of different energy sources in a manner that ensures that the entire load is met within established constraints. The algorithm in designing the controller is based on allocating linguistic variables and setting conditions and constraints for the controller. However, in this study, the fuzzy logic controller has three inputs and three outputs that are carefully designed within the established constraints. The inputs linguistic are the water level (water level), solar PV power output (P_PV), and the power demand (P_Load1) and the output linguistic variables are Load1_on, Load2_on, and pumped hydro storage_on (PHP_on). Where each input variable has three linguistic values designated as Low, Medium, and High and the output variables has Load1_on + PHP_on, Load1_on + Load2_on, Load1_on only. For easy understanding and simplicity of computation, triangles, and trapezoids membership function, Mamdani inference system for rule processing and centre of gravity for Defuzzification evaluation and process by fuzzy logic is utilized. Normally, fuzzy system comprises of a membership function, rule base, interference algorithm and rule viewer as presented subsequently.

Therefore, this section presents the fuzzy logic controller algorithm implemented in this study.

4.7.1 Fuzzy interface model

The fuzzy interface model used in this study showing the input linguistic variables (water level, solar PV power output, and power load 1) and output linguistic variables (primary load (Load1_on), secondary load (load2_on) and pumped hydro storage system (PHP_on)) are shown in figure 4.8.

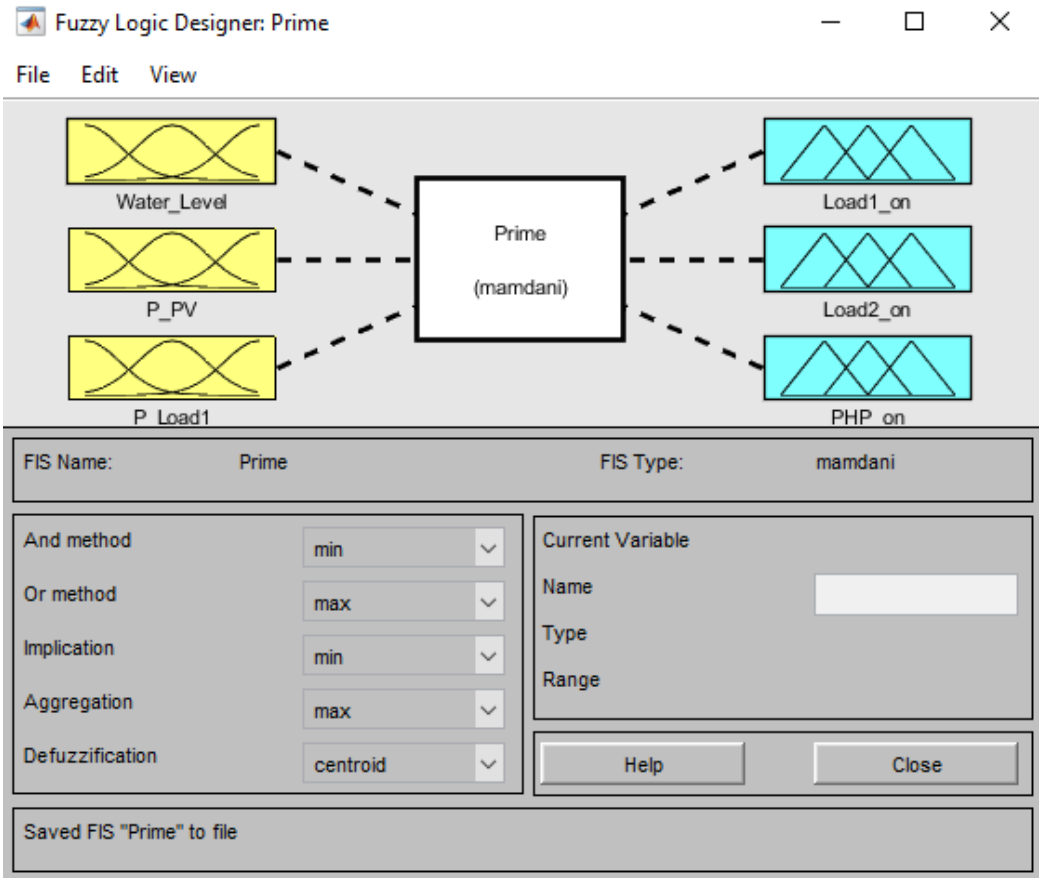

Figure 4.8: Fuzzy interface model

4.7.1.1 Water level membership function

The water level is one of the critical input linguistic variables with three overlapping linguistic values, Low (0 0 0.25 0.4), Medium (0.25 0.5 0.75) and High (0.5 0.75 1 1) as shown in figure 4.9. The display range is between 0 and 1 where 1 means that the reservoir is completely full.

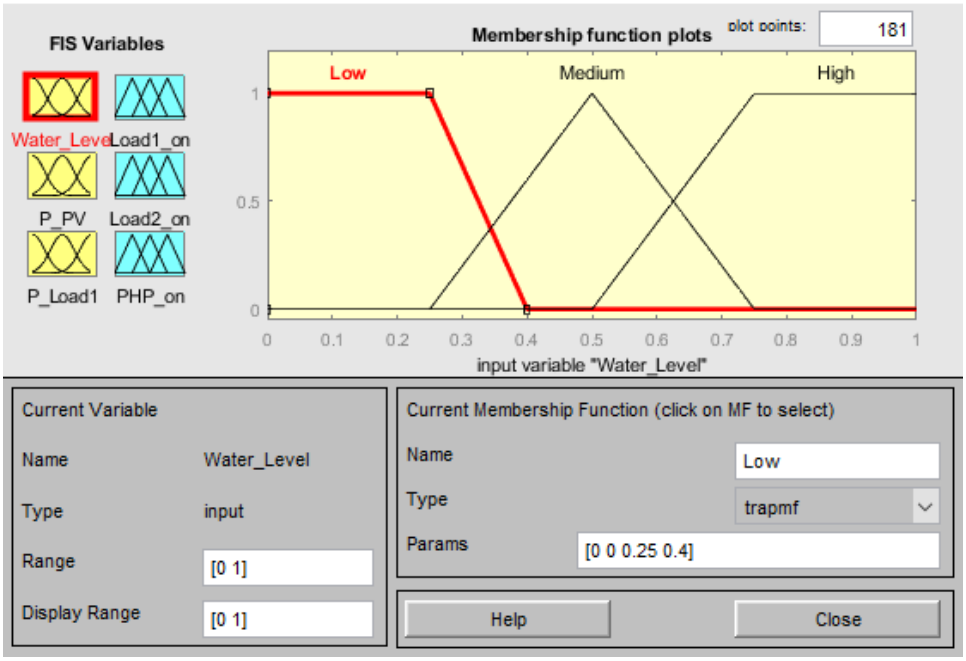

Figure 4.9: Membership function of water level

4.7.1.2 Membership function of Solar PV

The solar PV is the second input linguistic variables with three intersecting linguistic values, Low (0 0 2.5e+4 4e+4), Medium (2.5e+4 5e+4 7.5e+4), High (5e+4 7.5e+4 1e+5 1e+5) as shown in figure 4.10. The range display is between 0 and 100 kW.

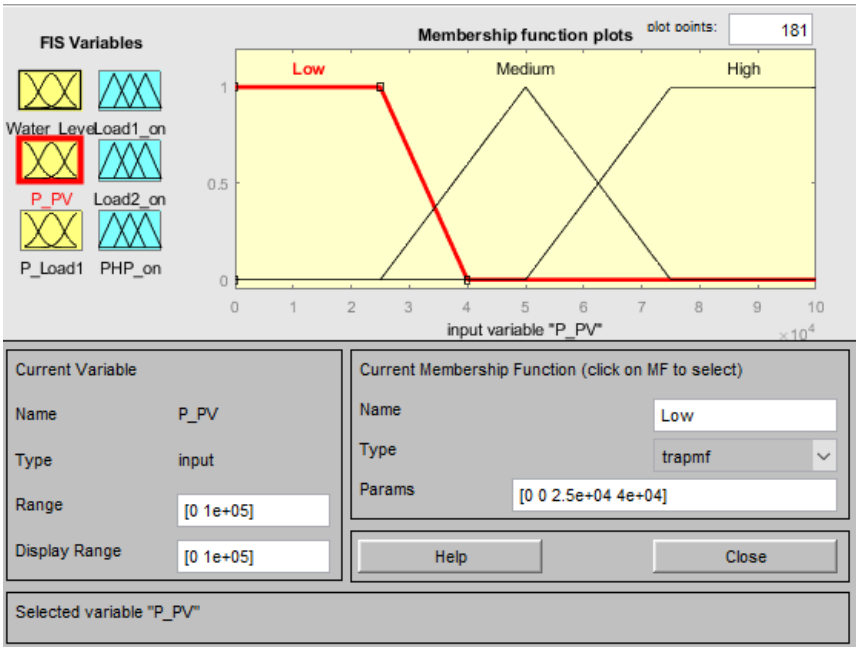

Figure 4.10: Membership function of Solar PV

4.7.1.3 Membership function of power load1

The power demand of load1 is the third input linguistic variables with three interweaving linguistic values, Low (0 0 1.2e+4 2.5e+4), Medium (1.2e+4 3.75e+4 5.6e+4), High (3.76e+4 5.6e+4 7.5e+4 7.5e+5) as shown in figure 4.11. The range display is between 0 and 7.5 kW.

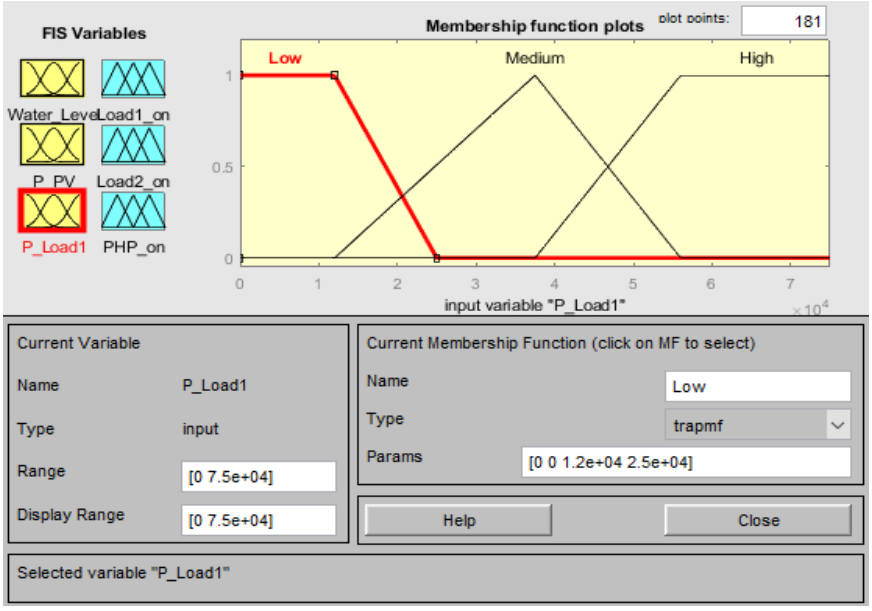

Figure 4.11: Membership function of power load1

4.7.1.4 Membership function of Load2

Membership function of Load2 is one of the three output variables with two linguistic values, Low (0 0 288 2 kW), high (1.5e+3 2.9e+3 3.3e+3 5.8e+3) as shown in figure 4.12.

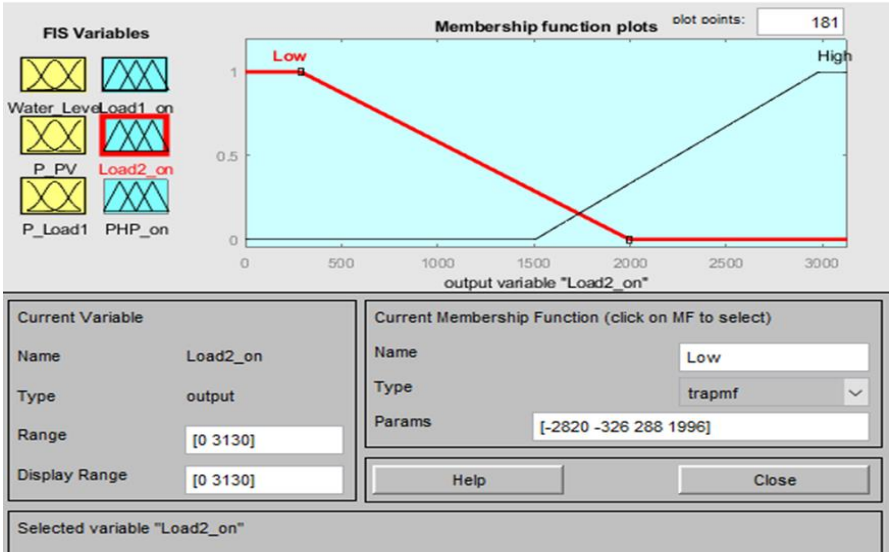

Figure 4.12: Membership function of load2

4.7.1.5 Membership function of Load1

Membership function of Load1 is one of the three output variables with two linguistic values, Low (0 0 7.5e+3 7.14e+4), high (6e+4 6.1e+4 8.25e+4 1.42e+5) as shown in figure 4.13.

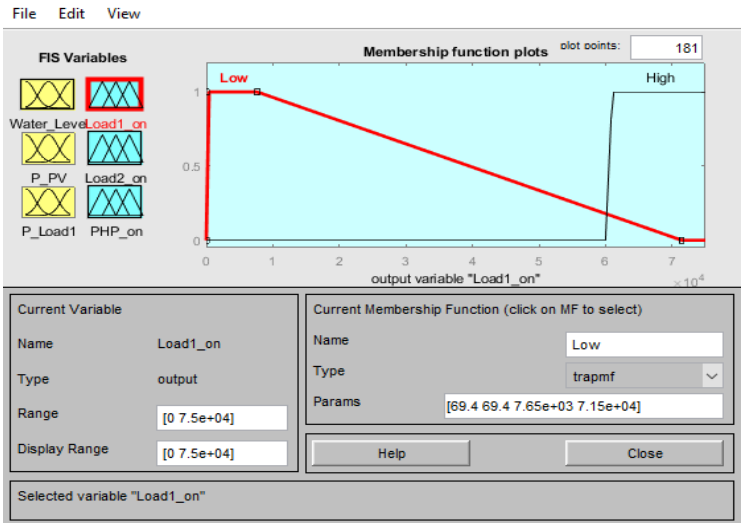

Figure 4.13: Membership function of load1

4.7.1.6 Membership function of pumped hydro storage

Membership function of pumped hydro storage is one of the three output variables with two linguistic values, Low (0 0 0.3), high (0.25 0.25 1 1) as shown in figure 4.14. The display range is from 0 to 1 which indicates a completely empty to completely full.

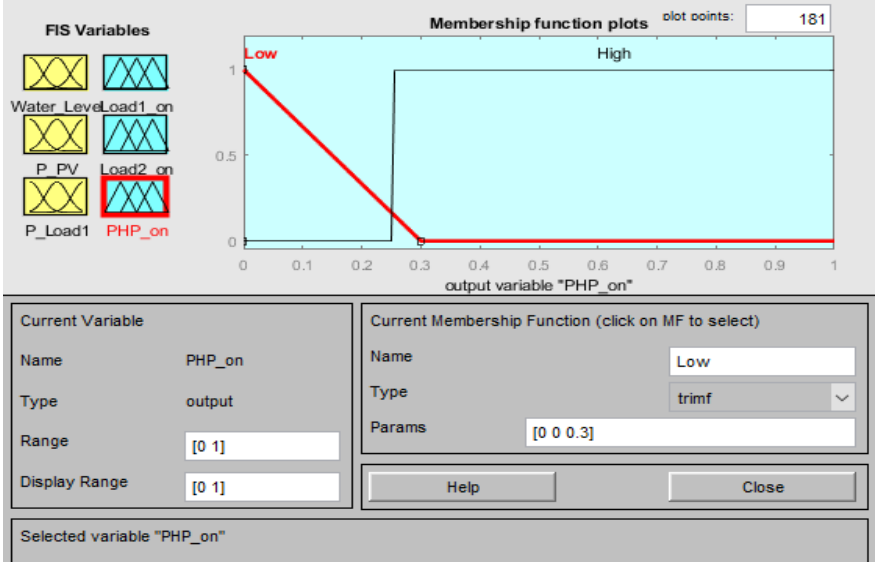

Figure 4.14: Membership of pumped hydro storage

4.7.1.7 Implemented fuzzy logic controller rules

Real time fuzzy logic controller is modelled with three inputs and three outputs. The system is controlled using some established set of rules that are written in the control box as shown in figure 4.15.

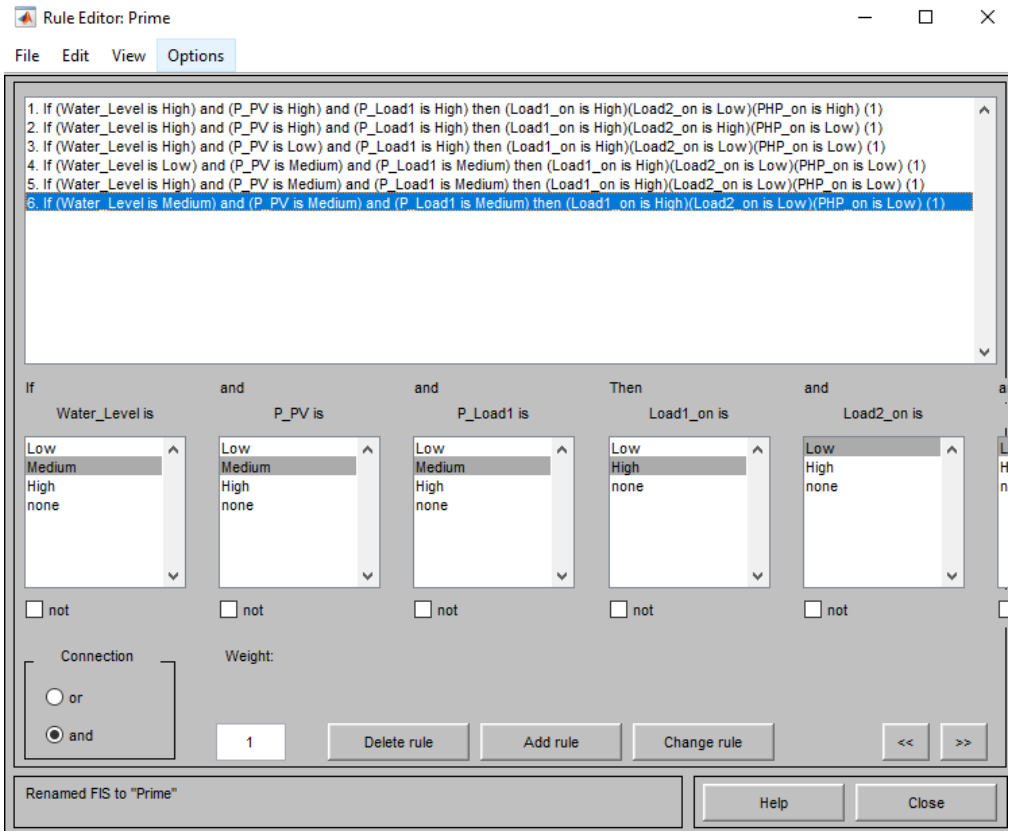

Figure 4.15: Fuzzy logic controller rule editor

4.7.1.8 Rule Viewer

The Rule Viewer is used to view the inference process of the fuzzy system. However, under the rule viewer, the input values can be adjusted to a corresponding output of each fuzzy rule, aggregated output fuzzy set, and the defuzzified output value. But the defuzzification procedure begins with the aggregation of the outputs of the fuzzy rules. Again, at the implementation stage, the aggregation is executed by combining the total output trigger values for each membership function over the set rules that affect that particular function. During the simulation process each membership function is determined by the sum of the triggering weights and combination of the outputs to compute a certain outcome using numeric integration as shown in figure 4.16a and 4.16b respectively.

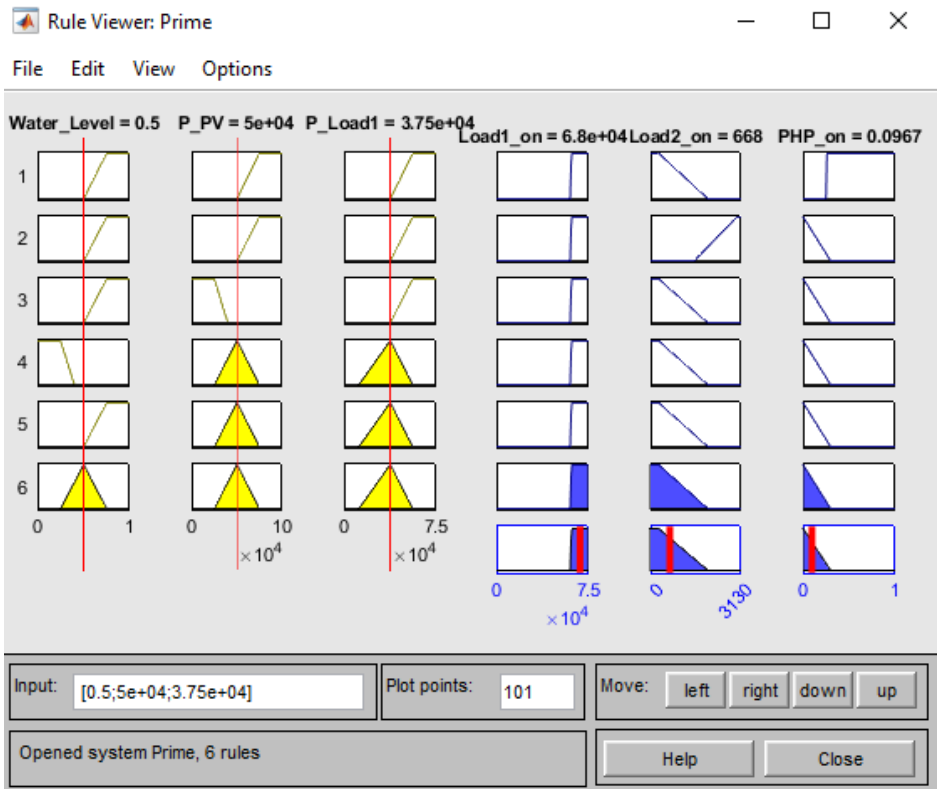

Figure 4.16a: Rule viewer

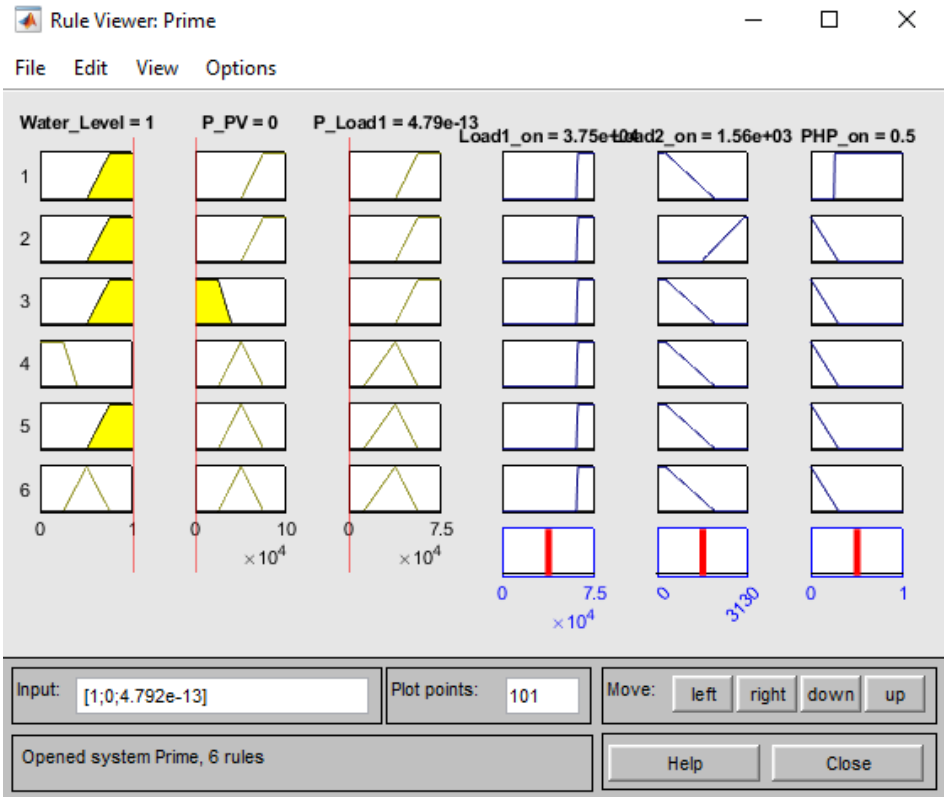

Figure 4.16b: Rule viewer

4.7.1.9 Complete fuzzy logic controller system

The input parameters of the fuzzy logic controller are the solar PV, pumped hydro storage system and the power load1 while Load2_on, Load1_on, and PHP_on are the corresponding outputs as shown in figure 4.17. However, the switches will respond according to input variables and the rules implemented in the fuzzy logic controller as shown in figure 4.18.

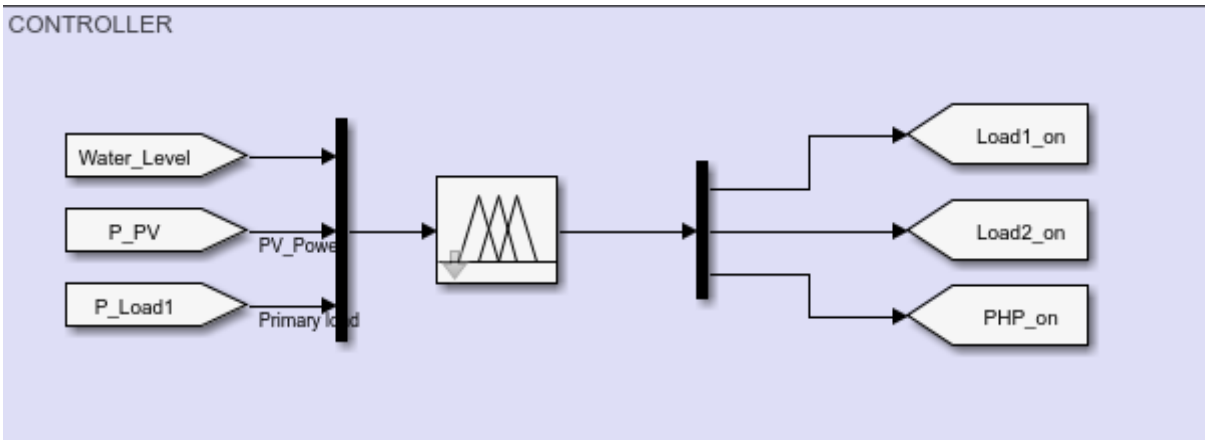

Figure 4.17: Complete fuzzy logic controller

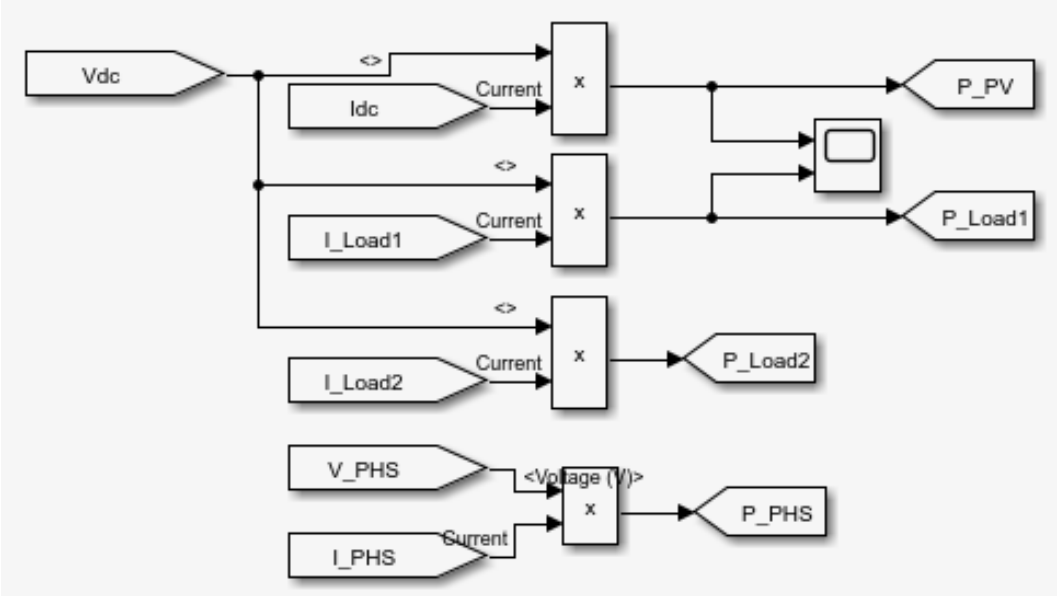

Figure 4.18: Fuzzy logic controller inputs

CHAPTER 5: SIMULATION RESULTS AND DISCUSSION

5.1 Introduction

This chapter presents simulation results of the different components of the microgrid system and discusses corresponding results. A PV microgrid network is modelled in the MATLAB/Simulink environment aimed at effective power distribution and optimisation. This is achieved using a pumped hydro storage system (PHSS) determined by the water level in both the lower and upper reservoirs. The remaining sections of this chapter presents the solar PV system simulation results and discusses its output in section 5.2. The DC-DC boost converter simulation results is presented in section 5.3. This section presents the voltage before and after the boost converter to indicate the boosted voltage value. In section 5.4 is the simulation results showing the water level in the upper reservoir, PHS current, voltage and available power. In section 5.5 three different scenarios are presented. The first case is when the power output from the solar PV is greater than the primary load (load 1) and the water level in the reservoir is less than 98% (recharge). The second case is when the solar PV power output is greater than the primary (load 1) and the water level in the reservoir is greater or equal to 98%, then, supply load 2. The third case is when the solar PV power output is less than the primary load and the water level is greater than or equal to 10% (discharge).

5.2 Simulation of PV array model

In this study, the PV system was modelled and simulated in the MATLAB/Simulink environment where it uses electronic components such as resistors, diodes and current source that is equivalent to a solar cell as shown in figure 5.1 and figure 5.2 respectively.

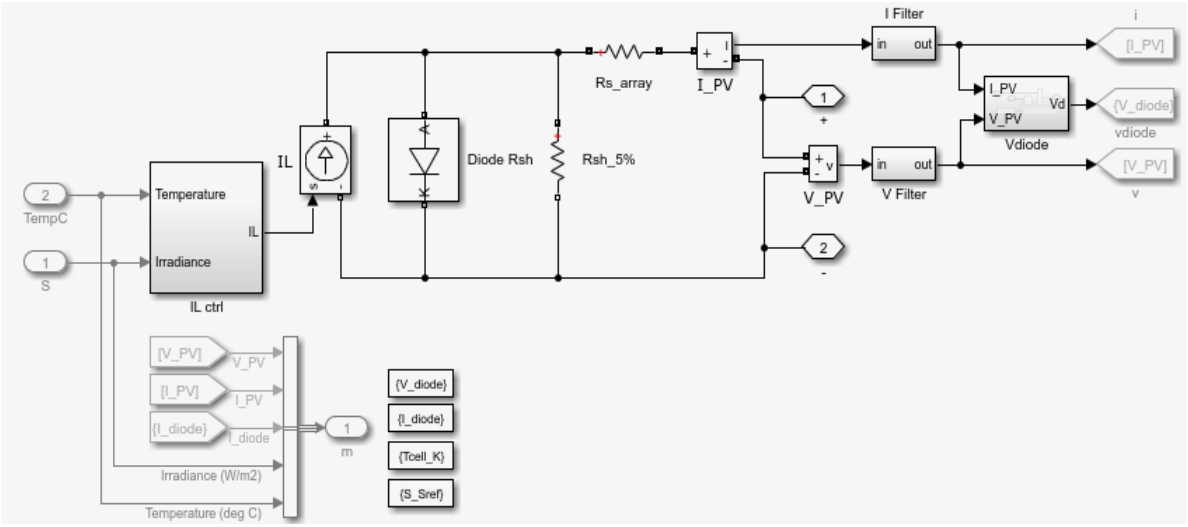

Figure 5.1: An illustration of a Solar cell characteristic in MATLAB/Simulink

Furthermore, the solar cells are further connected in series and parallel to form a PV array with a total generating capacity of 100 kW as indicated in the preceding chapters. The temperature was varied between 25℃ and 50℃ during the simulation to adequately understand the impact of temperature on the PV system output power.

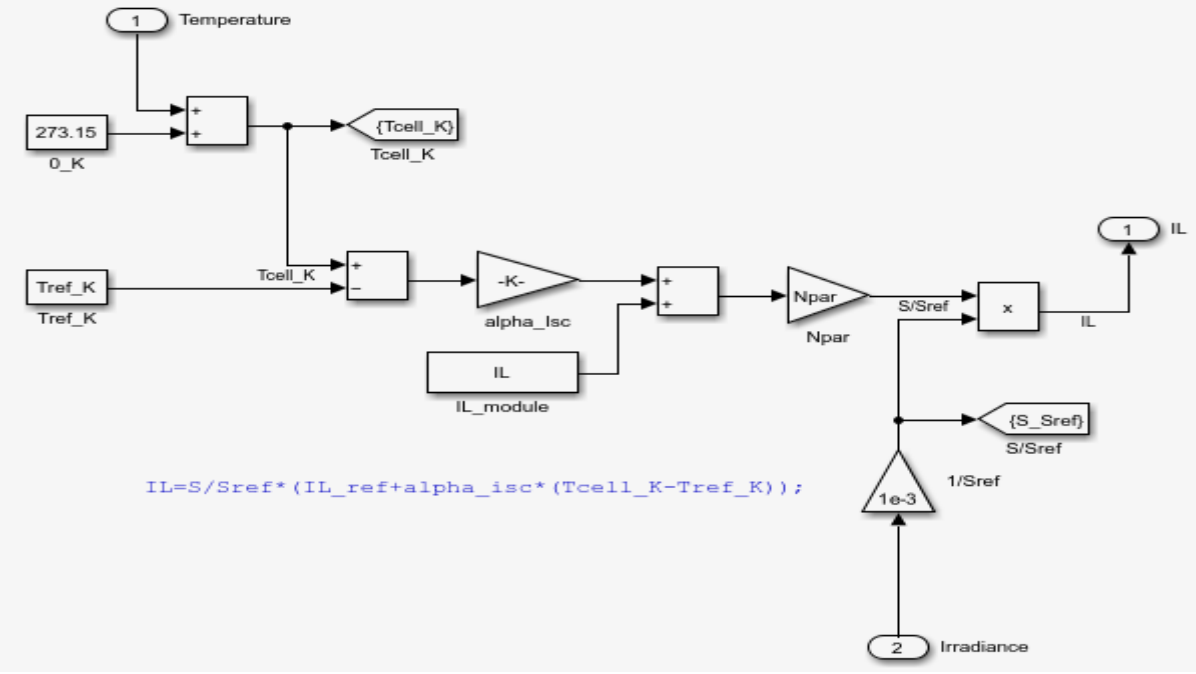

Figure 5.2: Equivalent circuit of a solar cell in MATLAB/Simulink

To maintain voltage stability and step up the voltage to the desired dc-link voltage, the PV system voltage is fed directly to a DC-DC boost converter. The PV system output voltage is 274 V_{dc} and stepped up to 584 V_{dc} with a duty cycle of 0.53. Again, because of the

fluctuation associated with PV system output, the duty cycle is used to control and implement a stable output voltage at 584 Vdc using equation 5.1. Hence, a change in the duty cycle is determined by the input voltage change to maintain a constant DC-link voltage.

$$D = 1 - \frac{V_{in}}{584} \tag{5.1}$$

The study has a primary load (Load 1) of 71.4 kW and a secondary load (Load 2) of 3.125 kW as shown in figure 5.3 while the corresponding control system is shown in figure 5.4. Again, the purpose of having two loads in the DCMGs is to highlight the effectiveness of the control system because it ensures that both charge and discharge cases are adequately implemented. The DCMG system measurements are shown in appendix 1 while the control variables and set conditions are shown in appendix 2 respectively.

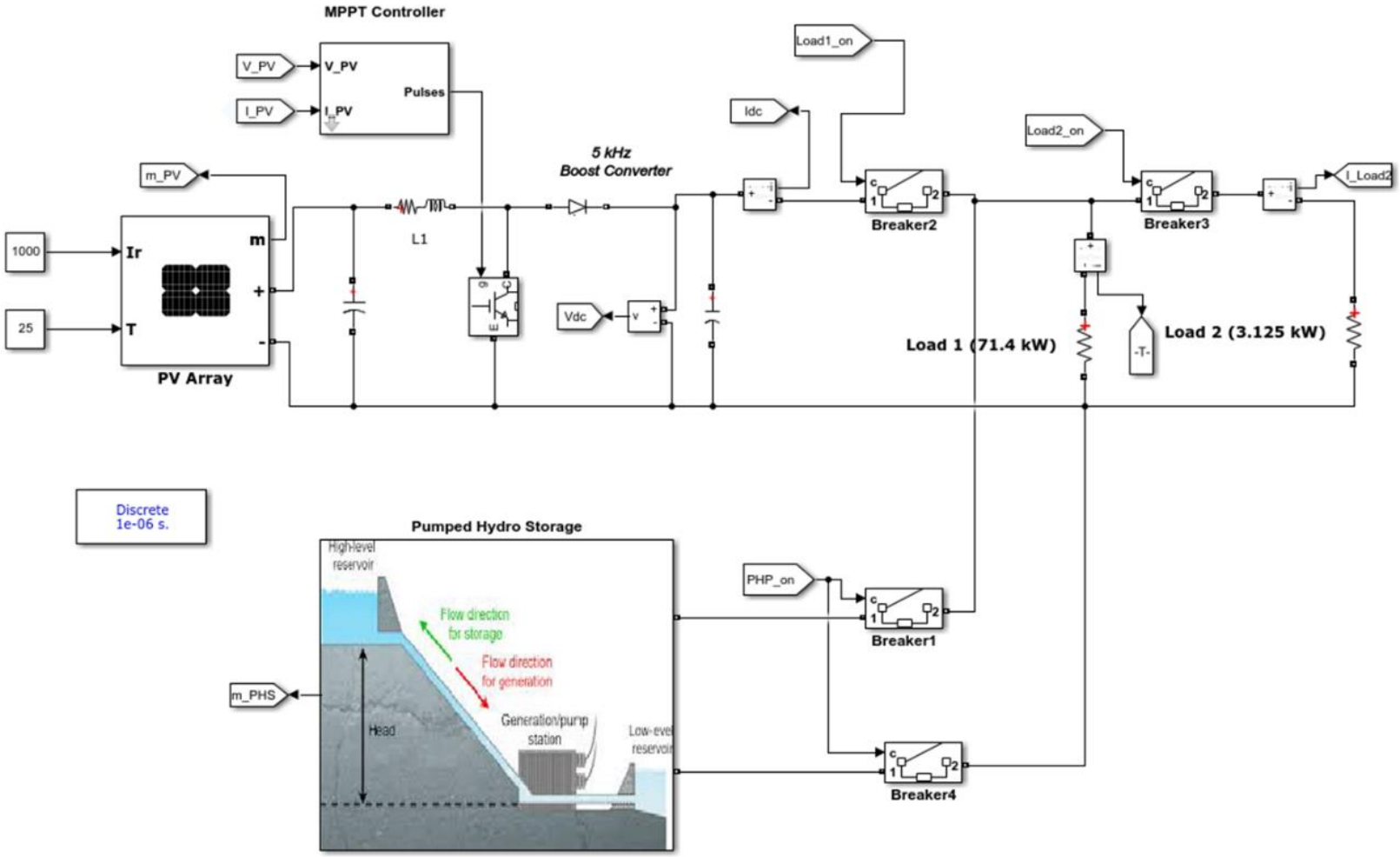

Figure 5.3: Solar PV–pumped hydro storage DC microgrid

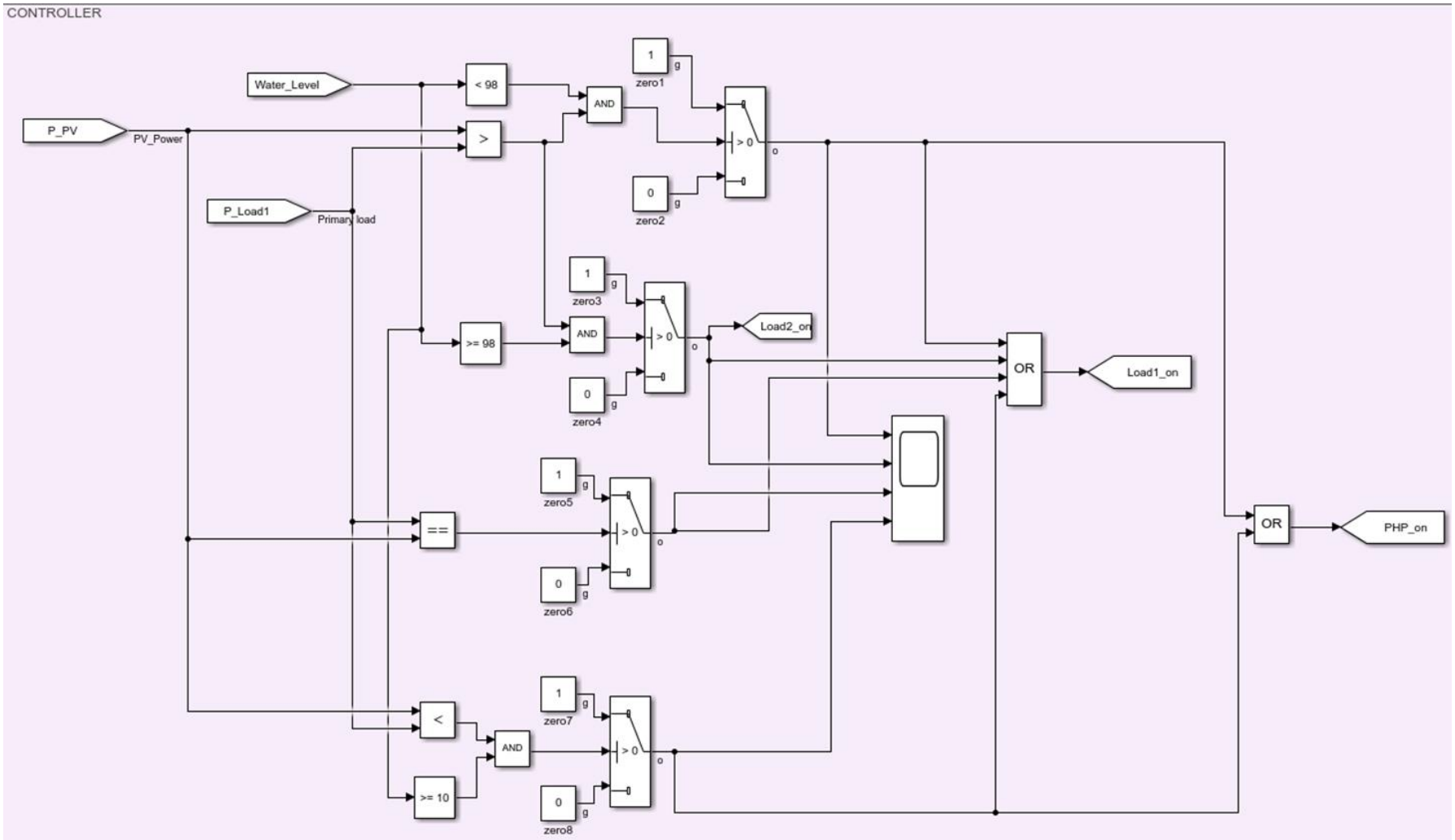

Figure 5.4: DCMG controller

The past decade has experienced significant improvement in solar PV technology. This has allowed the integration of different techniques capable of tracking the maximum power point of the PV module during operation. Some of such techniques are parasitic capacitance, perturbation and observation, incremental conductance, and current-based peak power tracking methods. However, in this study, the incremental conductance method was used in establishing the maximum power point as shown in figure 5.5. The incremental conductance technique is used to equate the incremental conductance and the conductance by calculating the product of the voltage and current at a particular point. The control method used in incremental conductance is less complicated in the MATLAB/Simulink environment as compared to other available tracking methods.

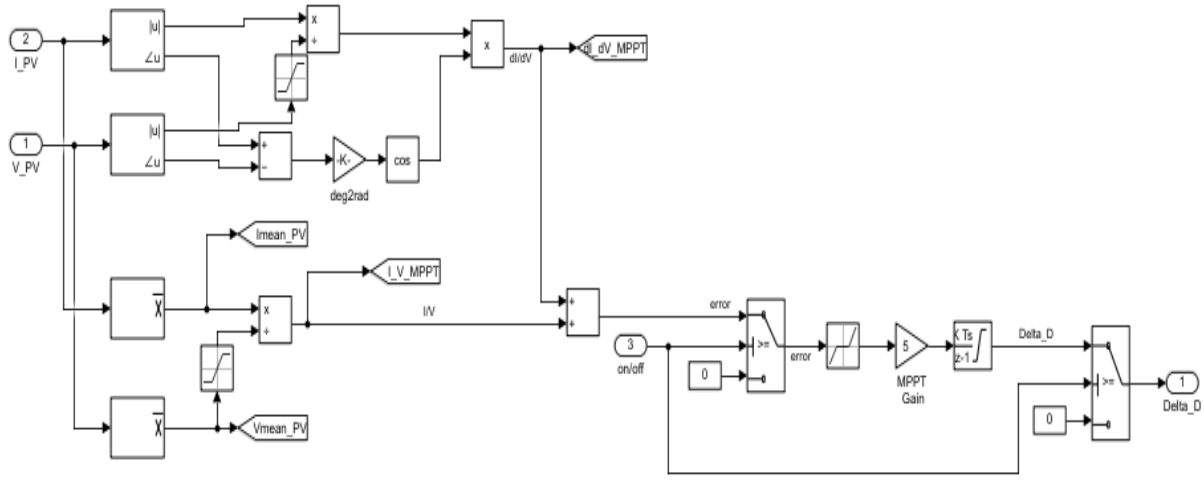

Figure 5.5: Maximum power point tracking by incremental conductance method

5.2.1 PV system simulation results

The type of PV system selected and modelled was aimed to reflect the desired output power and voltage. Again, to ascertain the effectiveness of the design and also offer an opportunity to evaluate basic performance. Hence, the PV system was modelled with a power rating of 100.7 kW, an output voltage of 273.5 Vdc, and output current of 365.5 A.

The PV system output current is shown in figure 5.6 at a constant solar irradiance of 1000 W/m^2. The value of the calculated output current of the PV system is 365.5 A as presented in the previous section. However, the simulated value is 366.5 A at 250 ms and 750 ms respectively as shown in figure 5.6 which is 1 A different from the calculated value due to losses in the system. This simulated result is an indication of the accuracy of the model.

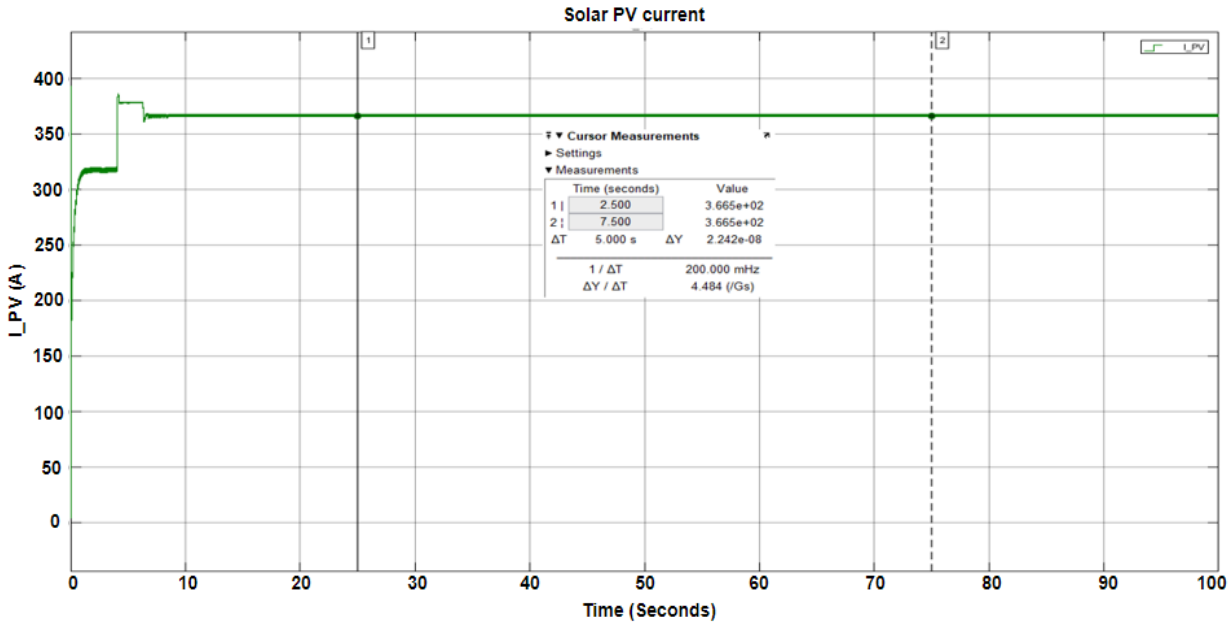

Figure 5.6: Solar PV system output current

The calculated output voltage of the PV system is 273.5 Vdc as presented in the previous chapter while the simulated value is 274.8 Vdc as shown in figure 5.7. Where the PV system input voltage serves as the input to the DC-DC boost converter. Hence, comparing the calculated value with the simulated value shows a difference of 1.3 Vdc which is equivalent to 0.47 %. This little difference in the value is caused by operational losses in the system. The system experienced a voltage dip due to system disturbance but regained stability after few microseconds.

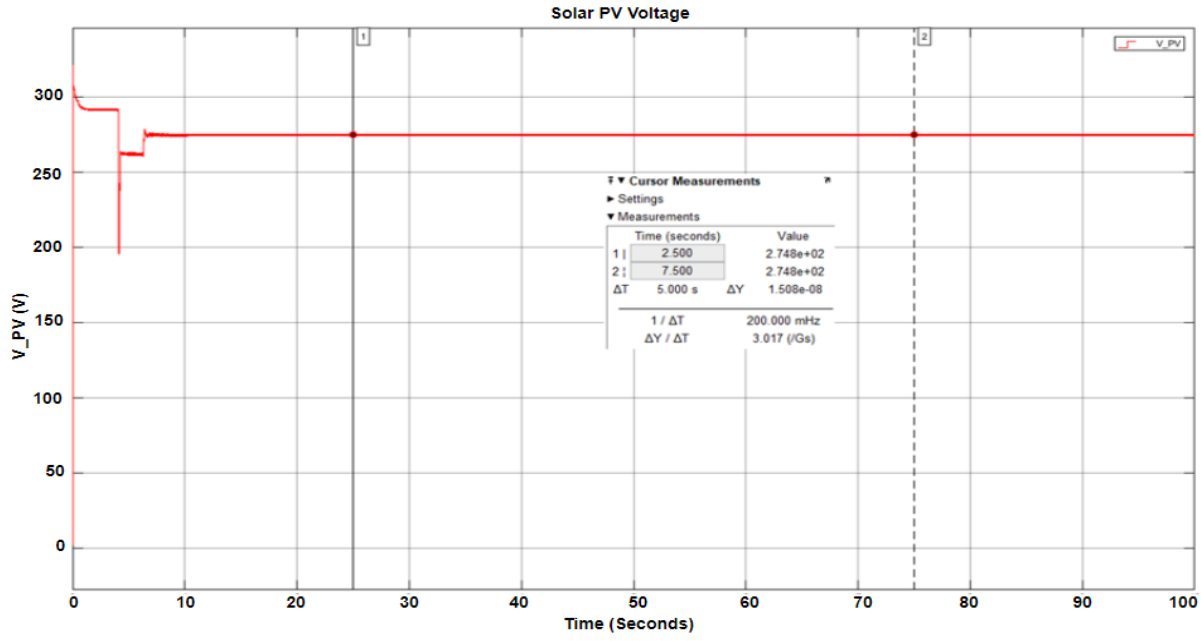

Figure 5.7: Solar PV system output Voltage

The simulated output power generated by the PV system that is time dependent is shown in figure 5.8. The power was initially unstable which a product of the fluctuating voltage and current is at that point, but it became stable throughout the simulation period (10 seconds) just before 1 second. The power generated starting from the point of stable state is 100.7 kW compared to the calculated value of 100 kW. A little discrepancy of 0.7 % between the simulated and calculated values can be attributed to the losses in the system caused by individual components within the system. However, this difference is very little and within allowable range of such design. This is the output power that is connected to the DC-DC boost converter when producing at maximum point.

However, the PV voltage is boosted to the desired voltage of 584 Vdc as shown in the preceding section using an equivalent duty cycle of the boost converter. The duty cycle was initially unstable during the transitory period of the input voltage but gained stability at 0.53 just before 1 second as shown in figure 5.9.

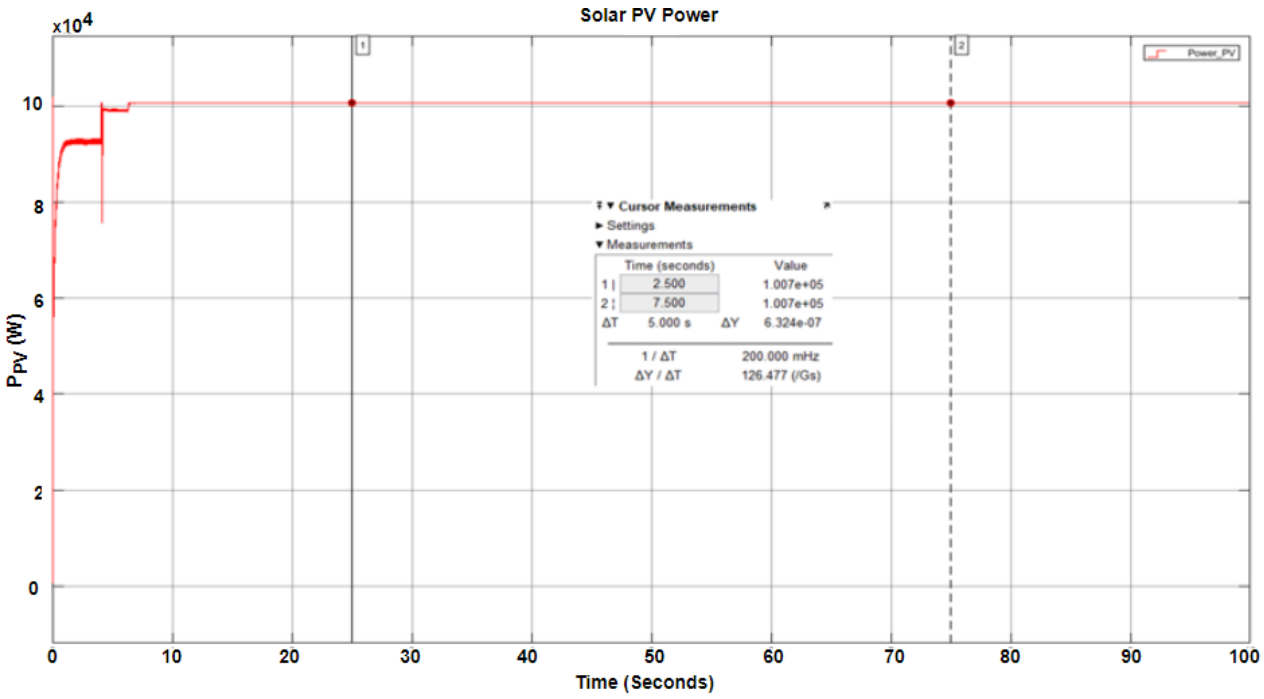

Figure 5.8: Solar PV system output power

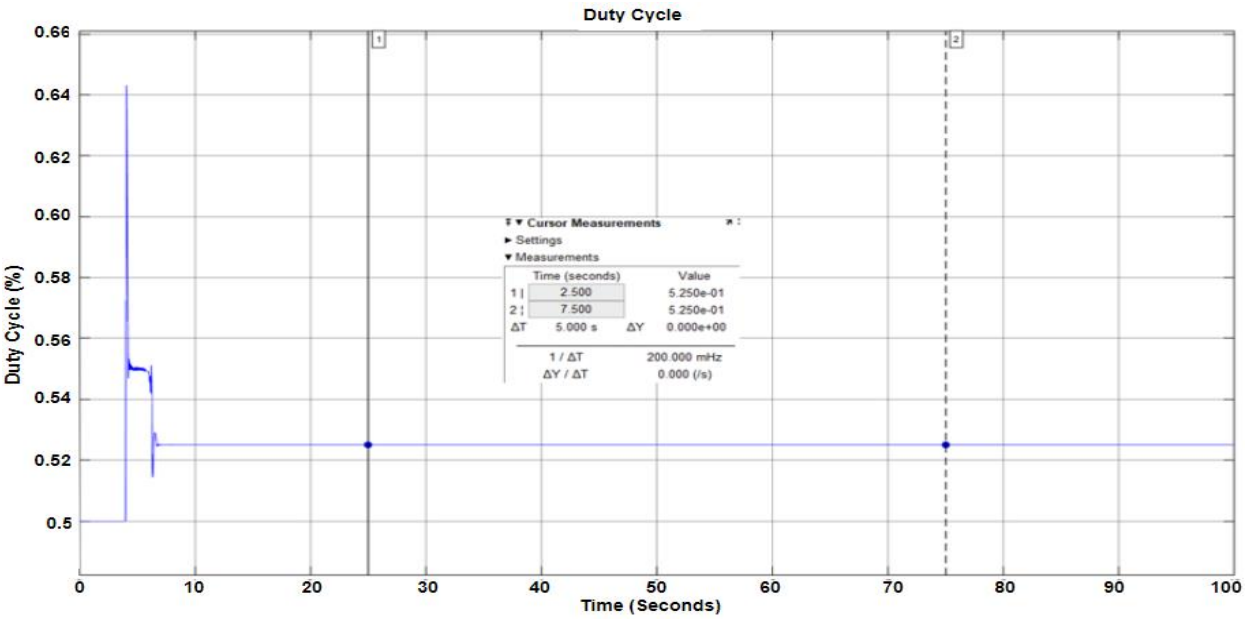

Figure 5.9: Solar PV system initial variation duty cycle

An overview of the simulated values of the PV system is shown in figure 5.10 and figure 5.11 respectively. These values are close to the calculated values in chapter 4 which is an indication of the correctness and reliability of the design and modelling. Though, and variation in the solar irradiance has a significant impact on the power output of the PV system likewise the temperature. Increasing the temperature will lead to a decrease in the PV system output power while an increase in the solar irradiance will cause an increase the power output of the solar PV. This relationship is very vital in the design and modelling of PV systems considering the geographical location.

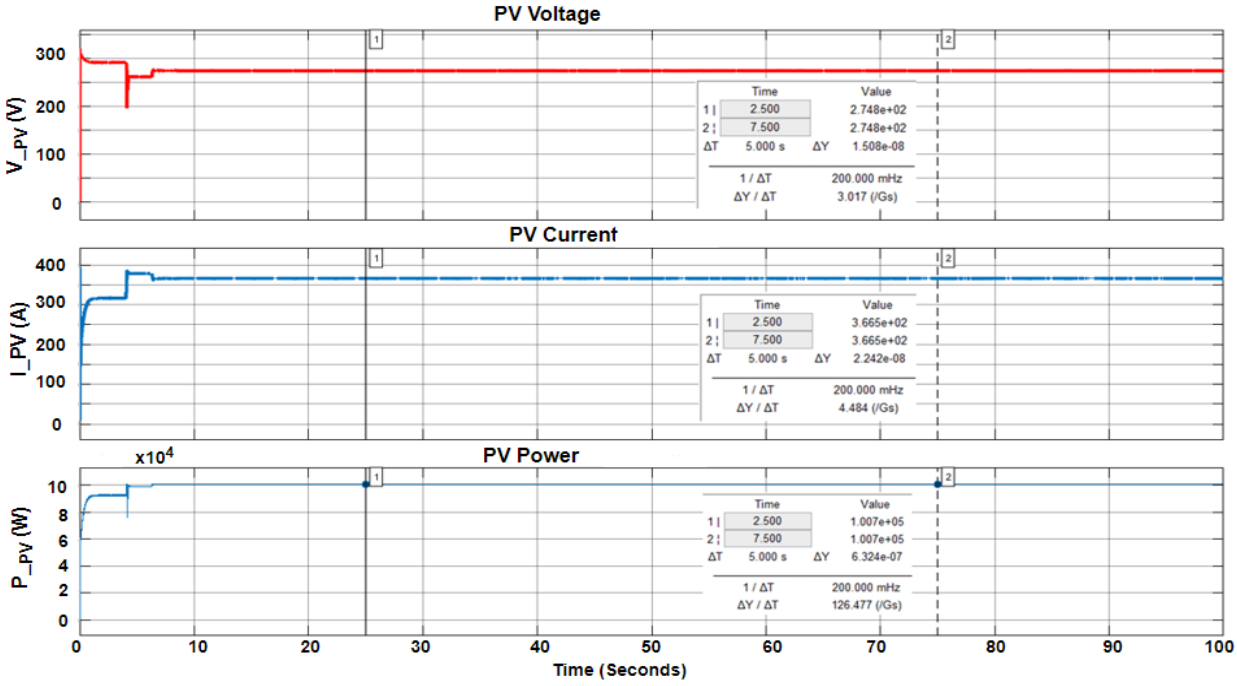

Figure 5.10: Simulated output values of the PV system

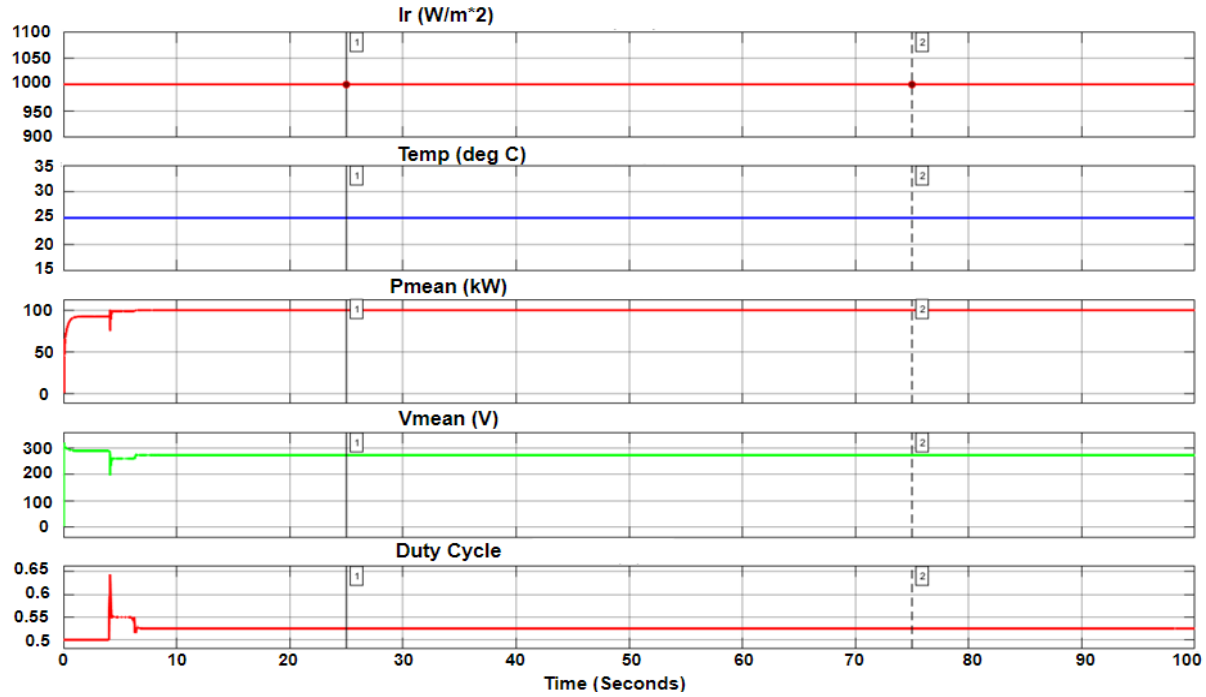

Figure 5.11: Solar PV system simulated values: solar irradiance, temperature, etc

5.3 DC-DC boost converter simulation results

The DC-DC boost converter output voltage in relation to simulation time is presented in figure 5.12 while the voltage before the boost converter is shown in figure 5.7. The output voltage is stable throughout the simulation period at 584 Vdc. Although, such design allows

a standard deviation of 1 %, the simulated boost voltage has the same value with the calculated boost voltage obtained in chapter 5. This shows an accurate, reliable, and stable output voltage immediately after the DC-DC boost converter.

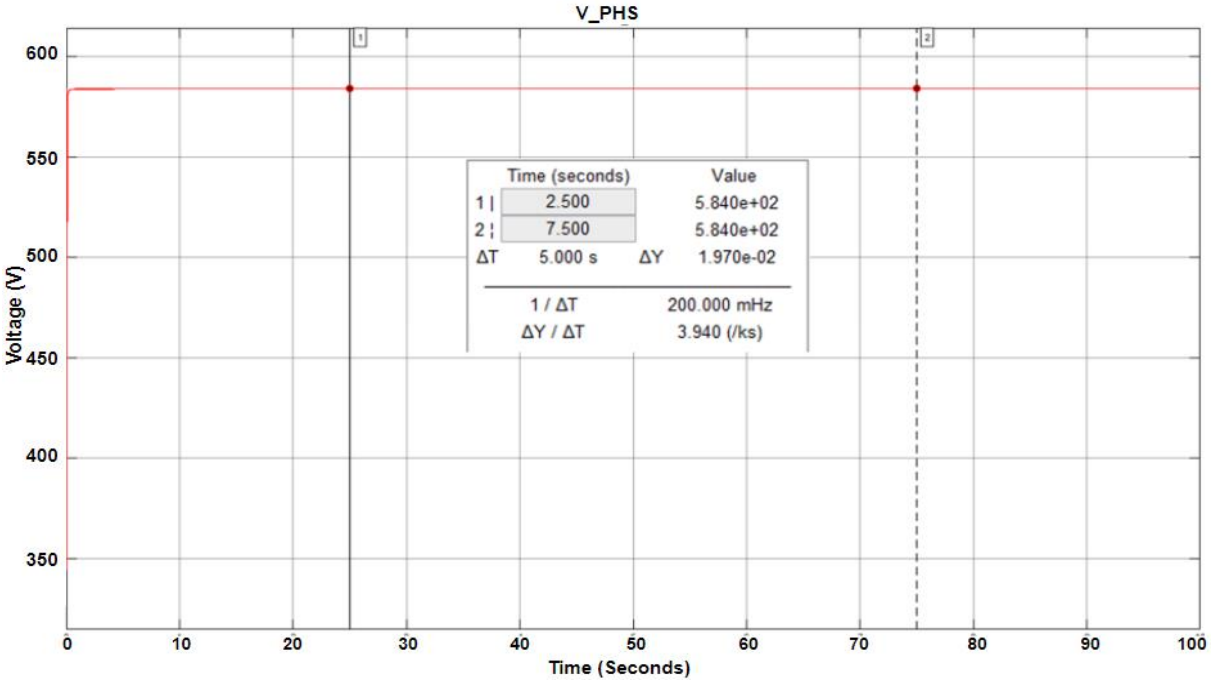

Figure 5.12: DC-DC boost converter Output voltage

5.4 Reservoir water level, PHS current, voltage and available power

The reservoir specification, which includes output power, water level current and voltage, is shown in figure 5.13. These values are very vital and provides much information about the reservoir capacity including how much power it can generate and the load it can supply.

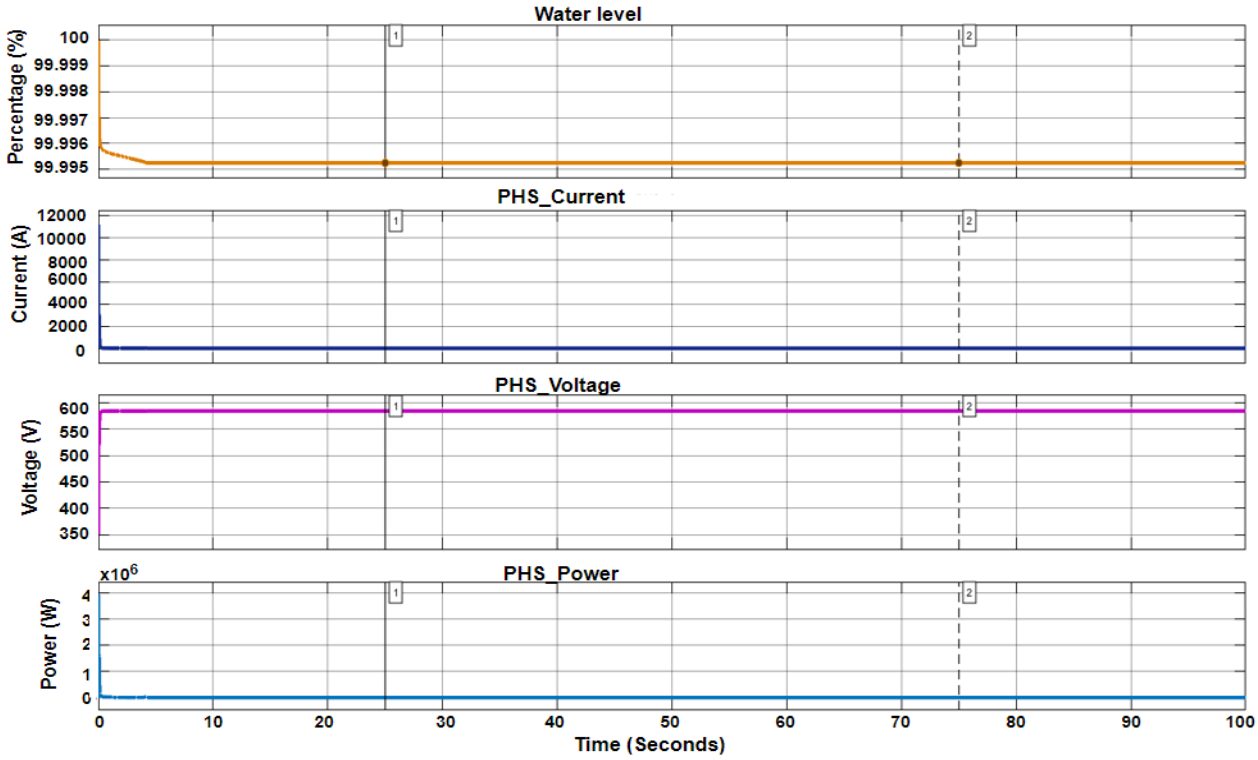

Figure 5.13: Reservoir water level, PHS current, voltage and available power

5.5 DC Microgrid simulation results

In this study, simulation results are conducted in the MATLAB/Simulink environment to validate the controller performance on the DCMG system. Three scenarios are conducted to demonstrate the effective operation and control of the DC microgrid system based on the solar PV power output, solar irradiance, water level in the reservoir and load conditions. These are used to authenticate (evaluate) the entire DC microgrid and the pumped hydro storage system's capacity to meet the load demand and maintain stability in the DC microgrid network. In addition, using scenarios offers a tried-and-true methodology and approach, improves comprehension while keeping the main objective in mind, and provides helpful guidelines. Therefore, table 5.1 presents the various scenarios and operating modes.

Table 5.1: Scenarios, description and conditions

Description	L_{D1}	L_{D2}	PHSS
Scenario 1 ($P_{PV} > L_{DT}$)			
The total power produced by the solar PV is greater than the total load demand and the excess power is used to pump water up the reservoir.	ON	ON	ON
Scenario 2 ($P_{PV} = L_{DT}$)			
The total power generated is equal to the load demand. The reservoir was turned off during this time because the water level had reached the upper permissible limit while still supplying loads 1 and 2. As a result, the PHSS is kept in reserve mode.	ON	ON	OFF
Scenario 3 ($P_{PV} < L_{DT}$)			
The PHSS is discharging because the load demand exceeds the power generated. Because the PHSS and solar PV output is only enough to power load 1, the load 2 is disconnected.	ON	ON	OFF
Scenario 4 (PHSWL > 20%)			
In this scenario, the power from the PHSS was used to augment the power supply to meet the total load demand (L_{DT}).	ON	ON	ON
Scenario 5 (PHSWL < 20%)			
In this scenario, the PHSS has reached its limit of discharge, hence, it was disconnected and LD2 was shut down. The PHSS was charged with the excess power generated from the solar PV.	ON	OFF	OFF
Scenario 6 (PHSWL $\geq L_{DT}$)			
During this stage, the PHSS was used to supplement power to the load until the water level in the reservoir drops to 20% and gets disconnected.	ON	ON	ON

5.5.1 Scenario 1 (where $P_{PV} > L_{DT}$)

Power generated from the solar PV is greater than the primary load (Load 1) and the water level in the reservoir is less than 98%, then, the PHS is run as a motor to recharge the upper reservoir and load 1 is supplied. In this case, the secondary load (load 2) is disconnected because the excess power from the solar PV is used to recharge the reservoir which is a fundamental priority. Hence, figure 5.14 shows that the current through load 1 is 151.6 A at 2.5 seconds and 151.7 A at 7.5 seconds respectively. Figure 5.15 and 5.16 shows the voltage and power during scenario 1. The power dropped from 100 kW to 80.7 kW due to losses in the system but still within an acceptable range as shown in figure 5.16.

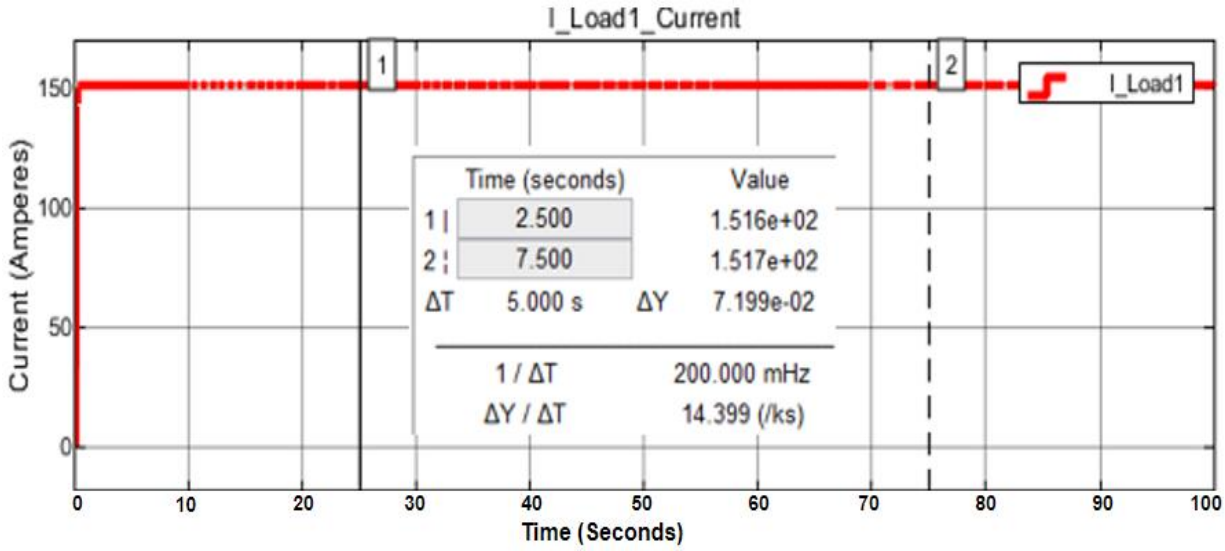

Figure 5.14: Current flowing through primary load (Load 1)

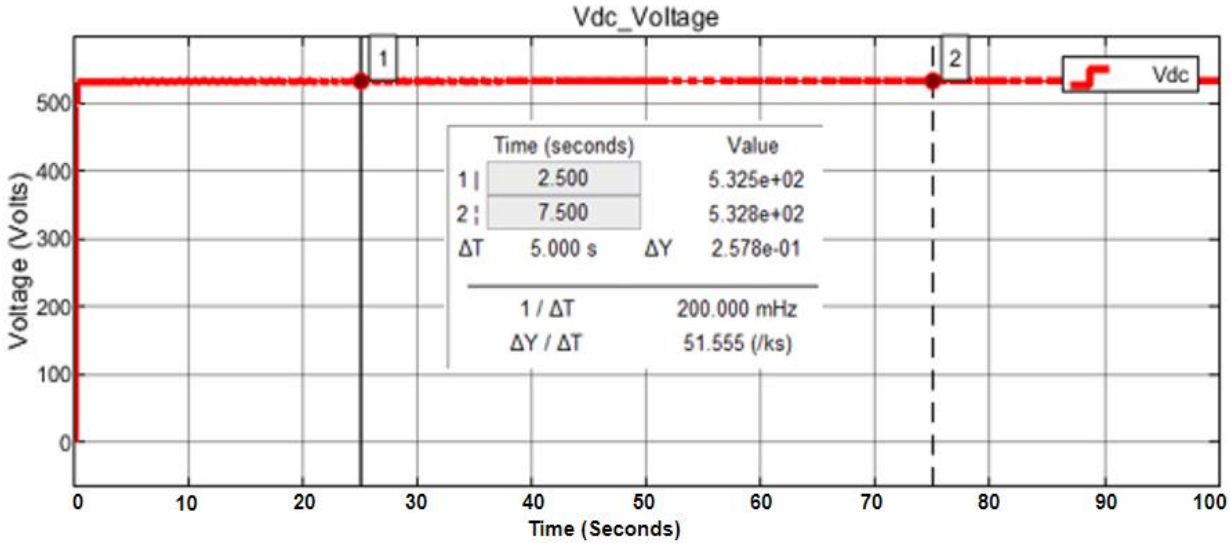

Figure 5.15: Voltage across primary load (Load 1)

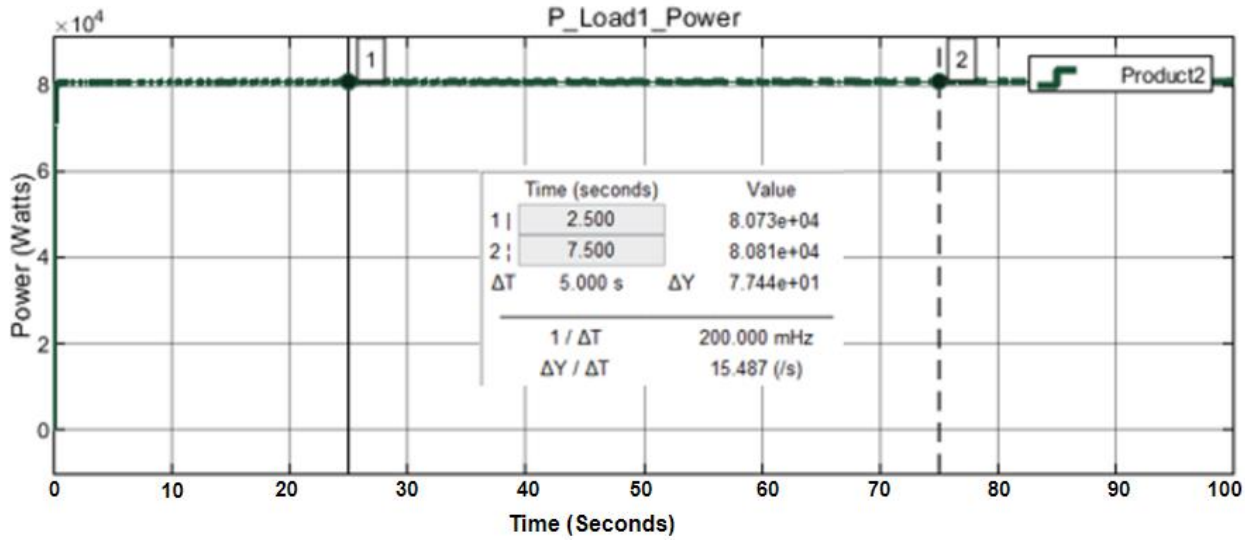

Figure 5.16: Input power to primary load (Load 1)

The current and power have both negative values as shown in figure 5.17 because the excess power generated from the solar PV is used to recharge the reservoir and load 2 is disconnected during this period.

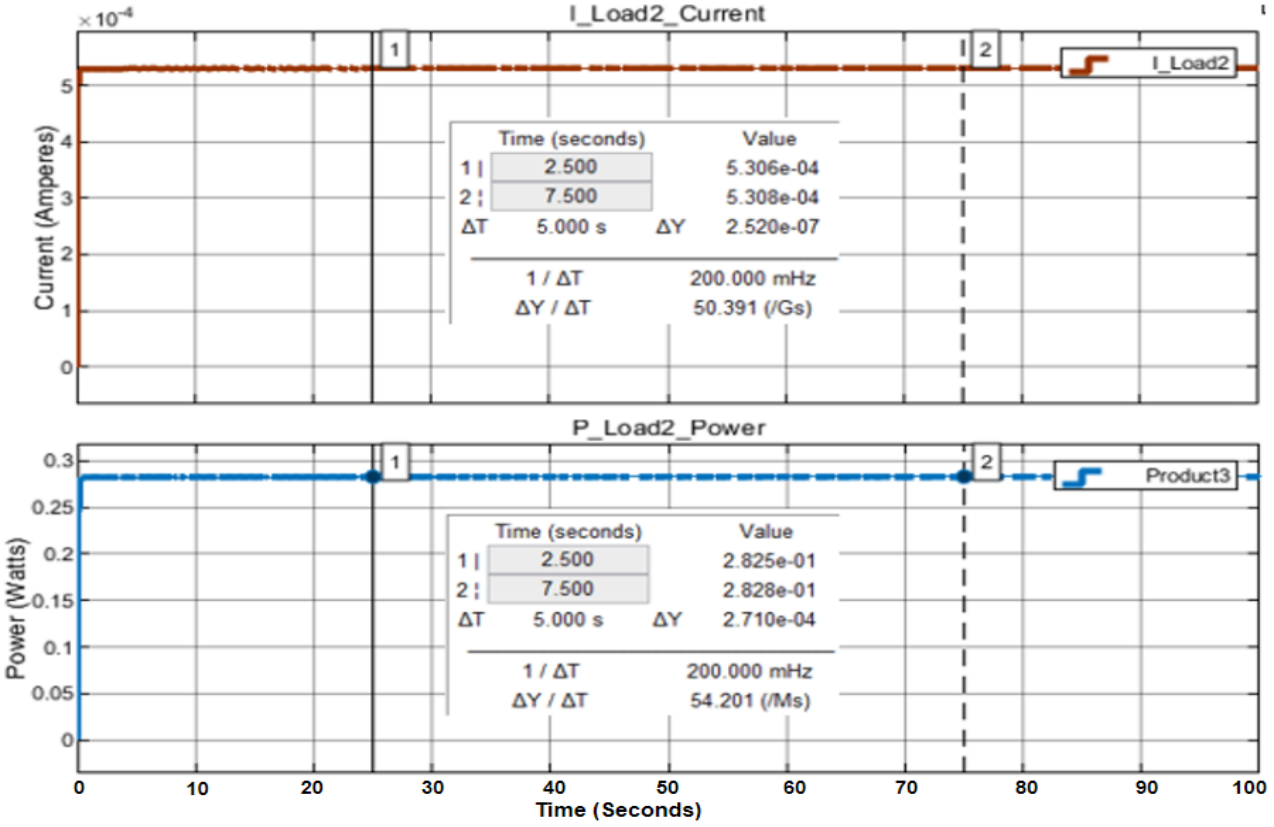

Figure 5.17: Current and power

5.5.2 Scenario 2 (where $P_{PV} = L_{DT}$)

The solar PV power output is greater than the primary load (load 1) and the water level in the reservoir is greater or equal to 98%, then supply both load 1 and the secondary load (load 2). In this case, the water reservoir is disconnected because the water level in the reservoir has reached the maximum allowable point, hence, the excess power generated by the solar PV is used to supply the secondary load.

The current flowing through load 1 using scenario 2 is shown in figure 5.18. The current is constant throughout the simulation time of 10 seconds at 165.2 A. In addition, the power input to load 1 using scenario 2 is shown in figure 5.19. The result indicated a power drop from 100.7 kW to 95.81 kW due to losses.

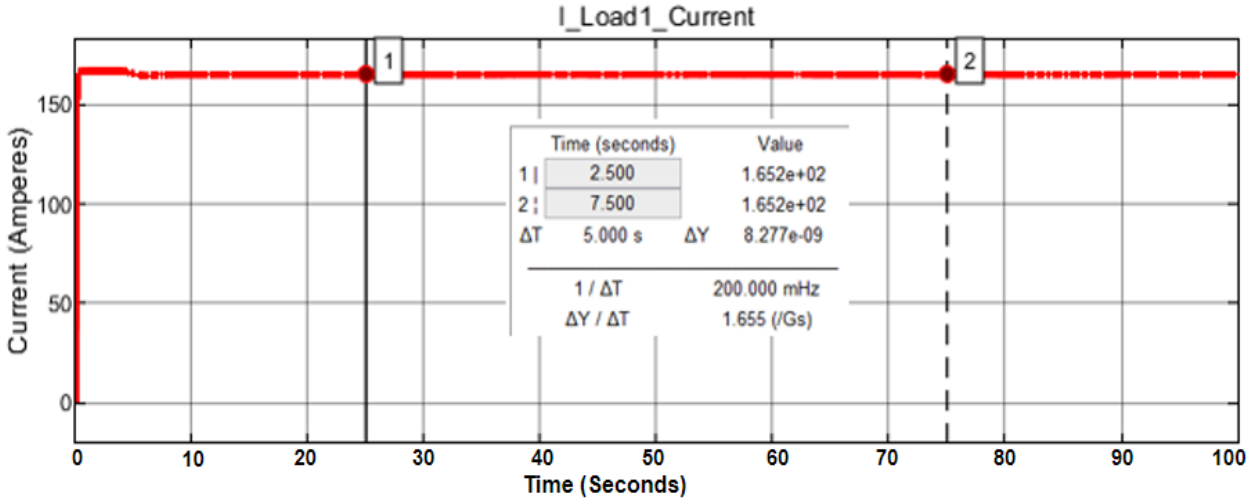

Figure 5.18: Current flowing through primary load (Load 1)

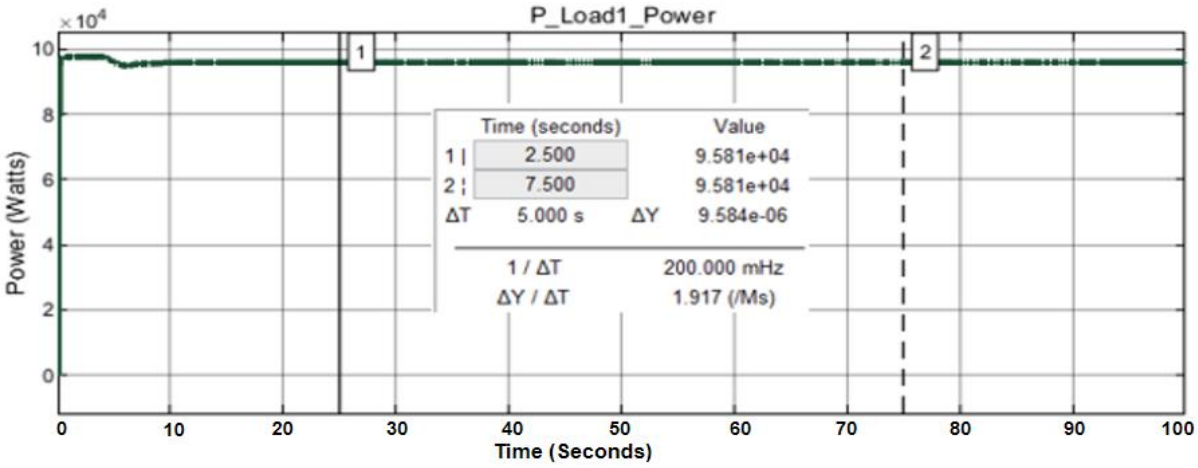

Figure 5.19: Input power to primary load (Load 1)

The current flowing through the secondary load (load 2) is shown in figure 5.20. A constant current of 7.23 A flows through the secondary load during case study 2. Furthermore, the power supply to load 2 is 4.191 kW as shown in figure 5.21. This is less than the power

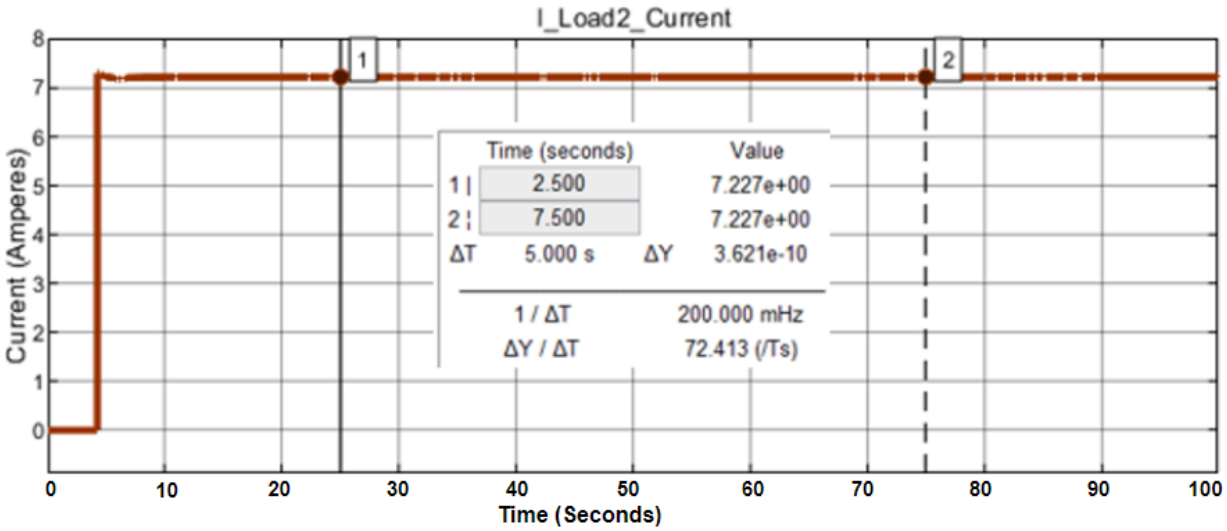

supply to load 1 during the same scenario due to difference in load demand.

Figure 5.20: Current flowing through secondary load (Load 2)

Figure 5.21: Input power to secondary load (Load 2)

The DC voltage and current is shown in figure 5.22 and 5.23 respectively. However, the same voltage seats across load 1 and load 2 because they are connected in parallel. The voltage is approximately 580 V, and the current is 172.4 A respectively.

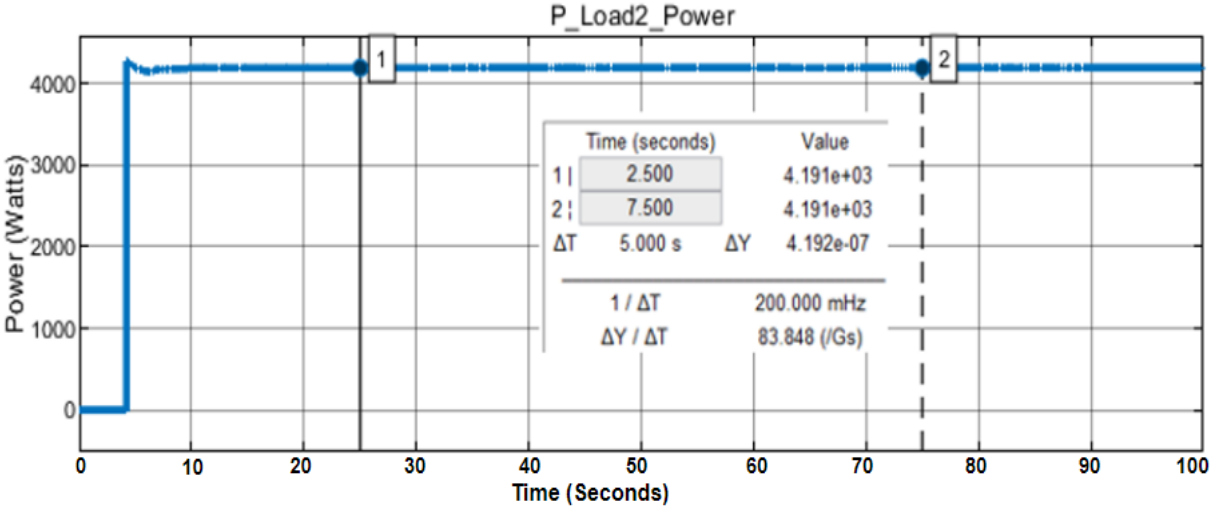

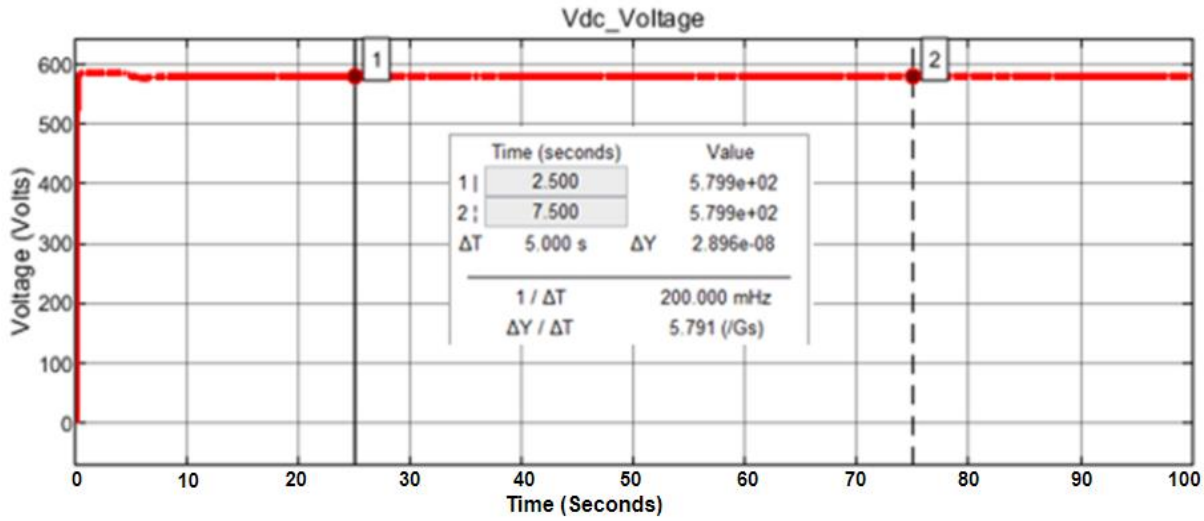

Figure 5.22: DC voltage across both loads

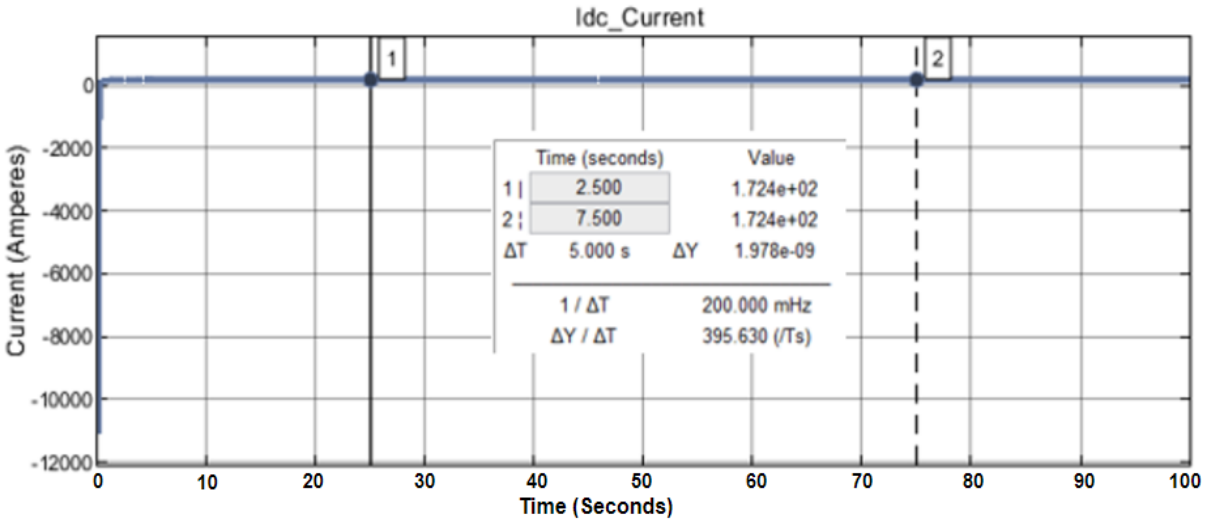

Figure 5.23: The supply current

5.5.3 Scenario 3 (where $P_{PV} < L_{DT}$)

The solar PV power output is less than the primary load demand and the water level in the reservoir is greater than or equal to 10%, then discharge the water in the upper reservoir enough to supply the primary load (discharge). In this case the secondary load (load 2) is disconnected because the total power generated by the solar PV is less than the primary load. Hence, load 1 is supplied from a combination of power from both the solar PV and PHSS at an irradiance of 500 W/m^2 and temperature of 25 ℃ as shown in figure 5.24.

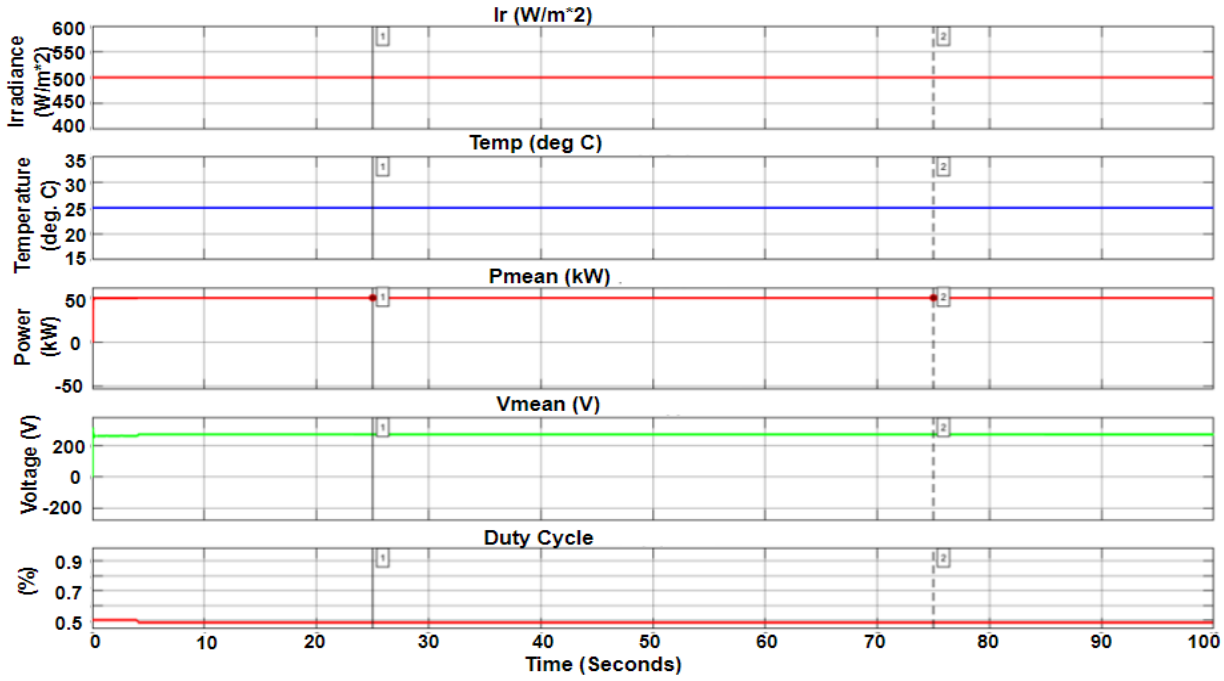

Figure 5.24: Solar PV parameters for case study 3

The DC link voltage and current indicating the amount of power available in scenario 3 is shown in figure 5.25 and 5.26 respectively. The product of these values represents the total power generated by both the solar PV and the PHSS when discharging because the amount

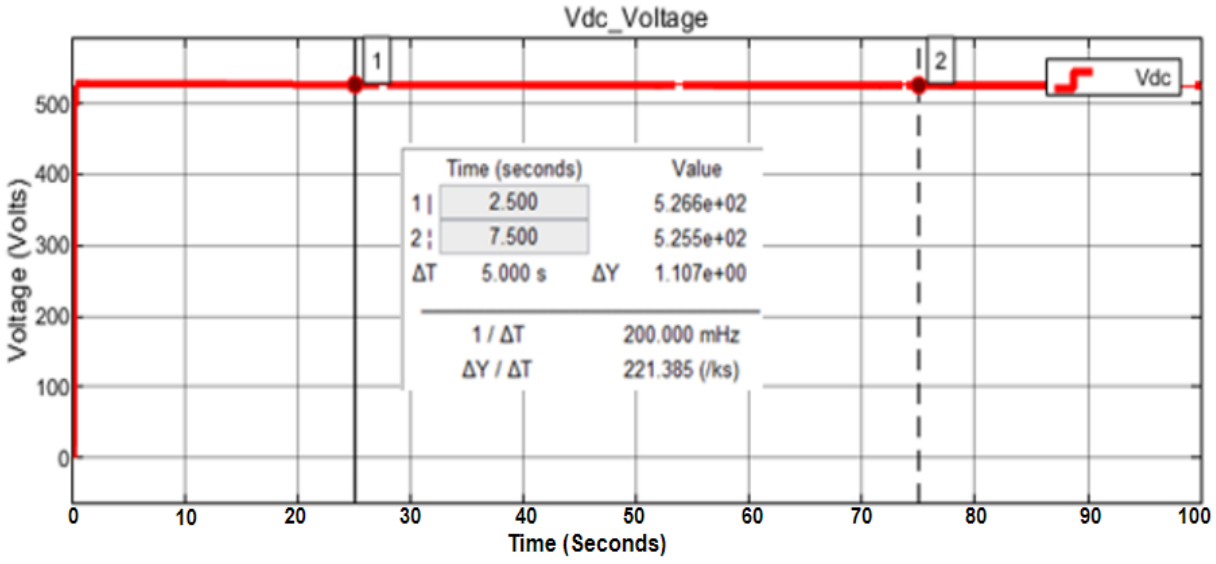

of power generated by the solar PV is less than the primary load.

Figure 5.25: DC link voltage (Vdc)

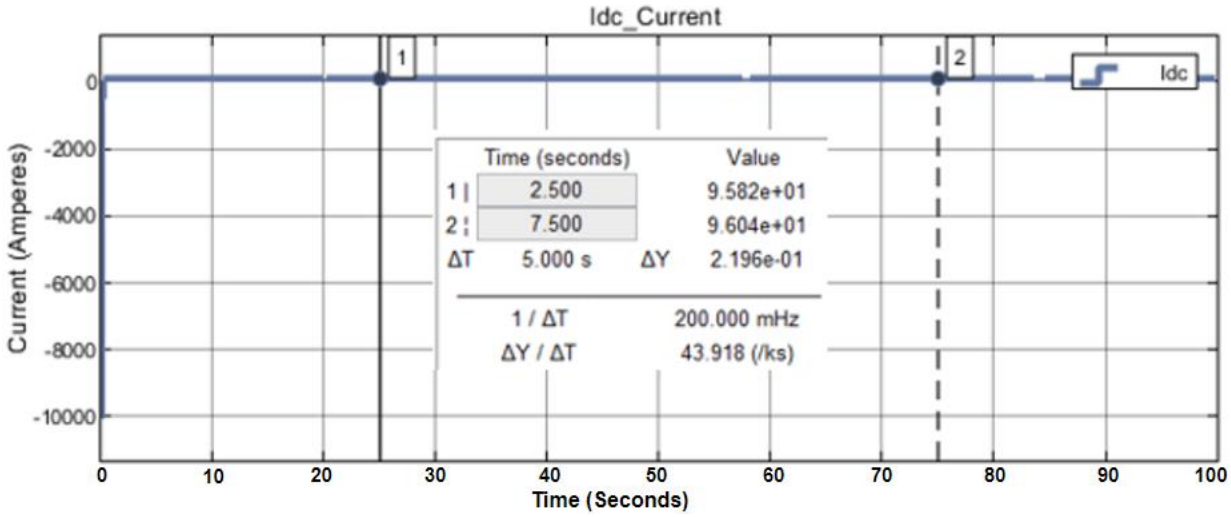

Figure 5.26: Input current

Approximately, a current 150.2 A flows through load 1 in scenario 3 as shown in figure 5.27. This indicates that the primary load (load 1) is supplied. In addition, a total power of 78.7 kW is available to load 1 as shown in figure 5.28. This shows an adequate power supply to load 1 which is a combination of both power supply from the solar PV and PHSS.

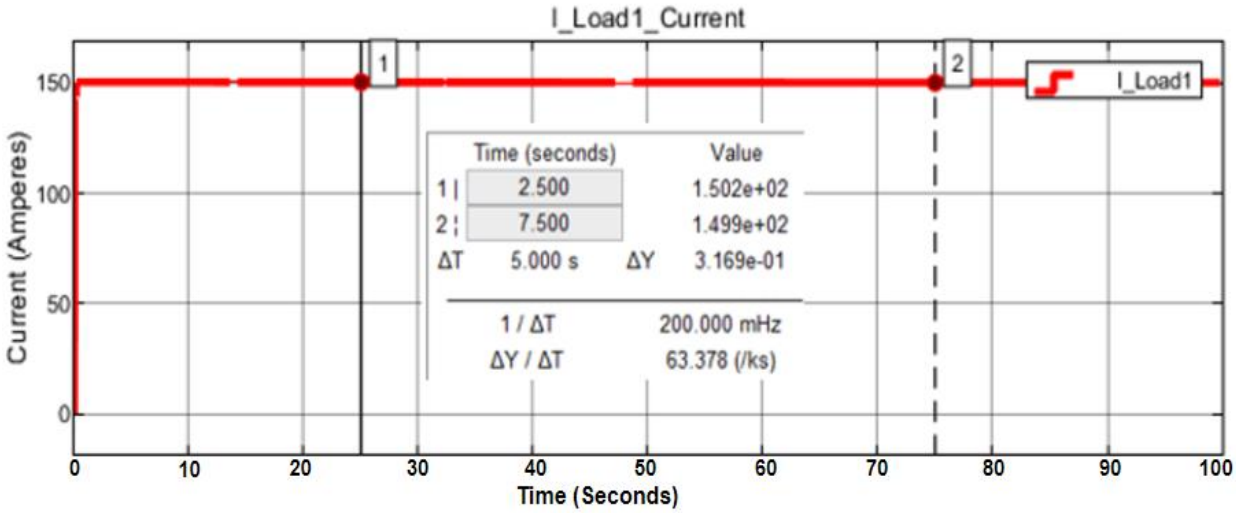

Figure 5.27: Current flowing through primary load (Load 1)

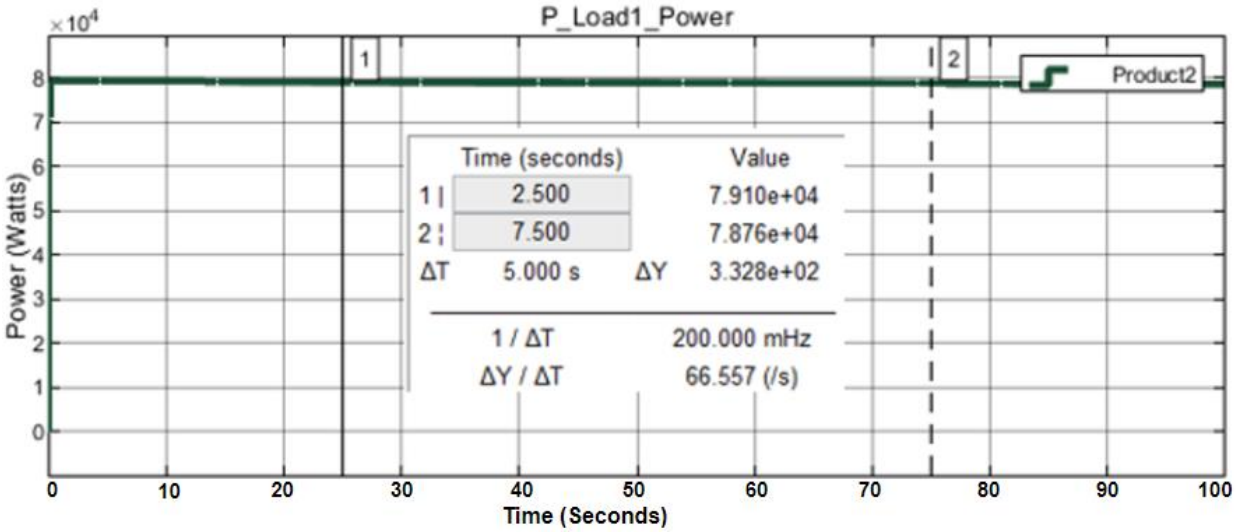

Figure 5.28: Power supply to primary load (Load 1)

The current flow through load 2 and the available power are both negatives as shown in figure 5.29 and 5.30 respectively because the available power was only enough to supply the primary load (load 1). This is also due to the fact that the secondary load (load 2) is disconnected because the power available is not enough to supply both loads in the system.

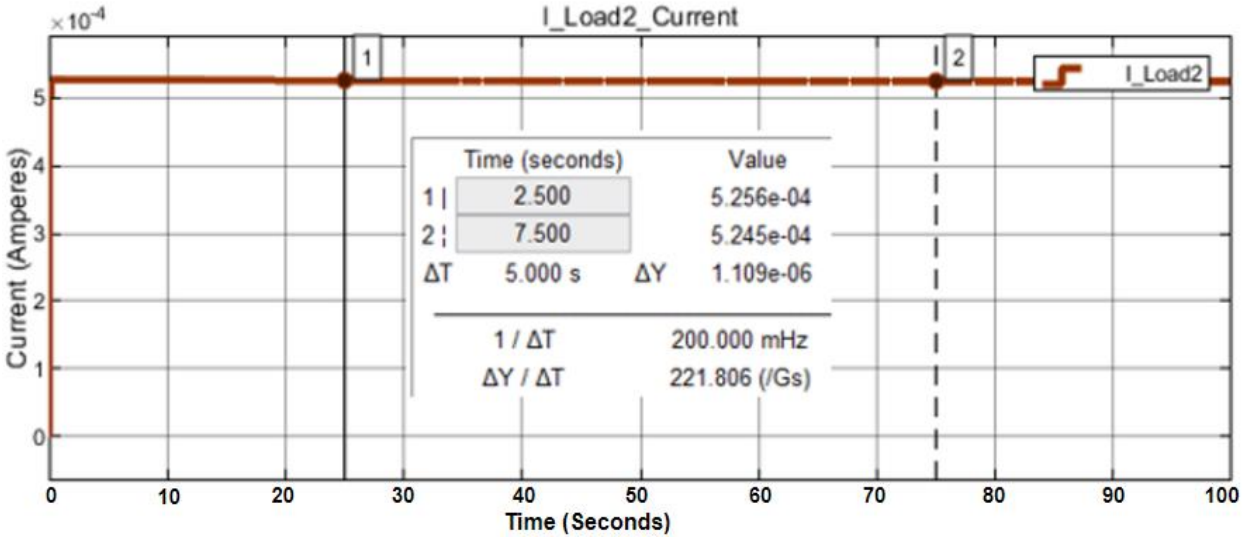

Figure 5.29: Current flowing through secondary load (Load 2)

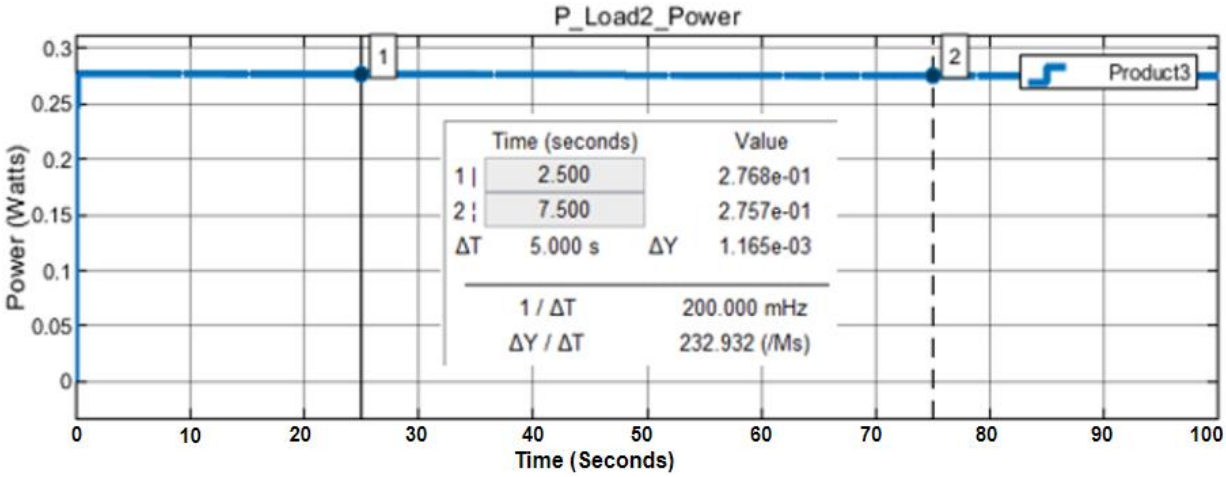

Figure 5.30: Input power to secondary load (Load 2)

5.6 Conclusion

This chapter presented the simulation results obtained for the DCMG system. The model was developed to ensure effective energy management of a pumped hydro storage system in an off-grid DCMG system. This was developed in the MATLAB/Simulink environment using fuzzy logic and the simulation results are presented accordingly. The simulation result of the solar PV system was presented in section 5.2 and DC-DC boost converter result was presented in section 5.3, showing the voltage before and after the boost converter. Thereafter, the simulation results showing the water level in the upper reservoir, PHS current, voltage and available power were presented in section 5.4. In section 5.5 was the simulation results showing the three different scenarios were presented. Firstly, the power output is greater than the load demand and the water level in the reservoir is less than 98% (recharge). The second case is when the solar PV power output is equal to the total load demand and the water level in the reservoir is greater or equal to 98%. The third case is when the solar PV power output is less than the primary load and the water level is greater than or equal to 10% (discharge). Energy management in a DCMG system is very important to ensure effective power distribution due to the intermittent nature of the renewable energy sources. Hence, the energy management system in this study is aimed at ensuring effective power distribution between the solar PV and the PHSS with keen interest in optimizing both sources. Summary of all scenarios are presented in table 5.2 where, P_{PV} is solar PV power output, PHSS is pumped hydro storage system, L_{DT} is total load demand, L_{D1} is primary load, L_{D2} is secondary load and PHSWL is pumped hydro storage water level.

Table 5.2: Summary of scenarios and results

Scenarios	L_{D1}	L_{D2}	PHSS	Evaluation
$P_{PV} > L_{DT}$	1	1	1	In this scenario, the total power produced by the solar PV was 80.7 kW and the load demand was 71.4 kW. The excess power produced was used to pump water into the reservoir as shown in figures 5.14, 5.15 and 5.16 respectively.
$P_{PV} = L_{DT}$	1	1	0	In this scenario, the power generated was 99.7 kW and the load demand was 99 kW as shown in figure 5.19, 5.21, 5.22 and 5.23 respectively. During this period, both load 1 and load 2 were supplied and water reservoir was disconnected because the water level in the reservoir has reached the maximum allowable point. Hence, the PHSS was maintained in the reserve mode.
$P_{PV} < L_{DT}$	1	1	1	In this scenario, the total power generated was less than the load demand and the PHSS was used to augment the power shortage. The secondary load was disconnected because the total power generated from the solar PV and the PHSS was only sufficient for load 1.
PHSWL = 80%	1	1	1	During this stage, the PHSS was used to supplement power to the load until the water level in the reservoir gets to 20% and gets disconnected.

PHSWL < 20%	1	0	0	In this scenario, the PHSS has reached its limit of discharge, hence, it was disconnected and L_{D2} was shut down. The PHSS was charged with the excess power generated from the solar PV.
PHSWL > 20%	1	1	1	In this scenario, the power from the PHSS was used to augment the power supply to meet the total load demand (L_{DT}).

The results showed that the proposed energy management system is effective and ensured optimization of the solar PV and PHSS in all three scenarios. When comparing the proposed energy management system and PHSS capacity and efficiency, the energy management system increased both solar PV and PHSS efficiencies. A typical PHSS efficiency is about 80 to 95% but the efficiency of the proposed PHSS is about 92%. The result of this study is compared with two other studies conducted in the past that used different method other than fuzzy logic and different energy storage systems other than PHSS. The comparison on the DC bus voltage regulation and energy storage efficiency are shown in table 5.3 where, the first scenario is for this study.

Table 5.3: Technical parameters

Studies	DC bus voltage	ESS optimization
My study	The fuzzy logic was very efficient for DC bus voltage regulation at about 97%.	92%
(Singh et al., 2012)	The efficiency of the PI controller used for the DC bus voltage regulation was about 93%	87%
(Chauhan et al., 2015)	The efficiency of the PID controller for DC bus voltage regulation was about 92%.	85%

Based on the above evaluation using table 5.3, the proposed EMS using fuzzy logic implemented in the MATLAB/Simulink environment has shown to be more suitable for DC bus voltage regulation and the PHSS has better efficiency when compared to other types of energy storage system (ESS). Consequently, the proposed EMS ensures effective power distribution between the solar PV and the PHSS hence improving the DCMG system resilience and reliability.

CHAPTER 6: CONCLUSION AND RECOMMENDATION

6.1 Conclusion

The primary aim of this research was to implement an efficient power flow control system in an autonomous solar PV-hydro DC microgrid system using fuzzy logic controller strategy. This was efficiently achieved by designing a suitable controller for the DC microgrid system in the MATLAB/Simulink environment using fuzzy logic controller. The system is designed for an islanded DC microgrid with voltage and power control function. It comprises of three basic components namely: solar PV as the main power supply, pumped hydro storage system that serves as an energy storage system and a variable load implemented in the MATLAB/Simulink environment. The performance was analysed using variable loads under different time scales. The load is grouped into two categories: the primary load (load 1) and the secondary load (load 2) which depends on water level in the reservoir and the power generated by the solar PV. A bi-directional communication between the load, solar PV, and pumped hydro storage system is implemented using a fuzzy logic controller and switches to ensure effective power distribution in the system determined by the availability of power and load demand at any particular moment. The load was properly supplied using both sources at different times to proof the effectiveness of the controller.

The second and third objectives was to present a detailed literature review on autonomous hybrid solar PV-hydro applications in DC microgrid and a feasibility study on fuzzy logic controller as a mechanism capable of DC microgrid power control. The literature indicated that fuzzy logic controller is appropriate for DC microgrid system power distribution and control. Other methods were studied but fuzzy logic controller offered unique advantage and flexibility in power regulation. Fuzzy logic controllers can easily be configured, applied to both small and large non-linear power systems, and used in a variety of operating situations. They also have no effect when parameter values are changed. The logic is robust and simple, it can handle various input variables, and it can make a precise choice with the help of a precise function, all of which make FLC an excellent solution to complicated problems. FLC is an artificial decision maker that operates in a closed-loop system in real-time.

The fourth objective of this research was to model a solar PV-hydro system using MATLAB/Simulink software. This was achieved by carefully simulating the solar PV and the pumped hydro system in the MATLAB/Simulink environment. A solar PV with a power rating of 100 kW was properly calculated and modelled as the primary renewable energy source in the network. In addition, a proper specification of the upper and lower reservoirs, pump motors and hydro turbine for the hydro storage system were implemented. To ascertain that

the objective was met, a fuzzy logic controller (FLC) was implemented to control the power flow from the solar PV and the pumped hydro storage (PHS) system. The result showed that power control was effective and the FLC functioned as predicted. The PHS was modelled to operate between 20% and 80% hence, it stops charging when it gets to the maximum water level or begin discharging. The PV system output current is 366.5 A, voltage is 274.8 Vdc and the actual power generated by the solar PV is 100.7 kW.

The fifth objective was to model a control system capable of balancing the unstable solar power supply and the ever-changing load demand using fuzzy logic controller in the MATLAB/Simulink environment. This objective was achieved by ensuring that load is shared equally between the solar PV and the PHS based on the power demand and availability. The results obtained in MATLAB/Simulink showed that the power was effectively distributed and the load was properly supplied at all times using the reservoir water level, solar PV power output and the load demand. The PHS responded swiftly in events that the solar PV output power was less than the load in the DC microgrid system.

The sixth objective was to develop a system that will control the amount of power generated and consumed in the system using fuzzy logic controller in the MATLAB/Simulink environment. To proof the success of this objective, the amount of power available at any particular point was measured against the load demand. The results obtained showed that the amount of power produced was equal to the load demand and any excess power was used to charge the PHS. This was also compared with existing literature to further ensure its effectiveness to meet the power demands when required. The solar PV produced 78 kW, which is greater than the primary load, and the PHSWL was less than 20%.

The last objective was to model varying solar irradiances that will mimic the unbalanced power supply from the solar PV using MATLAB/Simulink including a system that will implement a load-shedding strategy when the power generated is less than the power demand. To achieve this objective and to ascertain the effectiveness of the controller and effective power distribution in the system, three scenarios were tested. In the first scenario, the total power generated by the solar PV was greater than the primary load (Load 1), water level in the reservoir was less than 98%, PHSS was operated as a motor to recharge the upper reservoir and load 1 was supplied. In this scenario, the secondary load (load 2) was disconnected because the excess power from the solar PV was used to recharge the upper reservoir. The solar PV output power was 100 kW while the load demand was 71.2 kW and the excess power of 28.8 kW was used to recharge the reservoir. In the second scenario, the solar PV power output was greater than the primary load (load 1) and the water level in the reservoir was greater or equal to 98%, hence, both primary and secondary loads were

supplied. In this scenario, the water reservoir was disconnected because the water reservoir was completely full hence, the excess power generated by the solar PV was used to supply the secondary load (load 2). In the third scenario, the solar PV power output was less than the primary load and the water level in the reservoir was greater than or equal to 20%, hence, the water from the upper reservoir was discharged to supply the primary load (discharge mode). In this scenario the secondary load (load 2) was disconnected because the total power generated by the solar PV was less than the primary load, i.e., load 1 was supplied from a combination of the solar PV and PHSS powers at an irradiance of 500 W/m2 and temperature of 25 ℃. The solar PV output was 50 kW while the load demand was 71.2 kW.

The DCMG system can be remodelled using different parameters and sizes of individual components according to design requirements aimed at effective energy management. Again, the results showed that it is practical to use pumped hydro storage system in autonomous DCMG system for effective energy management. In addition, based on the commanded signals and the prevailing power availability and load demands, the pumped hydro storage system can respond swiftly and participate in DC microgrid power stability. The system used independent, easy to implement and not complex control techniques such as switches. The control method used can be implemented using multiple renewable energy sources and the system is also scalable depending on what the research is set to accomplish. The choice of pumped hydro storage system showed a major advantage in power management because the power from the pumped hydro storage system can be regulated by offering flexibility to the user according to reservoir size and water level.

6. 2. Recommendations and future work

Since energy storage systems are essential to DCMG stability, various energy storage technologies, such flywheels, supercapacitors, and others, should be researched to determine the optimal technical and financial choice over a range of timescales. In addition, integrating fuel cells to DC microgrid will improve the reliability of the network, improve power quality and provide a more sustainable network. Therefore, a study is required in this regard. Again, the interconnection of DC microgrid to AC grid network should be studied with different power sources because implementing this will offer scholars the opportunity to understand the network's response to certain power sources and its ability to support ancillary services such as frequency regulation. However, in the case of low inertia AC grid network, adequate study is required on the integration of renewables to AC grid using DC microgrid. Finally, a study should be conducted on low cost and commercially viable DC-DC

converters capable of connecting the DC loads to distribution lines because there are several DC loads that are in use globally at the moment.

REFERENCES

Abolhosseini, S., Heshmati, A. & Altmann, J. 2014. *A Review of Renewable Energy Supply and Energy Efficiency Technologies*. Bonn, Germany.

Adefarati, T. & Bansal, R.C. 2016. Integration of renewable distributed generators into the distribution system: A review. *IET Renewable Power Generation*, 10(7): 873–884.

Alanazi, A., Lotfi, H. & Khodaei, A. 2017. Coordinated AC/DC Microgrid Optimal Scheduling. *arXiv*.

Aliyu, M., Hassan, G., Elamin, I.M., Said, S.A., Siddiqui, M.U. & Alawami, A.T. 2018. A review of solar-powered water pumping systems. , 87(March 2017): 61–76.

Aminu, M. & Solomon, K. 2016. A Review of Control Strategies for Microgrids. *Advances in Research*, 7(3): 1–9.

Aneke, M. & Wang, M. 2016. Energy storage technologies and real life applications – A state of the art review. *Applied Energy*, 179: 350–377. http://dx.doi.org/10.1016/j.apenergy.2016.06.097.

Augustine, S., Quiroz, J.E., Reno, M.J. & Brahma, S. 2018. *DC Microgrid Protection : Review and Challenges*. California, USA.

Baboli, P.T., Shahparasti, M., Moghaddam, M.P., Haghifam, M.R. & Mohamadian, M. 2014. Energy Management and Operation Modelling of Hybrid AC-DC Microgrid. *IET Generation, Transmission and Distribution*, 8(10): 1700–1711.

Bagyaveereswaran, V., Mathur, T.D., Gupta, S. & Arulmozhivarman, P. 2016. Performance comparison of next generation controller and MPC in real time for a SISO process with low cost DAQ unit. *Alexandria Engineering Journal*, 55(3): 2515–2524. http://dx.doi.org/10.1016/j.aej.2016.07.028.

Bajpai, P. & Dash, V. 2012. Hybrid renewable energy systems for power generation in stand-alone applications : A review. *Renewable and Sustainable Energy Reviews*, 16(5): 2926–2939.

Benavente, F., Lundblad, A., Campana, P.E., Zhang, Y., Cabrera, S. & Lindbergh, G. 2019. Photovoltaic/Battery System Sizing for Rural Electrification in Bolivia: Considering the Suppressed Demand Effect. *Applied Energy*, 235(October 2018): 519–528.

Bevrani, H., Watanabe, M. & Mitani, Y. 2014. *Power System Monitoring and Control*. Hoboken, New Jersey.: John Wiley & Sons, Inc.

Bhandari, B., Lee, K., Lee, G., Cho, Y. & Ahn, S. 2015. Optimization of Hybrid Renewable Energy Power Systems : A Review. , 2(1): 99–112.

Bharath, K.R., Krishnan Mithun, M. & Kanakasabapathy, P. 2019. A Review on DC Microgrid Control Techniques, Applications and Trends. *International Journal of Renewable Energy Research*, 9(3): 1328–1338.

Blasi, B.R. 2013. *DC Microgrids: Rewiev and Applications*. Kansaa State University.

Chauhan, R.K., Rajpurohit, B.S., Hebner, R.E., Singh, S.N. & Longatt, F.M.G. 2015. Design and Analysis of PID and Fuzzy-PID Controller for Voltage Control of DC Microgrid. In *Proceedings of the 2015 IEEE Innovative Smart Grid Technologies - Asia, ISGT ASIA 2015*.

Chen, H., Cong, T.N., Yang, W., Tan, C., Li, Y. & Ding, Y. 2009. Progress in Electrical Energy Storage System: A Critical Review. *Progress in Natural Science*, 19(3): 291–312. http://dx.doi.org/10.1016/j.pnsc.2008.07.014.

Chong, L.W., Wong, Y.W., Rajkumar, Rajprasad Kumar, Rajkumar, Rajpartiban Kumar & Isa, D. 2016. Hybrid energy storage systems and control strategies for stand-alone renewable energy power systems. *Renewable and Sustainable Energy Reviews*, 66: 174–189. http://dx.doi.org/10.1016/j.rser.2016.07.059.

Connolly, D., Lund, H., Mathiesen, B. V., Pican, E. & Leahy, M. 2012. The Technical and Economic Implications of Integrating Fluctuating Renewable Energy Using Energy Storage. *Renewable Energy*, 43: 47–60. http://dx.doi.org/10.1016/j.renene.2011.11.003.

Cordón, O. 2011. A Historical Review of Evolutionary Learning Methods for Mamdani-Type Fuzzy Rule-Based Systems: Designing Interpretable Genetic Fuzzy Systems. *International Journal of Approximate Reasoning*, 52(6): 894–913.

Dhivya, B. & Prabu, V. 2018. A Review of Renewable Energy Supply and Energy Efficiency Technologies. *International Research Journal of Automotive Technology (IRJAT)*, 1(6): 49–59.

Dong, C., Jia, H., Xu, Q., Member, Student, Xiao, J., Xu, Y., Tu, P., Member, Student, Lin, P., Li, X., Wang, P. & Member, Senior. 2018. Time-Delay Stability Analysis for Hybrid Energy Storage System With Hierarchical Control in DC Microgrids. *IEEE Transactions on*

Smart Grid, 9(6): 6633–6645.

Eid, B.M., Member, Student, Rahim, N.A., Member, Senior, Selvaraj, J. & Khateb, A.H. El. 2016. Control Methods and Objectives for Electronically Coupled Distributed Energy Resources in Microgrids : A Review. *IEEE Systems Journal*, 10(2): 446–458.

Ellabban, O., Abu-Rub, H. & Blaabjerg, F. 2014. Renewable Energy Resources: Current Status, Future Prospects and their Enabling Technology. *Renewable and Sustainable Energy Reviews*, 39: 748–764. http://dx.doi.org/10.1016/j.rser.2014.07.113.

Gao, F., Kang, R., Cao, J. & Yang, T. 2019. Primary and secondary control in DC microgrids: a review. *Journal of Modern Power Systems and Clean Energy*, 7(2): 227–242. https://doi.org/10.1007/s40565-018-0466-5.

Gil-Antonio, L., Saldivar, B., Portillo-Rodríguez, O., Ávila-Vilchis, J.C., Martínez-Rodríguez, P.R. & Martínez-Méndez, R. 2019. Flatness-based control for the maximum power point tracking in a photovoltaic system. *Energies*, 12(10).

He, F., Ma, J. & Zhao, Z. 2015. Line Loss Optimization Based OPF Strategy by Hierarchical Control for DC Microgrid. In *IEEE Energy Conversion Congress and Exposition, ECCE*. Beijing, China: IEEE: 6212–6216.

Hesse, H.C. 2017. *Lithium-Ion Battery Storage for the Grid — A Review of Stationary Battery Storage System Design Tailored for Applications in Modern Power Grids*.

Hinov, N.L., Stanev, R.H. & Vacheva, G.I. 2016. A Power Electronic Smart Load Controller for Nanogrids and Autonomous Power Systems. In *2016 XXV International Scientific Conference Electronics (ET)*. Sozopol, Bulgaria: IEEE: 1–4.

Hossain, M.S., Jahid, A., Islam, K.Z. & Rahman, M.F. 2020. Solar PV and Biomass Resources-Based Sustainable Energy Supply for Off-Grid Cellular Base Stations. *IEEE Access*, 8: 53817–53840.

Hu, J., Shan, Y., Guerrero, J.M., Ioinovici, A., Chan, K.W. & Rodriguez, J. 2021. Model predictive control of microgrids – An overview. *Renewable and Sustainable Energy Reviews*, 136(August 2020): 110422. https://doi.org/10.1016/j.rser.2020.110422.

Jia, L. & Tong, L. 2016. Renewables and Storage in Distribution Systems: Centralized vs. Decentralized Integration. *IEEE Journal on Selected Areas in Communications*, 34(3): 665–674.

John, T. 2017. *Operation and Control of Multi-Area Multi-Microgrid Systems*. Nanyang Technological University.

Kakigano, H., Miura, Y. & Ise, T. 2013. Distribution Voltage Control for DC Microgrids Using Fuzzy Control and Gain-Scheduling Technique. *IEEE Transactions on Power Electronics*, 28(5): 2246–2258.

Khoa, T.D., Trigueiro, L., Santos, D., Sechilariu, M. & Locment, F. 2016. Load Shedding and Restoration Real-Time Optimization for DC Microgrid Power Balancing. *2016 IEEE International Energy Conference (ENERGYCON)*: 1–6.

Kumar, J., Agarwal, A. & Agarwal, V. 2019. A review on overall control of DC microgrids. *Journal of Energy Storage*, 21(September 2018): 113–138. https://doi.org/10.1016/j.est.2018.11.013.

Kumar, M.B. 2016. *Modeling and Control of PV/Wind Microgrid*. Halmstad University.

Liu, Y., Yu, S., Zhu, Y., Wang, D. & Liu, J. 2018. Modeling, planning, application and management of energy systems for isolated areas: A review. *Renewable and Sustainable Energy Reviews*, 82(September 2017): 460–470. http://dx.doi.org/10.1016/j.rser.2017.09.063.

Lotfi, H. & Khodaei, A. 2017a. AC versus DC Microgrid Planning. *IEEE Transactions on Smart Grid*, 8(1): 296–304.

Lotfi, H. & Khodaei, A. 2017b. Hybrid AC/DC microgrid planning. *Energy*, 118: 37–46.

Lu, X., Sun, K., Guerrero, J.M., Vasquez, J.C. & Huang, L. 2014. State-of-Charge Balance Using Adaptive Droop Control for Distributed Energy Storage Systems in DC Microgrid Applications. *IEEE Transactions on Industrial Electronics*, 61(6): 2804–2815.

Ma, T., Yang, H., Lu, L. & Peng, J. 2014. Technical Feasibility Study on a Standalone Hybrid Solar-Wind System with Pumped Hydro Storage for a Remote Island in Hong Kong. *Renewable Energy*, 69: 7–15. http://dx.doi.org/10.1016/j.renene.2014.03.028.

Ma, W., Wang, J., Member, S. & Lu, X. 2016. Optimal Operations Mode for a DC Microgrid. *IEEE Transactions on Smart Grid*, 7(6): 1–9.

Mahmoudimehr, J. & Shabani, M. 2018. Optimal Design of HJybrid Photovoltaic-Hydroelectric Standalone Energy System for North and South of Iran. *Renewable Energy*, 115: 238–251.

Mousavi, N. 2020. *The integration of pumped hydro storage systems into PV microgrids in rural areas*. Edith Cowan University.

Muhsen, D.H., Khatib, T. & Abdulabbas, T.E. 2018. Sizing of a standalone photovoltaic water pumping system using hybrid multi-criteria decision making methods. *Solar Energy*, 159(December 2017): 1003–1015. https://doi.org/10.1016/j.solener.2017.11.044.

Philip, J., Jain, C., Kant, K., Singh, B., Mishra, S., Member, S., Chandra, A. & Al-haddad, K. 2016. Control and Implementation of a Standalone Solar Photovoltaic Hybrid System. *IEEE Transactions on Industry Applications*, 52(4): 3472–3479.

Prakash, K., Lallu, A., Islam, F.R. & Mamun, K.A. 2016. Review of Power System Distribution Network Architecture. In *Asia-Pacific World Congress on Computer Science and Engineering*. Fiji: Researchgate: 124–130.

Reddy, G.H., Mounika, P. & Kumar, P.V. 2017. Implementation of a Standalone Solar Photovoltaic Hybrid System Using Fuzzy Logic Controller. , 6495(5): 157–163.

Rehman, S., Al-Hadhrami, L.M. & Alam, M.M. 2015. Pumped Hydro Energy Storage System: A Technological Review. *Renewable and Sustainable Energy Reviews*, 44: 586–598.

REN21. 2020. *Renewables 2020 Global Status Report*. Paris. https://abdn.pure.elsevier.com/en/en/researchoutput/ren21(5d1212f6-d863-45f7-8979-5f68a61e380e).html.

Šćekić, L., Mujović, S. & Radulović, V. 2020. Pumped Hydroelectric Energy Storage as a Facilitator of Renewable Energy in Liberalized Electricity Market. *Energies*, 13(22): 6076.

Shafiee, Q., Dragičević, T., Vasquez, J.C. & Guerrero, J.M. 2014. Hierarchical control for multiple DC-microgrids clusters. *IEEE Transactions on Energy Conversion*, 29(4): 922–933.

Shehadeh, H., Siam, J. & Abdo, A. 2019. Operation Scheme of a Microgrid to Maximize Photovoltaic System Utilization in Blackouts: A Case Study. *Proceedings - 2019 IEEE International Conference on Environment and Electrical Engineering and 2019 IEEE Industrial and Commercial Power Systems Europe, EEEIC/I and CPS Europe 2019*: 0–4.

Showers, S.O. 2019. *Enhanced Frequency Regulation of a Grid-Connected PV System*. Cape Peninsula University of Technology.

Siad, S.B. 2019. *DC MicroGrids Control for Renewable Energy Integration*. Université Paris-

Saclay.

Singh, B., Shahani, D.T. & Verma, A.K. 2012. Power Balance Theory Based Control of Grid Interfaced Solar Photovoltaic Power Generating System with Improved Power Quality. In *IEEE International Conference on Power Electronics, Drives and Energy Systems (PEDES)*. Bengaluru, Karnataka, India.: Researchgate: 1–8.

Singh, O. 2016. Hybrid renewable energy system integration in the micro-grid : Indian context. *2016 International Conference on Control, Computing, Communication and Materials (ICCCCM)*, (Iccccm): 1–5.

Smith, R.D. 2014. *DC Microgrid Stabilization Through Fuzzy Control of Interleaved , Heterogeneous Storage Elements*. Michigan Technological Universitty.

Somano, G.Z. & Shunki, G. 2016. American Journal of Electrical Power and Energy Systems Design and Modelling of Hybrid PV-Micro Hydro Power Generation Case Study Jimma Zone. *American Journal of Electrical Power and Energy Systems*, 5(6): 91–98. http://www.sciencepublishinggroup.com/j/epes.

Subkhan, M. & Komori, M. 2011. New concept for flywheel energy storage system using SMB and PMB. *IEEE Transactions on Applied Superconductivity*, 21(3 PART 2): 1485–1488.

Swe, W. 2018. Application of Pumped Hydroelectric Energy Storage for Photovoltaic based Application of Pumped Hydroelectric Energy Storage for Photovoltaic based Rural Electrification. , (January).

Torres, F.G. 2015. *Advanced Control of Renewable Energy Microgrids with Hybrid Energy Storage System*. Universidad De Sevilla. https://idus.us.es/xmlui/bitstream/handle/11441/32946/thesis.pdf?sequence=1&isAllowed=y.

U.S. Department of Energy Microgrid Exchange Group. 2011. *DOE Microgrid Workshop Report*. San Diego, California.

Velázquez-Abunader, I. 2013. Modeling and Simulation of Fuzzy logic based Hybrid power for Electrification System in case of Ashuda Villages. *Journal of Chemical Information and Modeling*, 53(9): 1689–1699.

Verma, S., Singh, S.K. & Rao, A.G. 2013. Overview of control Techniques for DC-DC

converters. , 2(8): 18–21.

Vijayaragavan, K.P. 2017. *Feasibility of DC Microgrids for Rural Electrification*. Dalarna University.

Wang, P., Member, Senior, Jin, C., Zhu, D., Member, Student, Tang, Y., Loh, P.C. & Choo, F.H. 2015. Distributed Control for Autonomous Operation of a Three-Port AC / DC / DS Hybrid Microgrid. *IEEE Transactions on Industrial Electronics*, 62(2): 1279–1290.

Xu, B., Chen, D., Venkateshkumar, M., Xiao, Y., Yue, Y. & Xing, Y. 2019. Modeling a pumped storage hydropower integrated to a hybrid power system with solar-wind power and its stability analysis. *Applied Energy*, 248: 446–462.

Yang, Y., Chen, W. & Blaabjerg, F. 2014. Foreword. In *Introduction to Renewable Energy Systems*. Switzerland: Springer International Publishing: 41–60.

Zhang, F., Ignatius, J., Lim, C.P. & Zhao, Y. 2014. A New Method for Ranking Fuzzy Numbers and its Application to Group Decision Making. *Applied Mathematical Modelling*, 38(4): 1563–1582. http://dx.doi.org/10.1016/j.apm.2013.09.002.

Zhang, L., Tai, N., Huang, W., Liu, J. & Wang, Y. 2018. A Review on Protection of DC Microgrids. *Journal of Modern Power Systems and Clean Energy*, 6(6): 1113–1127. https://doi.org/10.1007/s40565-018-0381-9.

APPENDICES

Appendix 1: DCMG system measurements

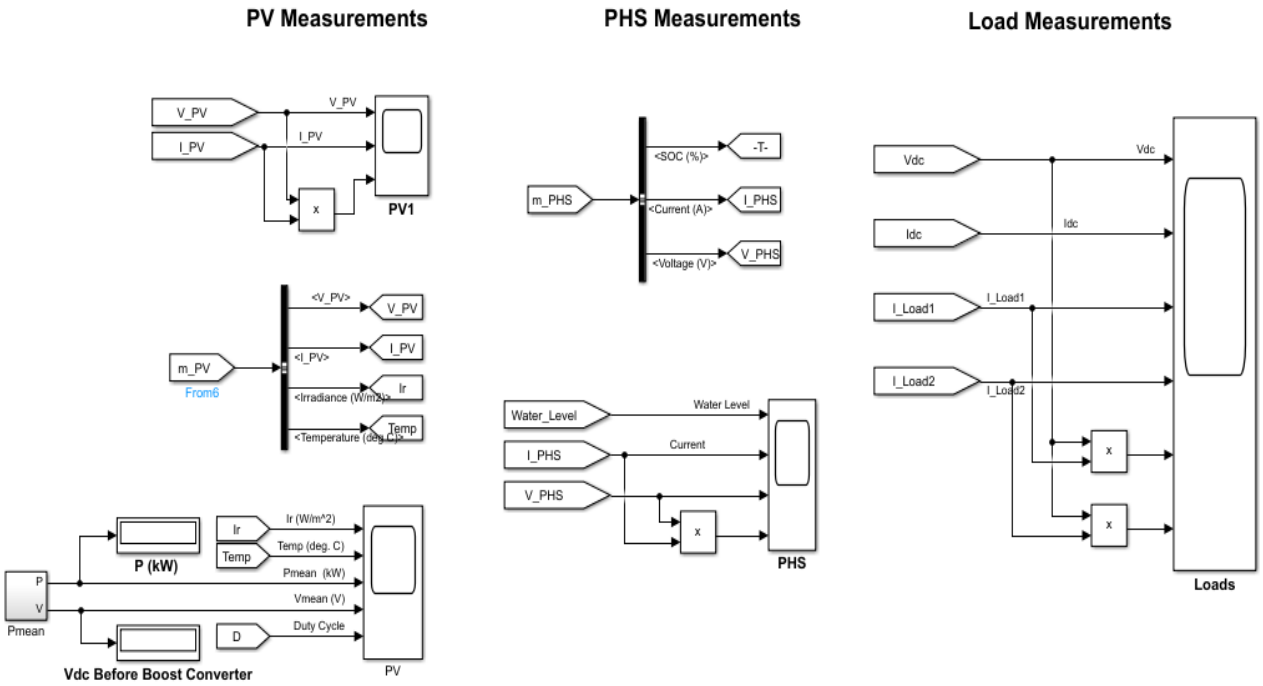

Appendix 2: DCMG system control variables and set conditions

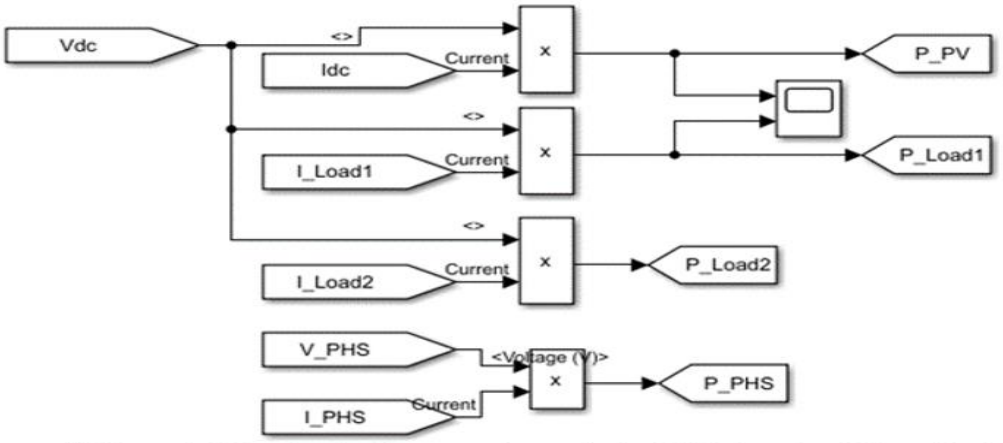

If PV power is higher than load1 power and water level of PHP is less than 98% supplies load1 and run the PHS as a motor to fill the upper reservoir (Irradiance=1000 and Water level less than 98%)

If PV power is higher than load1 power and water level is greater than or equal to 98% supplies load1 and load2 (irradiance=1000 and Water level=98%)

if PV power is equal equal to load1 supplies load 1 supplies Load1 only

if PV power is lesser than load1 power and water level is higher than or equal to 10% supplies load1 from both PV and PHP (Irradiance=500)

Else PV and PHP are off